IN VIVO CHARACTERIZATION OF A NEW TRANSPEDICULAR APPROACH TO THE INTERVERTEBRAL DISC IN A LARGE ANIMAL MODEL

Director of the School: Prof. Gianfranco Gabai

Supervisor: Prof. Marco Bernardini

PhD student: Francesca de Strobel

SUMMARY - Back pain (BP) is a common clinical condition that leads to high morbidity with significant psychosocial and economic effects. It is the leading cause of disability in people under 45 years of age, and it results in enormous national economic losses in developed countries. The wide majority of BP is associated with degenerative changes of the intervertebral disc (IVD). Intervertebral disc degeneration (IVDD) is an age-related chronic process that is characterized by a progressive reduction of proteoglycans and water content in the nucleus pulposus (NP) with loss of the IVD's ability to resist compressive forces. Current treatment options for BP and IVDD range from conservative measures to invasive procedures however, these treatment modalities have limited efficacy and do not produce predictable and reliable outcomes. Therefore, there is a clear need for more effective early treatment of BP that may prevent, slow down, or reverse the degenerative changes. To evaluate the efficacy of novel IVD regenerative treatments, prior to translation into humans, *ex vivo* and *in vivo* animal model systems are needed.

In the present study, a novel transpedicular approach to the IVD was validated in 12 sheep. Under fluoroscopy, a 2-mm Kirshner wire was introduced through the vertebral body with a cranio-medial inclination of approximately 45° in all plans direction to reach the center of the NP. In each animal four IVDs, from L1 to L5, were addressed by performing different surgical techniques, respectively: (I) nucleotomy, (II) tunnel, (III) nucleotomy + polyurethane (PU) scaffold, and (IV) tunnel + PU scaffold. Intact IVDs (L5-6) were used as controls. Intra- and post-surgical morbidity rates were low; CSF leakage was recorded in two spinal segments whereas discospondylitis and vertebral luxation occurred respectively at L1-2 and L3-4 in two different animals. The quantitative and qualitative analysis of MRI, radiologic, histologic and macroscopic data, collected at four different time points (before and 1, 3 and 6 months after surgery), suggested that the injury induced in the present model represents a reliable method for initiating a progressive IVDD process, obtaining different degrees of IVDD depending on the type of lesion performed. The endplate damage itself, caused by the realization of the

transpedicular tunnel, led to IVD degenerative changes, although to a lesser extent than those caused by performing nucleotomy. Furthermore, the sealing of the tunnel with the PU scaffold resulted in a lack of cells leakage throughout the tunnel.

The transpedicular approach represents a feasible alternative route to the IVD, with respect to the traditional ventral and ventrolateral approaches through the annulus fibrosus. This new pathway to the IVD provides a new valid model to study biologic and biomechanical alterations in relation either, to IVD degenerative processes and to potential NP regenerative therapies.

RIASSUNTO - La lombalgia è una condizione clinica molto frequente associata ad elevata morbidità, con effetti sia dal punto di vista psicosociale che della spesa sanitaria nazionale. La lombalgia é la principale causa di disabilità nella popolazione al di sotto dei 45 anni, e rappresenta una della principali voci di spesa nei paesi sviluppati. La grande maggioranza dei casi di lombalgia è associata alla degenerazione del disco intervertebrale (IVDD). L'IVDD è un processo cronico età-correlato caratterizzato da una progressiva riduzione del contenuto di proteoglicani ed acqua nel nucleo polposo (NP), con perdita della capacità del disco di resistere a forze compressive. Le attuali opzioni di trattamento disponibili per lombalgia e IVDD comprendono sia approcci conservativi che procedure invasive. Tuttavia, queste modalità di trattamento hanno un'efficacia limitata e non producono risultati prevedibili e riproducibili. Per queste ragioni, vi è una chiara necessità di trattamenti che siano efficaci nel prevenire, rallentare o invertire le modificazioni degenerative causate dal processo di IVDD. Al fine di valutare l'efficacia di nuove tecniche di rigenerazione discale e prima di trasferirle all'uomo, é necessario testarle su modelli animali *ex vivo* ed *in vivo.*

Questo studio ha permesso di validare, in 12 pecore, un nuovo approccio al disco intervertebrale (IVD) per via transpeduncolare. Tramite guida fluoroscopica, un filo di Kirshner di 2-mm di diametro é stato introdotto attraverso il corpo vertebrale con un'inclinazione di circa 45° in tutti i piani dello spazio e in direzione cranio-mediale, tale

da raggiungere il centro del NP. In ciascun animale sono stati trattati quattro IVD, da L1 a L5, effettuando in ciascuno una diversa tecnica chirurgica: (I) nucleotomia, (II) tunnel, (III) nucleotomia + scaffold in poliuretano (PU) e (IV) tunnel + scaffold PU. I dischi non trattati (L5-6) sono stati considerati come gruppo controllo. Le percentuali di morbiditá intra- e post-operatoria si sono rivelate basse; in due occasioni é stata riportata fuoriuscita di liquor in fase chirurgica, inoltre lussazione di L3-4 e discospondilite a livello di L1-2 si sono verificate in due soggetti. Le analisi quantitative e qualitative, effettuate sui dati ricavati in quattro diversi time point (prima e 1, 3 e 6 mesi dopo la chirurgia) dalle immagini radiografiche e di risonanza magnetica e dai campioni macroscopici e istologici, hanno rivelato l'efficacia del metodo presentato nell'ottenere un modello progressive di IVDD. Inoltre, attraverso l'approccio transpeduncolare é stato possibile ottenere diversi gradi di IVDD, dipendentemente dalla tipologia di lesione effettuata. Il solo danno al piatto vertebrale ha determinato alterazioni degenerative del IVD, tuttavia inferiori rispetto a quelle causate effettuando la nucleotomia. Inoltre, l'utilizzo dello scaffold in PU per sigillare il tunnel é servito a prevenire la fuoriuscita di cellule attraverso il tunnel.

L'approccio transpeduncolare rappresenta una via alternativa per raggiungere il IVD rispetto ai tradizionali approcci ventrali e ventrolaterali attraverso l'anello fibroso. Questa nuova tecnica fornisce un nuovo modello per lo studio di alterazioni biologiche e biomeccaniche in relazione sia ai processi di IVDD sia a potenziali terapie regenerative.

INDEX

INTRODUCTION

Back pain (BP) is a common clinical condition that leads to high morbidity with significant psychosocial and economic effects. It is the leading cause of disability in people under 45 years of age, and it results in enormous national economic losses in developed countries. The wide majority of BP is associated with degenerative changes of the intervertebral disc (IVD) (Luo et al., 2004). Intervertebral disc degeneration (IVDD) is an age-related chronic process that is characterized by a progressive reduction of proteoglycans (PGs) and water content in nucleus pulposus (NP) with loss of the IVD's ability to resist compressive forces, therefore to assure spinal stability. BP is the first symptom of IVDD that may progress to multiple spinal disorders such as disc herniation, degenerative spondylolisthesis, instability, and spinal stenosis (Figure 1) associated with neurological signs due to radiculopathy and myelopathy that often require surgical treatments (Wilste et al., 1976).

Currently, there are no treatment options able to reverse the degenerative process targeting the pathophysiology involved in IVDD. Nowadays, there is a strong effort to develop an effective early treatment of BP that may prevent, slow down, or reverse the degenerative changes in the IVD. Recovering the IVD's ability to repair the extracellular matrix (ECM) and re-establishing the PG content may have a significant therapeutic effect by increasing IVD hydration and thereby improving its biomechanics.

Animal models are widely used to study IVDD and to evaluate treatment methods because of the availability of the tissue, the dicreased variability between subjects compared with humans, and the feasibility to perform *in vivo* experiments. *In vivo* animal models are essential to study the aetiopathogenesis of IVDD, how it evolves over time either spontaneously or following experimental injury, and to show how therapeutic strategies may ameliorate, resolve, or prevent it. Animal models must be ethical,

controllable, reproducible, and cost-effective; in addition, they should be able to model

human pathologic processes.

Figure 1
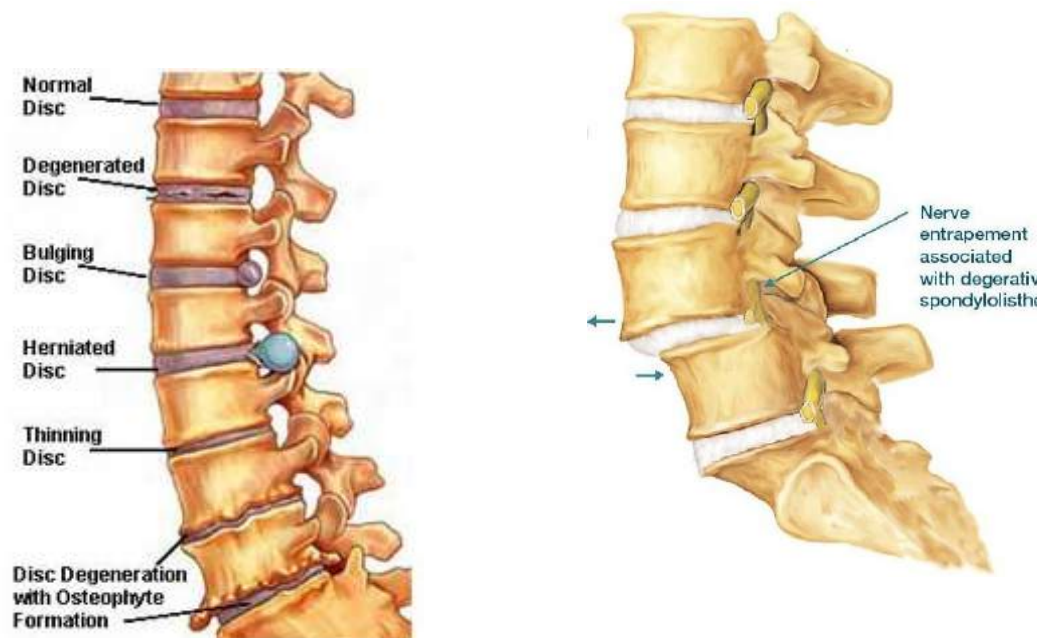
Spinal stenosis - Progressive narrowing of the spinal canal could be either a congenital or acquired condition. It is most common in the cervical and lumbar areas. The canal components that contribute to acquired stenosis include the facets (hypertrophy, arthropathy), ligamentum flavum (hypertrophy), posterior longitudinal ligament, vertebral body (spondylosis), IVD, and epidural fat. Spinal stenosis implies spinal canal narrowing with possible subsequent neural compression. Congenital stenosis may predispose an individual with mild degenerative changes to become symptomatic earlier in life.

Spondylolisthesis – It is defined as the translation of one vertebra in relation to the adjacent level and is commonly referenced as an anterolisthesis of the cranial segment on the caudal segment. Five different types of spondylolisthesis have been described: dysplastic, isthmic, degenerative, traumatic, and pathologic (Wilste et al., 1976). Spondylolisthesis can be either congenital or acquired.

Numerous *in vivo* animal models for IVDD are described in literature, and each

model has its own advantages and disadvantages. There are several important aspects to

consider in relation to using animals for studying IVDD such as development and anatomy

of the spine, loading and size differences, the mechanical, biochemical and nutritional conditions.

o **INTERVERTEBRAL DISC**

▪ *EMBRYOGENESIS AND POSTNATAL DEVELOPMENT*

The embryonic development of the vertebral column centers on the notochord, a rod-like mesoderm-derived structure (Fleming et al., 2001; Stemple, 2005). The notochord is important both as a signaling center that mediates cell migration, differentiation and survival, and as a structure that physically gives rise to the NP (Peacock, 1951; Walmsley, 1953; Choi et al., 2008). Embryonic morphogenesis of the disc, as well as key molecules implicated in this process, are illustrated schematically in Figure 2.

The annulus fibrosus (AF) and NP regions of the IVD arise concurrently along distinct developmental pathways. During human fetal gestation, at approximately 30 days (12 days in the mouse), cells of the sclerotome migrate medially from pairs of paraxial somites (Figure 2A) to condense around the notochord (Figure 2B) (Peacock, 1951; Hunter et al., 2003a), adopting a metameric pattern of more condensed and less condensed regions (Figure 2C), which later give rise to the AF and vertebral bodies, respectively (Aszodi et al., 1998). Cells in the future AF region adopt a fibroblastic morphology. These cells align and orient to form the template for ECM deposition that later defines the AF angle-ply lamellar structure (Figure 2E) (Rufai et al., 1995).
Concurrently with AF morphogenesis, the notochord contracts within the forming vertebral body rudiments, simultaneously expanding within the intervertebral regions to form the NP (Figure 2D) (Peacock, 1951; Pazzaglia et al., 1989; Aszodi et al., 1998).
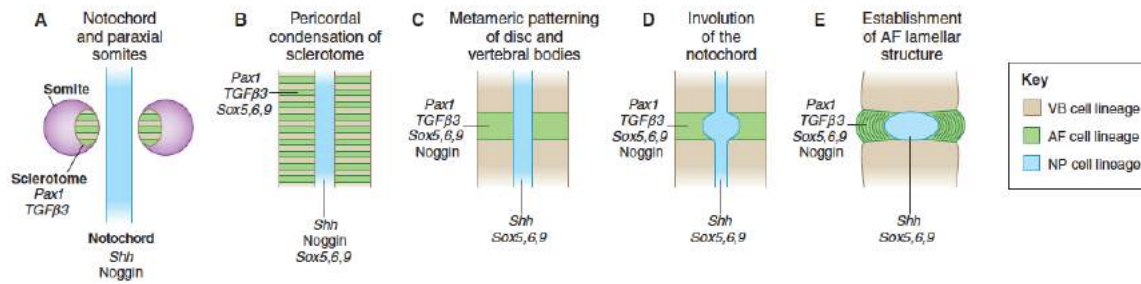
Figure 2. Schematic representation of embryonic morphogenesis of the mammalian IVD. Colours represent origins and destinations of cell populations. Also indicated are key morphogens and transcriptional regulators implicated in the growth and differentiation of the disc structures at each developmental stage. (A) The notochord adjacent to pairs of paraxial somites, which contain sclerotome cells. (B) Sclerotome cells condense around the notochord. (C) Cells adopt a metameric pattern of more condensed (green) and less condensed (brown) regions that give rise to the AF and vertebral bodies, respectively. (D) The notochord contracts within the vertebral body rudiments and expands within the future intervertebral disc to form the NP. (E) Basic structures of the disc are established, and AF cells adopt orientations and alignments that form the template for the lamellar structure. VB, vertebral body.

Once the basic structures of the IVD are established, several developmental changes occur. In humans, during the early postnatal years, blood vessels that have penetrated the AF and cartilage endplates (EPs) from as early as 35 weeks gestation begin to recede, determining the avascular structure of the IVD (Urban and Roberts, 1995; Nerlich et al., 2007). The vascular regression has been hypothesisied to be a consequence of decreased nutrient requirements following the initial period of rapid growth or, more likely, of the inability of circulatory pressure to compete with large physiological stresses in the surrounding ECM. Poor nutritional supply to the cells of the avascular IVD has been implicated in the pathogenesis of IVDD.

Further changes characterising the resident cell populations, and specifically those of the NP, begin to occur very early in life. Soon after birth, the cells that populate the NP exhibit morphological characteristics that are similar to the cells that populate its notochord precursor (Peacock, 1952; Wolfe et al., 1965; Trout et al., 1982a; Trout et al., 1982b). Notochordal cells (NCs) in the postnatal NP are large (30-40 µm in diameter), frequently appear in clusters and possess actin-filament-bounded intracellular vacuoles

that occupy more than 25% of the cell area (Hunter et al., 2003b; Hunter et al., 2004) (Figure 3b).

In the first 10 years following birth, the number of NCs declines, and no NCs are present by adulthood (Peacock, 1952; Trout et al., 1982a; Hunter et al., 2004). Concurrently, a second population of chondrocyte-like cells appears, characterised by apparent morphological similarities with cartilage chondrocytes (Urban and Roberts, 1995) (Figure 3). In comparison with NCs, the chondrocyte-like NP cells are smaller (~10 µm in diameter) and lack intracellular vacuoles (Hunter et al., 2004).

In many species (mouse, rat, cat, mink, chondrodystrophoid dog, pig and rabbit) the NCs persist through most of adult life, whereas in other species they gradually disappear during aging (human, sheep, non-condrodystrophoid dog, cow) (Hunter et al., 2004). Horses apparently have no NCs at birth (Table 1). The exact mechanism of transition from NCs to chondrocytic-like cells is not precisely known; however, developmental changes to both mechanical and nutritional microenvironment have been implicated (Rastogi et al., 2009; Guehring et al., 2010). It is unclear whether this change in cell populations is due to continued differentiation of the NCs into chondrocytic phenotype (Choi et al., 2008; Risbud et al., 2010), or due to apoptosis of the resident cells with the subsequent migration to the NP by cells derived from the cartilaginous EPs or AF (Kim et al., 2003).

Considered that altered cellularity represents a hallmark of IVDD, the relevance of NCs in animal models used to study IVDD can be great since this is a completely different cell type in terms of morphology and function to the cells populating the adult human NP (Hunter et al., 2003a).

Another key factor in early IVDD is the decrease in the PG content in the NP. NCs have been shown to synthesize ECM in a distinct manner respect the mature NP cells (Cappello et al., 2006). PGs synthesized by NCs are evenly distributed between the inter- and pericellular regions, compared with mature NP cells, in which the majority of PGs are intercellular. Additionally, the rate at which PGs migrate to the intercellular regions is significantly greater for NCs than for mature NP cells (Cappello et al., 2006).

Table 1. Age of loss of notochordal cells in different species (Hunter et al., 2004)

Species	Age of skeletal maturity	Age of loss of notochordal cells	References
Dog (c)	12 months	12 months	Hansen, 1952; Hutton et al., 2000; Ganey et al., 2003
Dog (n/c)	12 months	60 months	Frick et al., 1994; Hansen 1952; Maldonado and Oegema, 1992; Katsuura and Hukuda, 1994; Matsuzaki et al., 1996; Hunter et al., 2004
Rabbit	10 months	6 months	Anderson et al., 2002; Smith and Serafini-Fracassini, 1968; Scott et al., 1980; Nomura et al., 2001; Hunter et al., 2004
Pig	12 months	Unknown	Holm et al., 2004; Kawchuck et al., 2001; Hunter et al. ,2004
Cat	24 months	Never	Hansen 1959; Butler 1989; Kathmann et al., 2000; Hunter et al., 2004
Ferret	n/d	Never	Hunter et al., 2004
Sheep	12 months	Unknown	Kadoya et al., 2001 ; Hunter et al., 2004
Rat	2 months	12 months	Adler et al., 1983; Moskowitz et al., 1990; Nishimura and Mochida, 1998; Iatridis et al., 1999; Mente et al., 1999; MacLean et al., 2003; Hunter et al., 2004
Mouse	4 months	n/d	Ariga et al., 2001; Lotz et al., 1998; Lotz and Chin, 2000; Wlash and Lotz, 2004; Hunter et al., 2004
Human	20 years	6-10 years	Horwitz, 1977

C, chondrodystrophoid (beagles); n/c, non-chondrodystrophoid (mongrels); n/d: no data available.

▪ *INTERVERTEBRAL DISC MORPHOLOGY AND BIOCHEMISTRY*

The human vertebral column consists of 24 mobile vertebrae: 7 cervical, 12 thoracic, and 5 lumbar. With the exception of the first and second cervical vertebrae, all vertebral bodies are connected by IVDs. IVDs form a strong and flexible connection between the vertebrae, allowing flexion, extension, and rotation of the spinal column and forming an amphiartrosis type of joint. Moreover, the IVDs constantly transmit loads arising from body weight and muscle activity through the spinal column (Twomey and Taylor, 1987; Roberts et al., 1989).

As described previously, developmentally the IVD is a unique structure formed from cells of at least two embryonic origins: the notochord and the somites. These lineages give rise to a tissue that is complex and specialized in terms of its microstructure, mechanical function and cell types (Smith et al, 2011). IVDs consist of a thick outer ring of fibrous cartilage (AF), which surrounds a more gelatinous core known as the NP; the NP is delimited cranially and caudally by cartilage EPs (Figure 4A), forming a symphysis type of cartilagineous joint.

Nucleus pulposus - The central NP contains large quantities of aggrecan, the major PG, which aggregates along chains of hyaluronan (Urban, 1996). The glycosaminoglycan (GAG) side chains of these PGs carry a fixed negative charge and generate an osmotic swelling pressure within an irregular meshwork of collagen II fibrils (Inoue, 1981) and elastin fibres, which are arranged radially (Yu et al., 2002). Interspersed at a low density (approximately 5000/mm^3) (Maroudas et al, 1975) are chondrocytes-like cells (Figure 3c; 4b).

Annulus fibrosus - Outside the NP is the AF, characterized by heterogeneous composition and architecture. The highly organized outer regions consist of concentric distinct lamellae (Figure 5A-B), which are composed of bundles of collagen I fibers oriented at oblique angles that alternate within each consecutive lamella to form an angle-ply structure (Marchand and Ahmed, 1990). In the inner AF, there is a transition to collagen II that, together with increasing PGs concentration, gives rise to a less fibrous and less organized structure (Humzah and Soames, 1988). Elastin fibres lie between the lamellae, possibly helping the IVD to return to its original arrangement following bending. They may also bind the lamellae together as elastin fibres pass radially from one lamella to the next (Yu et al., 2002). The cells of the AF, particularly in the outer region, tend to be fibroblast-like, elongated, thin and aligned parallel to the collagen fibres (Figure 3a), while toward the inner AF the cells can be more oval. Cells of the IVD, both in the AF and NP, can have several long, thin cytoplasmic projections, which may be more than 30 μm

long (Errington et al., 1998; Bruehlmann et al., 2002). Their function in the IVD is unknown but it has been suggested that they may act as sensors and communicators of mechanical strain within the tissue (Bruehlmann et al., 2002).
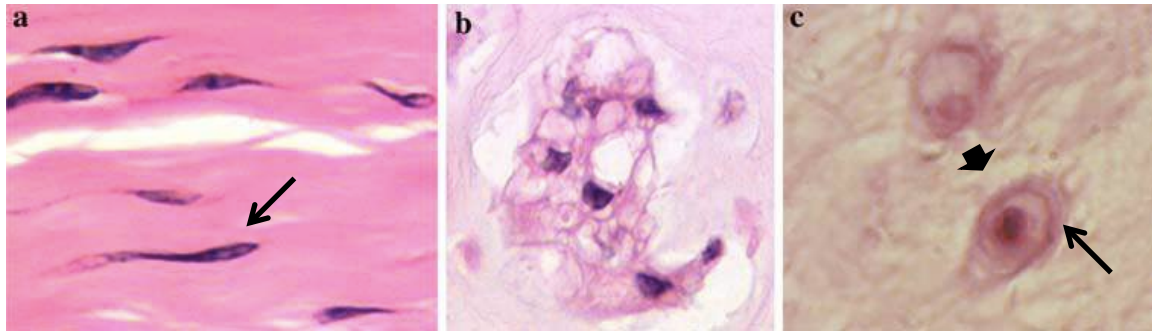
Figure 3. Morphology of IVD cells. Cells of the intervertebral disc differ in morphology according to the region of origin, age and species. (a) Annulus fibrosus cells (bovine disc): the cells in the outer fraction are fibroblast-like, therefore much more bipolar and elongated (arrow) than those in the inner fraction that are more rounded; (b) Notochordal cells (bovine disc): large highly vacuolated cells; (c) Nucleus pulposus cells (human disc) are rounded, often sitting inside a capsule (thin arrow) that may be surrounded by an obvious pericellular matrix (thick arrow) (Roberts et al., 2006; Alini et al., 2008).

Endplate - The third morphologically distinct region is the cartilage EP, a thin horizontal layer, usually less than 1 mm thick, of hyaline cartilage. The EPs extend cranially and caudally over the inner AF and NP to interface with the vertebral bodies (Figure 4), and function to regulate nutrient diffusion between the IVD and the vertebral bodies. In the outer regions of the AF, collagen fibres anchor directly into the vertebral bone, interfacing the IVD and the vertebral body. The collagen fibres within it run horizontal and parallel to the vertebral bodies, with the fibres continuing into the IVD (Roberts et al., 1989). During childhood and adolescence, the EP functions also as a growth plate of the adjacent vertebrae in humans, whereas the vertebral bodies of other mammals contain separate growth plates (Adam and Roughley, 2006).
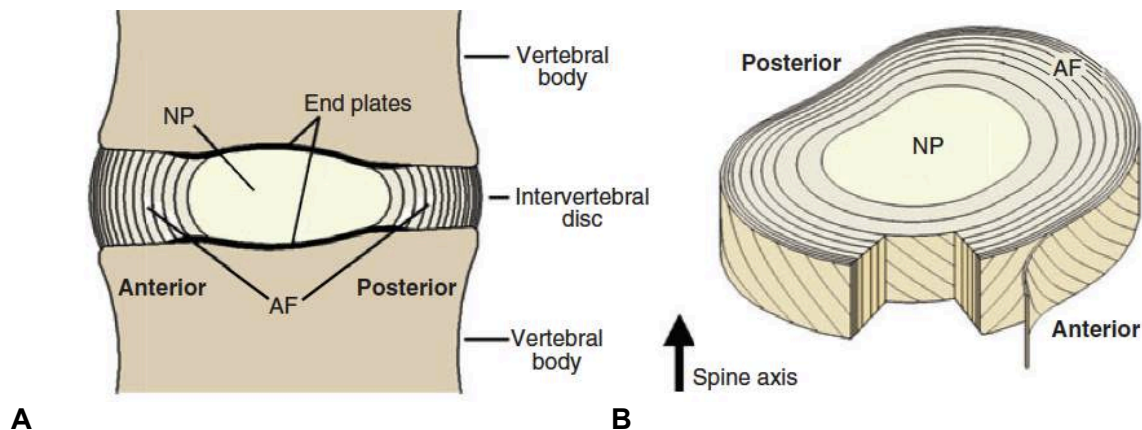
Figure 4. Schematic representations of the adult intervertebral disc. (A) Midsagittal cross-section showing anatomical regions. (B) Three-dimensional view illustrating the AF lamellar structure.

Extracellular matrix - The mechanical functions of the IVD are determined by the composition and organization of the ECM. The main mechanical role is provided by the two major macromolecular components, collagen and PGs. The collagen network, formed mostly of type I and type II collagen fibrils and making up approximately 70% and 20% of the dry weight of the AF and NP respectively (Eyre and Muir, 1977), provides tensile strengh to the IVD and anchors the tissue to the bone. Aggrecan, the major PG of the IVD (Johnstone and Bayliss, 1995), is responsible for maintaining tissue hydration through the osmotic pressure provided by its constituent chondroitin and keratan sulphate chains (Urban et al, 1979) (Figure 5B). The PGs and water content of the NP (around 50% and 80% of the wet weight, respectively) is greater than in the AF (approximately 20% and 70% of the wet weight, respectively) (Figure 5A). In addition, there are many other minor components, such as collagen types III, V, VI, IX, X, XI, XII and XIV; small PGs such as lumican, biglycan, decorin and fibromodulin; and other glycoproteins such as fibronectin and amyloid (Roberts et al., 1991; Melrose et al., 2001). The functional role of many of these additional matrix proteins and glycoproteins is not yet clear. Collagen IX, however, is thought to be involved in forming cross-links between collagen fibrils and is thus important in maintaining network integrity (Eyre et al., 2001).
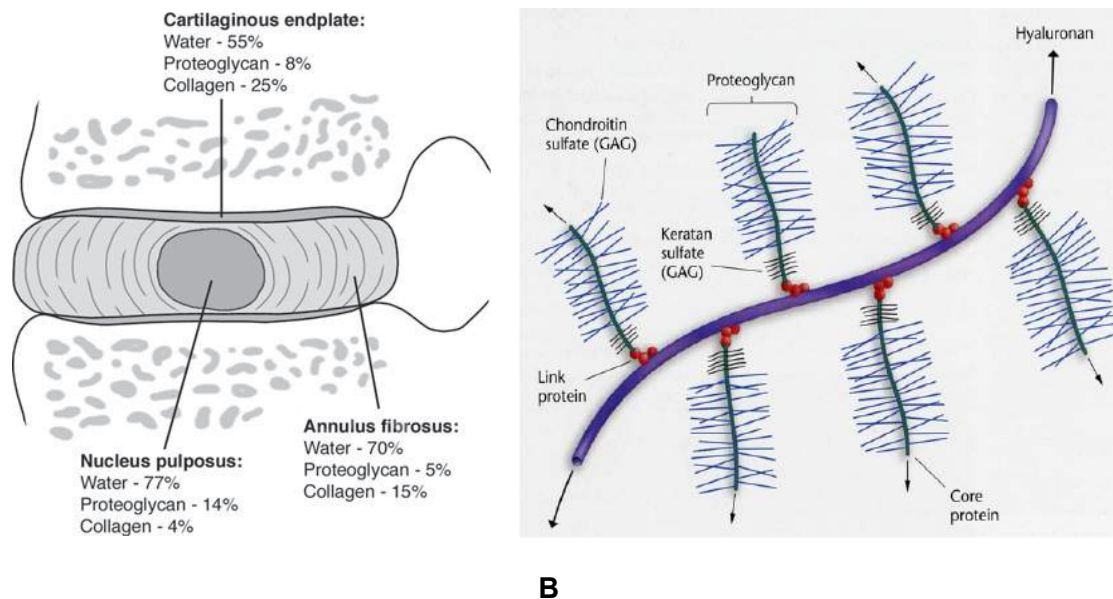
Figure 5. (A) Distribution of the main IVD constituents within the AF, NP and EPs (Prithvi, 2008). (B) Structure of an aggrecan type complex PG. Aggrecan is a high molecular weight PG, in which chondroitin sulfate and keratan sulfate GAG chains are attached to an extended protein core.

The ECM is a dynamic structure. Its molecules are continually being broken down by proteinases such as the matrix metalloproteinases (MMPs) and aggrecanases, which are also synthesized by IVD cells (Sztrolovics et al., 1997; Roberts et al., 2000; Weiler et al., 2002). The balance between synthesis, breakdown and accumulation of ECM macromolecules determines the quality and integrity of the ECM, and thus the mechanical behaviour of the IVD itself. The integrity of the ECM is also important for maintaining the relatively avascular and aneural nature of the healthy IVD.

- ***INTERVERTEBRAL DISC INNERVATION AND VASCULARIZATION***

The adult IVD is almost completely avascular (Figure 6B) (Nerlich et al., 2007), so resident cells must survive and function in an environment that is low in nutrients and oxygen (Urban et al., 2004). In the longitudinal ligaments adjacent to the IVD and in young cartilage EPs (less than about 12 months old) are present blood vessels which represent branches of the spinal artery (Crock et al., 1991) (Figure 6A). The cartilagineous EP, like other hyaline cartilages, is normally totally avascular and aneural in the healthy adult

(Groen et al., 1990).

The nerve supply of the IVD is complex. The healthy adult IVD innervation is mainly restricted to the outer lamellae where some branches terminate in proprioceptors (Roberts et al., 1995) (Figure 6). A meningeal branch of the spinal nerve, known as the recurrent sinuvertebral nerve, originates near the IVD space and innervates the dorsal circumference of the AF (Figure 7). This nerve stems from the rami communicantes, runs ventral to the nerve root, enters the foramen back to the spinal canal, where the nerve splits into finer branches (ascending and descending branches), which form nerve networks – one in the posterior longitudinal ligament (PLL) and a network in the ventral dura (Groen et al., 1990). It has been shown in animal studies that further afferent contributions to the sinuvertebral nerve arises via the rami communicantes from multiple superior and inferior dorsal root ganglia (Figure 7B). In addition, the anterior longitudinal ligament (ALL) also receives afferent innervation from branches originating in the dorsal root ganglion. The PLL is richly innervated by nociceptive fibers from the ascending branch of the sinovertebral nerve, which also innervate the adjacent outer layers of the AF (Figure 8). The sensory innervation of the IVD occurs via branches of the truncus sympathicus (Groen et al., 1990), supplying the ventral and lateral sides of the IVD. Some of the nerves in the IVD have glial support cells, or Schwann cells, alongside them (Johnson et al., 2001).

Afferent fibers from the IVD travel along with the sympathetic nerve and both nerve networks consist of interverconnected nerves with somatic and autonomic branches from various lumbar spinal nerves (Groen et al., 1990; Suseki et al., 1998; Oh and Shim, 2004).
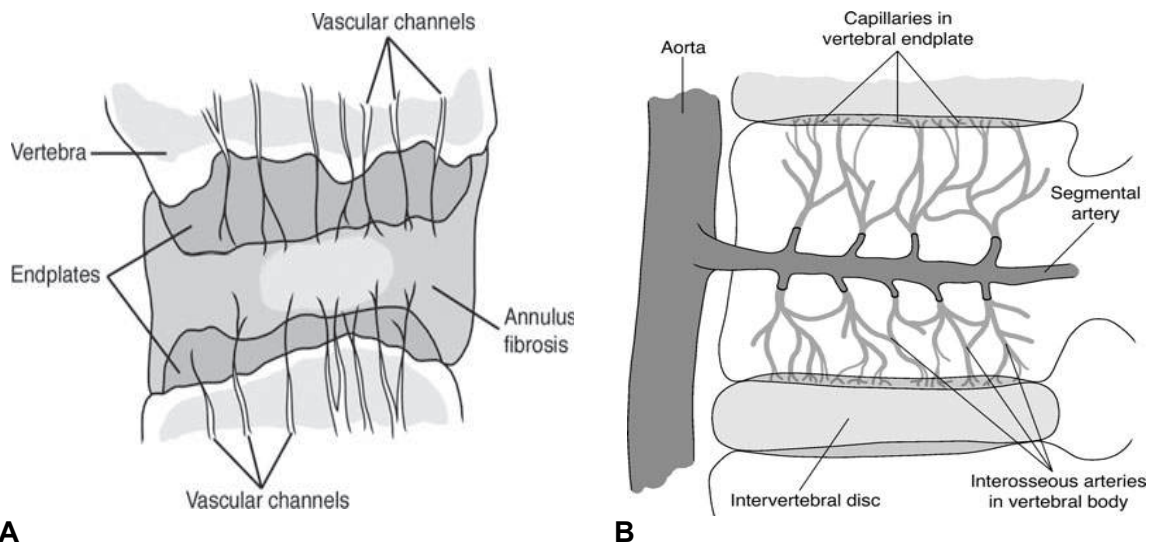
Figure 6. (A) An axial section of the IVDD of a 10-month-old girl. Numerous vascular channels and wide cartilaginous endplates traversing to the AF and the NP are present. The disc is gel-like and highly hydrated. **(B)** The organization of the blood vessels branching from the segmental artery entering the vertebral body and end as capillaries in the EP (Raj, 2008).
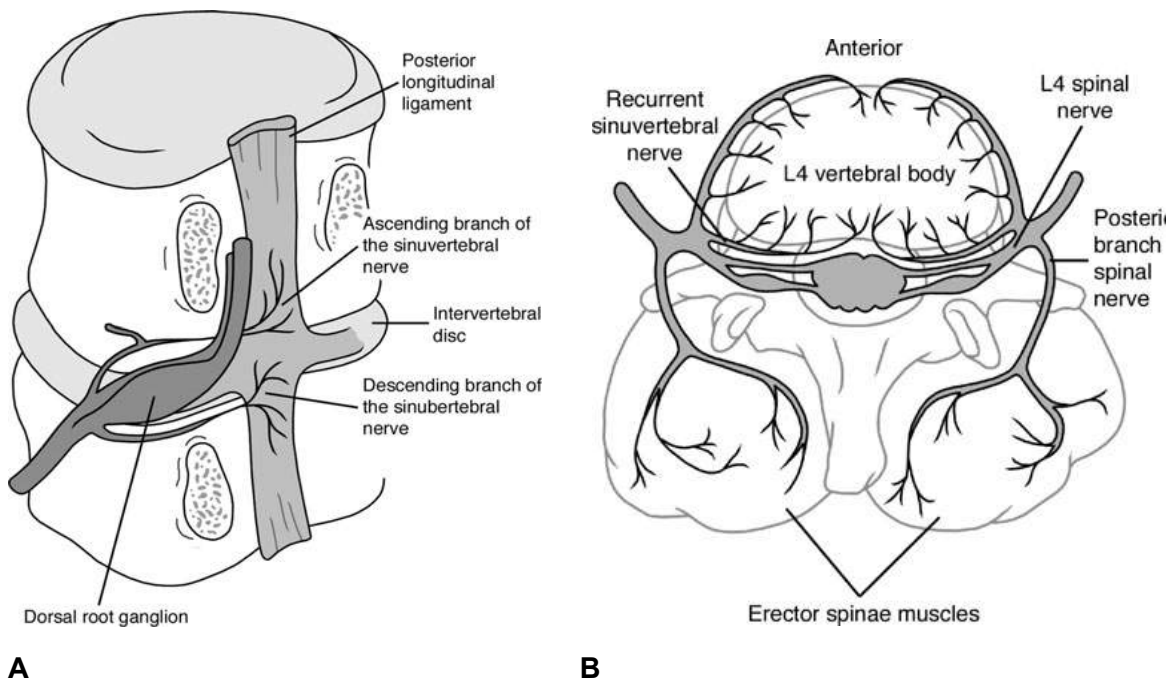
Figure 7. (A) Innervation of the PLL and the disc annulus by the ascending branch of the sinuvertebral nerve. **(B)** The course of the recurrent sinuvertebral nerve, which innervates the postero-lateral region of the disc. The nerve exits from the dorsal root ganglion and enters the vertebral foramen, where it divides into a major ascending and a lesser descending branch. The PLL is richly innervated by nociceptive fibers from the ascending branch of the sinuvertebral nerve (Raj, 2008).
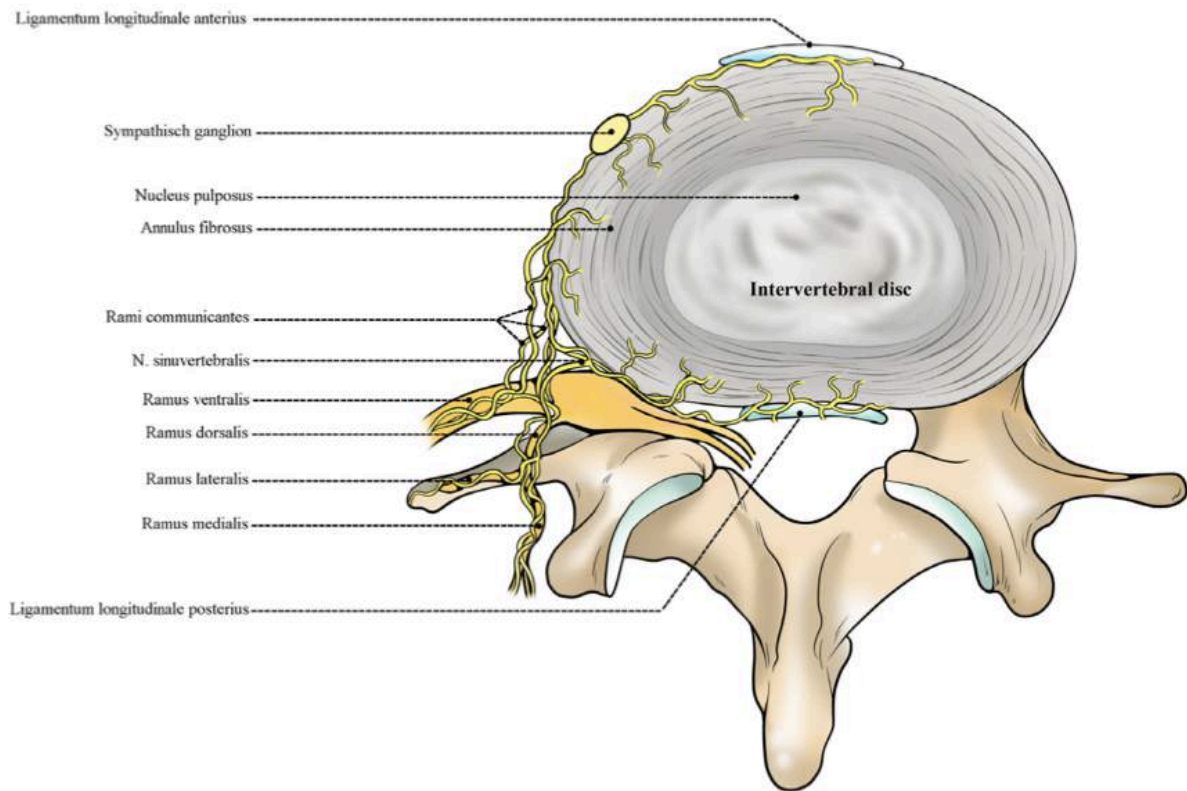
Figure 8. Schematic representation of the innervation of the normal IVD. The ventral and lateral sides of the IVD are supplied by branches of the rami communicantes, direct branches of the truncus sympathicus, and the ligamentum longitudinale anterius and ligamentum longitudinale posterius nerve plexus. In healthy adult animals and human beings, nerves extend no further into the IVD than the outer third of the annulus fibrosus.

- ▪ *INTERVERTEBRAL DISC DEGENERATION*

During growth and skeletal maturation the boundary between AF and NP becomes less obvious, the NP becomes progressively more fibrotic and less gel-like and the disc morphology becomes more disorganized (Buckwalter, 1995). The IVD degeneration process involves four main stages: dehydration, fissuring, neovascularization, and bony changes.

Dehydration of the IVD results from the reduced synthesis of the PG matrix. The morphological changes associated with IVDD are characterised by increased incidence of cell death with necrotic and apoptotic appearance (Trout et al., 1982b; Gruber and Hanley, 1998), cell proliferation leading to cluster formation particularly in the NP

21

(Johnson et al., 2001; Hastreiter, 2001), reduced ECM turnover and accelerated loss of PGs due to the production of interleukin-1 (IL-1) and tumour necrosis factor in response to repeated injury (Boos et al., 2002).

Over time, the AF becomes thickened and may develop radial fissures. The EPs are prone to fracturing under repeated loading. The nuclear material may leak out into either the AF or the EP. As nuclear material contains proinflammatory cytokines, this leads to an inflammatory response within this parts of the IVD. As these injuries heal, the healing process is accompanied by new vessel formation, or neovascularization within the AF (Figure 9) or EP. In conjunction with this neovascularization, sensory nerve endings spread into the inner layers of the AF and into the EPs. In severely degenerate IVDs, nerves fibers may extend all the way into the NP (Roberts et al., 1995).

IVDD is radiologically and histologically characterized by a loss of disc height (DH) which leads to altered spinal mechanics. Furthermore, subchondral sclerosis of the EP, osteophite formation, facet joint atrophy, radial bulging may occur over time (Lotz et al., 1998).

It is difficult to differentiate changes that occur solely due to ageing from those that might be considered "pathological". Examples of IVDs with advancing degrees of degeneration, as visualized by magnetic resonance imaging, are shown in Figure 10.

As mentioned previously, the most significant biochemical change that occurs in IVDD is loss of PGs (Lyons et al., 1981). The aggrecan molecules become degraded, with smaller fragments being able to leach from the tissue more readily than larger portions. This results in loss of GAG, which leads to a fall in the osmotic pressure of the disc ECM, therefore a loss of hydration. In degenerate IVDs, however, the IVD cells can retain the ability to synthesize large aggrecan molecules, with intact hyaluronan-binding regions, which have the potential to form aggregates (Johnstone and Bayliss, 1995).
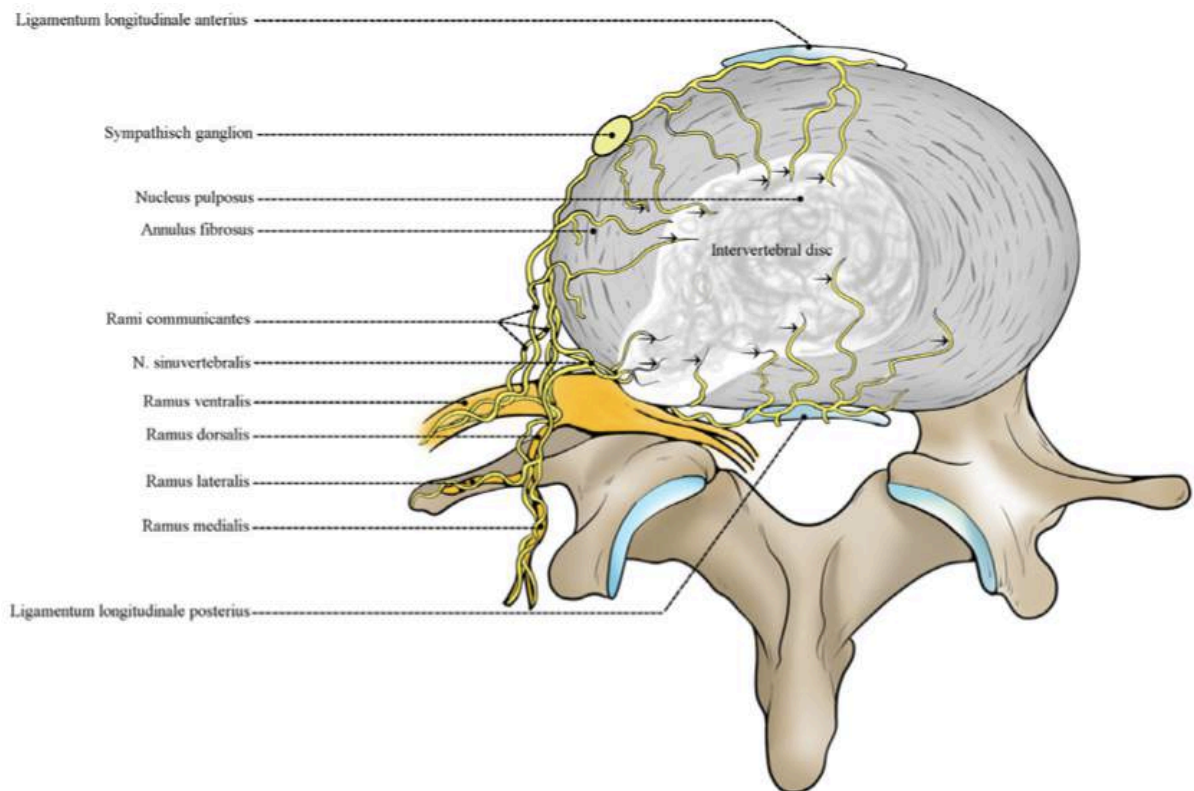
Figure 9. Schematic representation of the innervation of the injured IVD. The innervation of IVD is more extensive. Sensory nerve structures have been demonstrated in the AF, extending into the inner layers of AF, and even reaching up to NP.

Although the collagen population of the IVD also changes with degeneration of the ECM, the changes are not as obvious as those of the PGs. The main changes are related to the types and distribution of collagens rather than to the absolute quantity. In addition, the fibrillar collagens, such as type II collagen, become progressively more denatured with degeneration, apparently because of enzymatic activity (Antoniou et al., 1996; Hollander et al., 1996). However, as with PGs, new collagen molecules may be synthesized, at least early in IVDD, possibly in an attempt at repair (Duance et al., 1998).

At the molecular level, increased levels of cytokines and catabolic enzymes are associated with IVDD (Gruber et al, 2002). The catabolic process in IVDD is thought to be mediated by several cytokines: IL1β, IL6, IL8, IL10, and TNFα (Hansen, 1951; Lotz, 2004). The biochemistry of IVDD indicates that enzymatic activity contributes to this disorder, with increased fragmentation of the collagen, PG and fibronectin populations.

Several families of enzymes are capable of breaking down the various matrix molecules of IVD, including cathepsins, MMPs and aggrecanases; they may be produced by the cells of the IVD themselves as well as by the cells of the invading blood vessels (Eyre and Muir, 1977; Roberts et al., 2000; Ariga et al., 2001).
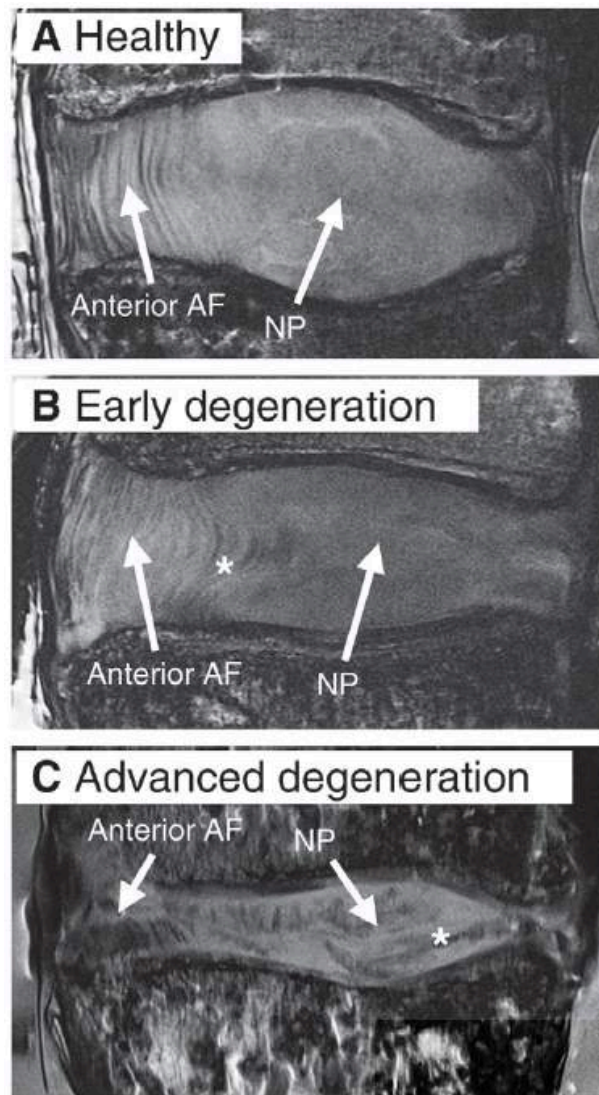
Figure 10. Magnetic resonance images illustrating different stages of human lumbar disc degeneration. (A) A healthy disc exhibiting distinct AF lamellae (AF) and central NP region (NP). (B) A disc exhibiting early stages of degeneration, inlcuding moderate height reduction, decreased NP signal intensity and inward bulging of AF lamellae (*). (C) A disc exhibiting advanced stages of degeneration, including severely reduced height, large fissure (*) and generalized structural deterioration. Images obtained using 7T Siemens scanner and a turbo spin echo sequence at 200 μm isotropic voxel resolution.

- ***AETIOLOGY OF DISC DEGENERATION***

Several mechanisms have been postulated to be involved in IVDD, however a clear understanding of the basic mechanisms of its pathogenesis and specific therapeutic agents is still lacking. Unquestionably, IVDD is a multifactorial process influenced by genetics, lifestyle conditions (e.g. obesity, occupation, smoking and alcohol consumption), biomechanical loading and activities, and other health factors (e.g. diabetes, aging) (Ariga et al., 2001; Boos et al., 2002; Gruber and Hanley, 2002; Lotz et al., 2002; Roughley et al., 2002; Ferguson and Steffen, 2003).

Nutritional pathways to IVDD – The pathway from the blood supply to the NP cells is precarious because these cells are supplied virtually entirely by capillaries that originate in the vertebral bodies, penetrating the subchondral plate and terminating just above the cartilaginous EP (Urban et al., 1978; Crock et al., 1991). Nutrients must then diffuse from the capillaries through the cartilaginous EP and the dense ECM of the NP to the cells. Considering that, like all cell types, IVD cells require nutrients such as glucose and oxygen to remain alive and active, failure of the nutrient supply has been proposed to be one of the primary causes of IVDD (Nachemson et al., 1970). *In vitro*, it has been demonstrated that IVD cells activity (ECM synthesis) is very sensitive to low extracellular oxygen and acidic pH (Ishihara and Urban, 1999; Ohshima and Urban, 1992), and that cells do not survive prolonged exposure to low pH or glucose concentrations (Horner and Urban, 2001). Several factors have been reported to affect the nutrient supply to the NP. Sclerosis of the subchondral bone is a well known characteristic of IVDD (Thompson et al., 1990). Atherosclerosis (Kauppila et al., 1997a; Kauppila, 1997b), sickle cell anaemia, Caisson disease and Gaucher's disease all appear to lead to a significant increase in IVDD, due to impaired blood supply to the vertebral body. Long-term exercise or lack of it appears to have an effect on diffusion of nutrients into the IVD, and thus on their concentration in the tissue (Holm and Nachemson, 1982; Holm and Nachemson, 1983). The mechanism is not known but could be related to an alteration of the architecture of

the capillary bed at the disc-bone interface. Finally, even if the blood supply remains undisturbed, nutrients may not reach the IVD cells if the cartilaginous EP calcifies or becomes sclerotic (Nachemson et al., 1970; Roberts et al., 1993; Roberts et al., 1996), due to a decreased subchondral bone's permeability (Holm and Nachemson, 1988; Urban et al., 2001).

Mechanical load and injury – Epidemiologic data suggest an associaton between spinal force and IVDD. In attempt to understand mechanisms for this phenomenon, several animal models have been reported where forces across the normal IVD are altered. While regular loading of the IVDs is assumed to be essential for maintaining a normal phenotype of IVD cells, excessive and repetitive loading can lead to the biochemical and radiological changes that are associated with IVDD (Sztrolovics et al., 1997; Eyre et al., 2001). Both occupational loading of the lumbar spine and obesity have been reported to increase the risk of IVD degeneration; instead, intense exercise does not appear to affect IVDs adversely (Puustjarvi et al, 1993) and IVDs are reported to respond to some long-term moderate loading regimens by increasing PG content (Iatridis et al, 1999). Further support for the role of abnormal mechanical forces in IVDD comes from findings that disc levels adjacent to a fused segment tend to degenerate more rapidly (Eck et al., 1999).

Genetic factors in IVDD – Although genetic factors by themselves are not a cause of disease, IVDD seems to have a strong genetic background (Ghosh et al., 1976; Silberberg, 1988). Several studies have reported familial predisposition for IVDD and herniation (Heikkila et al., 1989; Varlotta et al., 1991; Matsui et al., 1998). MRI twin studies have shown that the hereditability of low back pain ranges between 52%-81% (Eijkelkamp et al., 2002).

○ DISCOGENIC PAIN

The mechanisms for the provocation of discogenic pain have been associated to five main different causes:

1. stretching of the fibers of an abnormal AF;

2. extravasation of extradurally irritating substances such as glycosaminoglycans, lactic acid, and acidic media;

3. pressure on nerves posteriorly caused by bulging of the AF;

4. hyperflexion of posterior joints on disc injection (during discography) (Wiley et al., 1986);

5. presence of vascular granulation tissue, with pain caused by scar distension (Heggeness and Doherty, 1993).

The pathways for discogenic pain are still very controversial. The spreading of sensory nerve endings into the inner layers of the AF, the EPs and NP during the degenerative process seems to play an important role in the development of discogenic pain (Coppes et al., 1997; Freemont et al., 1997; Freemont et al., 2002; Hurri and Karppinen, 2004; Peng et al., 2005; Peng et al., 2006; Peng et al., 2009; Freemont et al., 2009). Indeed, as a consequence of annular fissure and tears formation, chronic pain may occur if the outermost third of the AF is involved. Furthermore, smaller insults within the IVD with repeated small extravasation of proinflammatory nuclear material lead to sensitization of nerve endings and pain. The release of inflammatory mediators from the nuclear material onto neural structures within the spinal canal is believed to promote the development of radicular pain as a result of IVD herniation (Rea et al., 2012). Herniation-induced pressure on the nerve root is not the only cause of pain because more than 70% of "normal", asymptomatic people have disc prolapses pressurizing the nerve roots but no pain (Boden et al., 1990; Boos et al., 1995). A hypothesis is that, in symptomatic

individuals, the nerves are somehow sensitized to the pressure (Cavanaugh, 1995), possibly by molecules arising from an inflammatory cascade from arachidonic acid through to prostaglandin E_2, thromboxane, phospolipase A_2, TNF-α, the interleukins and matrix metalloproteinasis (MMPs) (Kang et al., 1996). These molecules can be produced by cells of herniated IVDs, and because of the close physical contact between the nerve root and IVD following herniation they may be able to sensitize the nerve root (Kawakami et al., 1996; Olmarker et al., 2002).

Analyzing the innervation pattern, which has been described previously, it is possible to observe that the presence of the left-right connections in the nerve plexuses suggests that lateralized disorders, in which nociceptive stimuli reach the spinal cord via sinuvertebral nerve from the other side, can cause pain at the side that is controlateral to its origin. Another implication is that the majority of spinal structures, including the IVDs, are innervated multisegmentally (Groen et al., 1990). Via the mechanism of deep somatic referred pain, this innervations pattern lead to an overlap in distribution of referred pain areas from adjacent structures. As a result, the pain projections are not always reliable for determining the source of the pain. Traditionally, pain signals that originate in the nerve roots adjacent to the IVD move from that root, into the corresponding dorsal root ganglion and into the spinal cord (Figure 11A). However, has been suggested that pain signals from the lower lumbar IVDs (L4 and L5) are detoured up the sympathetic nerves (gray ramus communicans) and into the upper lumbar dorsal root ganglions—especially at the L2 level (Figure 11B) (Oh and Shim, 2004; Morinaga et al., 1996; Ohtori et al., 1999). Therefore, it would be possible that some patiens with L4 and L5 IVD pathology, manifest L1 or L2 dermatomal pain (groin and anterior thigh pain).
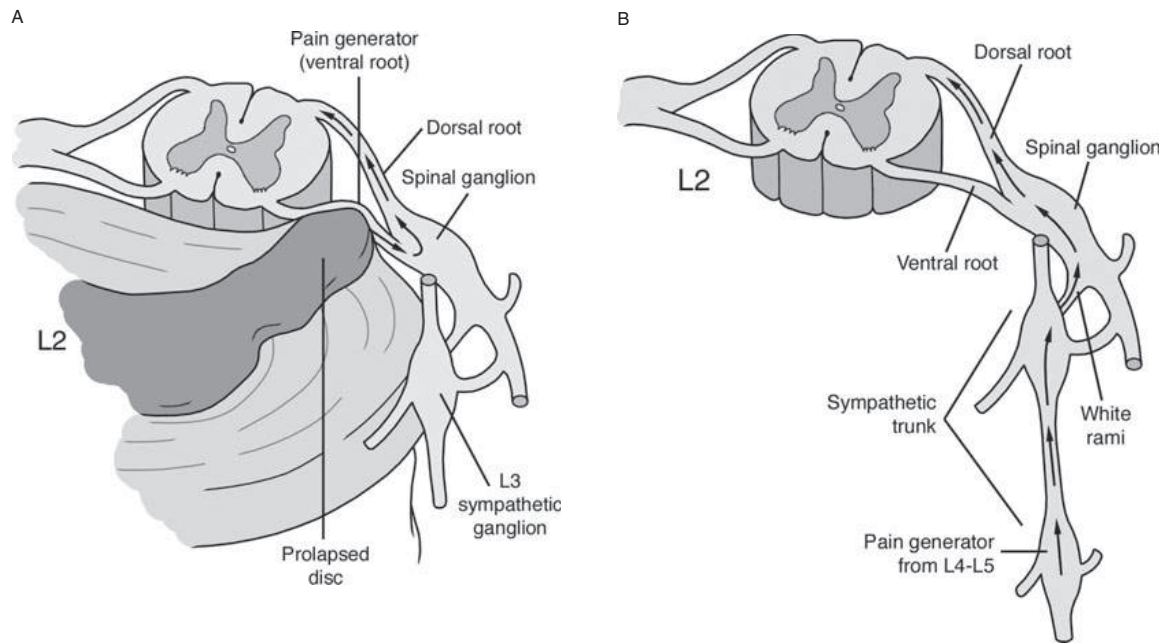
Figure 11. Pain pathways for discogenic pain. **(A)** Pain signals that generate from the IVD traverse pass into the corresponding dorsal root ganglion and into the spinal cord. **(B)** Pain signals from the lower lumbar IVDs (L4-L5) detour up the sympathetic nerves (grey ramus communicans) into the upper lumbar dorsal root ganglion, especially at the L2 level (Raj, 2008).

o **HISTOLOGIC AND MRI CLASSIFICATION OF IVDD**

▪ *THOMPSON GRADING SCALE*

A fine-category grading scheme for assessing the gross morphology of midsagittal sections of the human lumbar IVD has been developed by Thompson et al. (1990) (Table 2). The scheme has been applied to IVDs sectioned in midsagittal plane and permits to observe all four tissues of the IVD: NP, AF, EP and adjacent vertebral bodies, providing a valid overall assessment of the tissue.

Table 2. Description of morphologic histologic grades

Grade	NP	AF	EP	Vertebral body	Histology
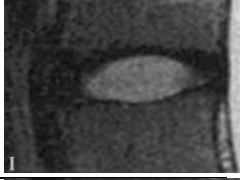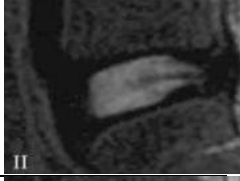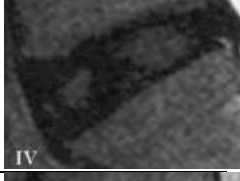
I	Bulging gel	Discrete fibrous lamellas	Hyaline, uniformly thick	Margins rounded	
II	White fibrous tissue peripherally	Mucinous material between lamellas	Thickness irregular	Margins pointed	
III	Consolidated fibrous tissue	Extensive mucinous infiltration; loss of anular-nuclear demarcation	Focal defects in cartilage	Early chondrophytes or osteophytes at margins	
IV	Horizontal clefts parallel to EP	Focal disruption	Fibrocartilage from subchondral bone, irregularity and sclerosis in subchondral bone	Osteophytes less than 2 mm	
V	Clefts extend through NP and AF		Diffuse sclerosis	Osteophytes greater than 2 mm	

- *PFFIRMANN GRADING SCALE*

A morphologic grading system relating to the MRI pathologic changes in the lumbar IVDs has been developed by Pfirrmann et al. (2001) (Table 3). This MRI grading system is based on a gross morphology grading scheme and evaluates, on sagittal T2-weighted (T2w) images, variations in MRI signal intensity, IVD structure, distinction between NP and AF, and IVD height. Degeneration of the NP and the anatomical structure of the IVD itself is readily seen in T2w sagittal images of the spinal column. Normal hydrated NP has a hyperintense signal compared to the AF. As the NP loses hydration, the signal becomes less intense and may appear iso- or hypointense relative to the AF.

Table 3. MRI classification of disc degeneration (Pfirrmann et al., 2001)

Grade	Structure	Distinction NP/AF	Signal intensity	Height of IVD	MRI

I	Homogeneous, bright white	Clear	Hyperintense, isointense to CSF	Normal	
II	Inhomogeneous with or without horizontal bands	Clear	Hyperintense, isointense to CSF	Normal	
III	Inhomogeneous, gray	Unclear	Intermediate	Normal to slightly decreased	
IV	Inhomogeneous, gray to black	Lost	Intermediate to hypointense	Normal to moderately decreased	
V	Inhomogeneous, black	Lost	Hypointense	Collapsed disc space	

The signal intensity of the IVD on T2w images correlates with the progressive degenerative changes of the IVD (Modic et al., 1988) and the brightess of the NP has been shown to correlate directly with the PG concentration, but not with the water or collagen content (Pearce et al., 1991). The DH is important mainly for distinguishing between Grades IV and V, while for Grades III and IV, the DH is not a discriminative feature.

o **CURRENT TREATMENT OPTIONS: MEDICAL / SURGICAL**

Current treatments for IVDD still remain a subject of debate. Conservative therapy of chronic low back pain may involve a vast group of treatment modalities, such as physiotherapy, analgesic and anti-inflammatory medications, acupuncure and chiropractics (Mirza and Deyo, 2007). Approximately 75-90% of all chronic low back pain patients obtain satisfactory results with conservative treatment (Burkus et al., 2004; Smith et al., 2011; Highes et al., 2012; Ludwinski et al., 2012). Analgesia, such as non-steroidal

anti-inflammatory drugs and muscle relaxants are very effective for both acute and chronic pain (Pye et al., 2004; Ludwinski et al., 2013). In the patients that remain symptomatic surgery becomes an option (Blummenkrantz et al., 2004). The two main surgical treatment alternative for IVDD are spinal fusion and the placement of an IVD prosthesis. Despite spinal fusion is considered the gold standard (Radin et al., 1986; Blummenkrantz et al., 2004), the results of three randomized controlled trials, which compared spinal fusion with conservative treatment, showed substantial clinical improvement in only a limited number of patients (Diamant et al., 1986; Thompson et al., 1990; Nguyen-minh et al., 1998; Haefeli et al., 2006). Furthermore, spinal fusion could accelerate the degenerative process in adjacent levels (Wang et al., 2007; Rutges et al., 2010) and it seeks only to alleviate painful symptoms without restoring disc mechanics and structure. Implantation of an IVD prosthesis (disc arthroplasty) has been introduced more recently to restore mobility. Randomized controlled trials, where prosthesis has been compared with spinal fusion, revealed comparable results with both techniques (Sandtrom, 1951; Radin et al., 1986; Feinberg et al., 1990; Prescher, 1998; Drissi et al., 2005). This technique has been reported to provide a statistically better clinical outcome when compared to conservative treatment (Huang et al., 2008), although with minor improvement; therefore, the peri-operative risks and possible complications do not out-weight these limited benefits of total disc prosthesis placement (Huang et al., 2008). Furthermore, disc arthroplasty do not reestablish the mechanical function of the native joint, is subject to wear and failure, and resection is a complex surgical procedure (Hanley et al., 2010).

Current surgical treatment strategies for chronic low BP yield far from optimal results and there is, therefore, a strong need for therapies that both alleviate painful symptoms and restore IVD structure and mechanical function by directly addressing the underlying biological causes of IVDD.

o **NOVEL THERAPEUTIC APPROACHES**

The aim of therapeutic approaches for IVDD is both to alleviate painful symptoms and to restore mechanical function. Depending on the stage of degeneration during which treatment strategies are designed to act, they can be classified as regenerative or reparative. In general, in the early stage of IVDD (grades II-III, Figure 12), protein factors such as growth factors or proteinase inhibitors may be effective. In the intermediate stage of degeneration (grade IV), cell or gene therapy may be required; in the advanced stage of IVDD (grade V, Figure 12), tissue engineering approaches are needed (Zhang et al., 2011).

▪ *REGENERATIVE STRATEGIES*

Regenerative strategies for the treatment of IVDD are focused on reviving or healing extant IVD tissue. This can be done either by altering the phenotype of cells native to the degenerate IVD or by introducing new cell populations (Smith et al., 2011).

Injections of **growth factors** into the IVD has been widely studied as a means to stimulate extracellular matrix production and cell proliferation (Masuda, 2008). Despite succesfull results obtained in certain animal models of IVDD (Masuda, 2008), the translation of such treatments to human application and clinical use is hampered by the inability to accurately recreate the progressive, life-long degenerative transformation of the disc in an animal model (Alini et al., 2008). Moreover, the potential success of anabolic factors injected directly into the disc might be limited, both owing to the short biological half-life of the factors and their rapid diffusion away from the delivery state (Smith et al., 2011).

Alternatively, cell populations within the IVD can be manipulated through **gene therapy** approaches, which involve the delivering of genes into cells through viral-vector-mediated gene transfer (Sobajima et al., 2004). The NP represents a promising site for gene introduction, as its avascular encapsulated nature can protect the vector form body's

own immune system, preventing damaging immune reaction against the transfected cells and prolonging gene expression (Kalson et al., 2008). Questions remain as to the best method for gene delivery (Wallach et al., 2006). Adenoviruses are currently the most commonly used vector owing to their high transfection rate, although safety concerns preclude their use in clinical trials. Alternatives are represented by non viral vectors such as the gene gun or liposomes, which deliver the gene as an episome into the host cell cytoplasm (Wells, 2004). These methods have the disadvantage of reduced duration of gene expression and lower transfection success rate.

Finally, a more recent regenerative approach under investigation is **cell therapy**, whereby cells are delivered locally to the degenerated IVD. The purpose of these cells is to either provide signaling cues that ameliorate the effects of *IVDD*, or adopt and/or maintain disc-like phenotypes themselves, producing extracellular matrix intended to re-establish healthy disc function (Sakai, 2005; Leung et al., 2006).

▪ *REPAIR STRATEGIES*

Reparative strategies are focused on, either augmenting or replacing degenerate IVD tissue to re-establish healthy IVD function. In IVDs with higher grades of degeneration (grade IV-V) (Figure 12), the number of cells responsive for example to growth factor stimulation diminishes (Zhang et al., 2011). In this setting, has been recently observed an increased interest in the tissue engineering approach. Cell therapy and cell-based gene therapy may be useful treatment strategies at most advanced stages of IVDD (grade V) (Figure 12), with the aim of restoring the IVD function (Zhang et al., 2011). The appeal of tissue engineering strategies is that, unlike non-biological materials that can wear with time, cell-generated tissues retain their capacity for remodeling and growth. A cell therapy approach has been described using different type of cells such as IVD cells, cartilaginous chondrocytes, and progenitor cells.

Autologous IVD cell transplantation are currently under clinical investigation, and two-year follow-up has shown a decrease of BP and prevention of IVD narrowing. However, this approach is limited by the poor expansion rates or the loss of phenotypic characteristic when expanded in monolayer cell culture, and it is applicable only when discectomy is required (Meisel et al., 2002; Meisel et al., 2006).

Autologous articular chondrocytes are phenotypically similar to IVD cells and can be obtained from non-weight bearing areas of the knee without significant donor site morbidity (Brittberg et al., 1994). Hydrogels sich as alginate-, collagen-, and hyaluronan-based gels, among others, have been shown to support the survival of mature NP cells and to be conducive to ECM deposition (O'Halloran and Pandit, 2007). However, although NP tissue engineering has been a particular focus over the years, interest has more recently turned to the AF and to whole IVD composite tissues (Bowles et al., 2010; Mizuno et al., 2006; Nerurkar et al., 2010; Nesti et al., 2008).

Adult stem cells are self-renewing cells that, because of their ability to differentiate into different cell types and to secrete a range of cytokines, have received considerable interest and shown promise in respect of treating chronic conditions such as IVDD. The potential use of different adult stem cells has been described for IVD regeneration, and recent studies have demonstrated that bone marrow mesenchymal stem/stromal cells (MSCs) therapies might be a feasible and effective approach to prevent and cure IVDD (Sakai et al., 2006). *In vivo* studies have demonstrated proof of efficacy of MSCs transplantation in reproducible animal models in terms of enhanced PG content, DH and hydration (Sakai et al., 2006). Therefore, adult stem cell therapy may be considered a powerful tool in the future treatment of IVDD. If stem cell therapy is convenient for the low harvest site morbidity, ease of *ex vivo* cell expansion, and favorable modulation of the cell phenotype before or after transplantation, many open questions remain in the translation of this new cell therapy in the medical arsenal, such as the most

reliable transplantation method including the surgical route to approach the IVD, the carrier choice and the optimal cell dose.
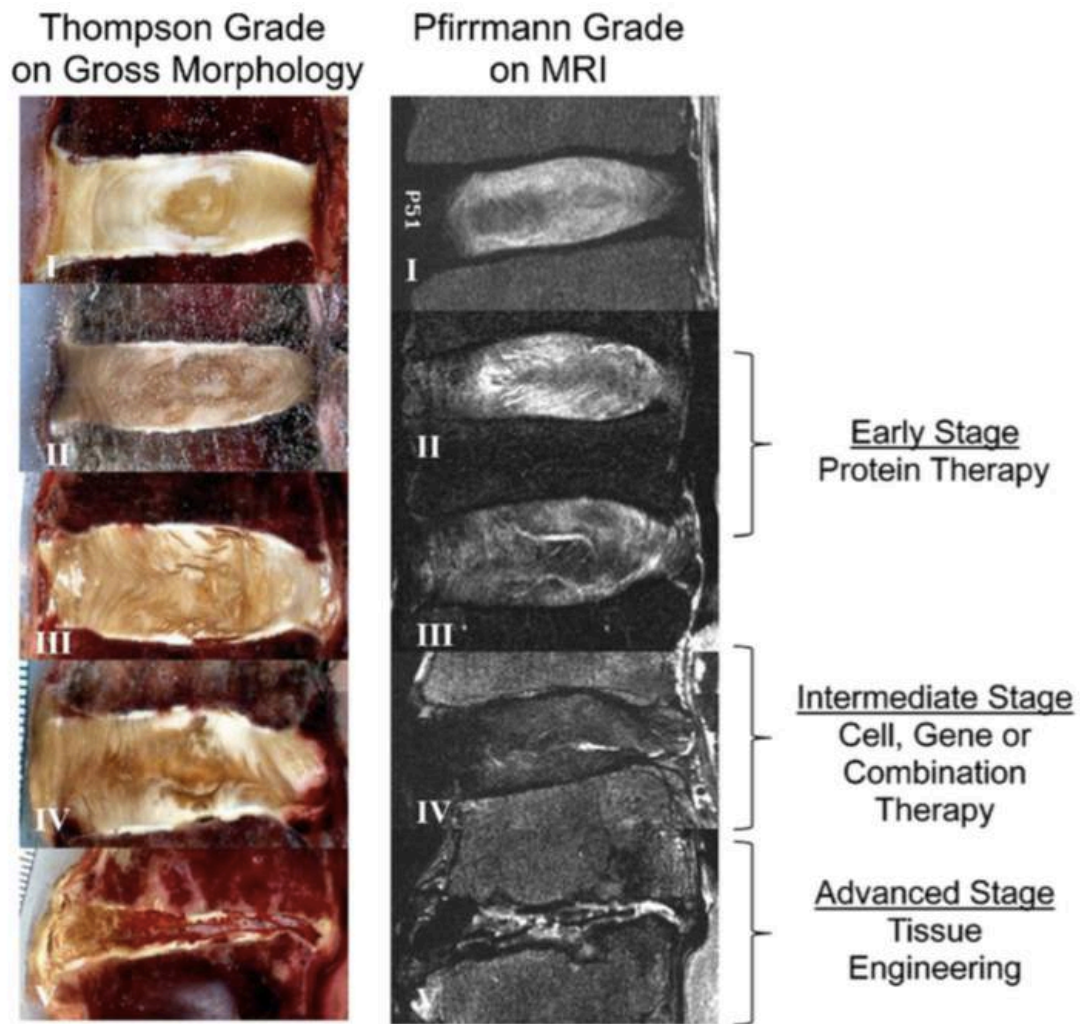
Figure 12. Human IVD with different degrees of degeneration classification according to the Thompson grading scale and Pfirrmann grading scale (Zhang et al., 2011)

o **ANIMAL MODELS**

Animal models are essentials in making the transition from scientific concepts to clinical applications. The scarse availability of primary human degenerate disc tissue, and the almost non-existence of healthy tissue for comparison in *in vitro* studies, means that model systems, despite their limitations, are indispensable for investigating the molecular and cellular pathways that maintain healthy IVDs and that characterize the degenerative cascade (Smith et al., 2011).

Certain fundamental principles must be followed for an animal model to be effective. The animal model must be ethical, controllable, reproducible and cost-effective and must adequately model the human pathologic process that is under investigation.

Ethical issus are always of concern. The Animal Welfare Act and the Public Health Service Animal Welfare Policy require that an Institutional Animal Care and Use Committee review and approve each protocol. The use of appropriate technologies to eliminate or reduce pain and to humanely euthanize the animals is required. The use of the minimum number of animals from which significant conclusions can be inferred is not only ethically necessary but also cost-effective. In addition, the species selected should be carefully chosen with serious consideration given to all applicable federal regulations, Public Health Service Policy and institutional policies (Singh et al., 2005).

The degree of IVDD obtained in an animal model should be controllable and selectable to aid the researcher in proving the hypothesis. The validation of the reproducibility of an animal model allows results from different scientific researchers to be compared. Furthermore, for validation, the interobserver variability of outcome measures should be fully studied. If a surgical technique or other environmental change is used, the procedure should be standardized in detail to increase the transferability of models to other groups (Singh et al., 2005).

The time period required to generate IVDD and the size of the animal used are other factors related to cost-effectiveness. The cost and availability of a specific strain of animal, the housing and husbandry requirements and the ease of handling by researchers and animal technicians are other factors to be taken into consideration. Generally, animal models of IVDD that use species higher in the phylogenetic tree and less invasive procedures show a slower progression. However, although these models are desirable to study the natural course of IVDD, the associated costs can be prohibitive. Ultimately, the selection of the proper animal model of IVDD depends on the stage of development of the investigational drugs or devices (Singh et al., 2005).

Most important, the animal model must be similar in nature to the human pathologic process that it is intended to mimic. Otherwise, conclusions made from dissimilar animal and human pathologic states may not be clinically appropriate (Singh et al., 2005).

The development and application of model systems in which to study the pathogenesis of IVDD and evaluate associated treatments is extremely challenging (Alini et al., 2008), due to the natural slow progression of the condition, multifactorial underlying causes and a poor understanding of the circumstances under which degenerative changes are associated with painful symptoms.

In vivo, animal models are important to study how degeneration evolves over time either spontaneously or following experimental injury, and to determine how constitutive, environmental, or biomechanical risk factors may initiate, promote, or otherwise regulate these changes (Lotz, 2004). Animal models are also needed to show how therapeutic strategies may ameliorate, resolve, or prevent IVDD. These models can be classified as either experimentally induced or spontaneous (Table 4) (Lotz, 2004). In IVDD research, experimentally induced models can be further subdivided into mechanical or structural perturbations. Mechanical perturbation is the alteration of the magnitude or distribution of forces on the normal joint. By contrast, structural models perturb tissue functioning by means of injury or chemical alterations. Spontaneous models include animals that develop IVDD naturally in a systematic fashion, including those that have been genetically altered or specially bred to develop this condition (Hansen, 1951; Gruber et al., 2002).

Table 4 *In vivo* animal models used to study disc degeneration (Alini et al., 2008).

Model type	Animal	Stimulus	References
Spontaneous	Mouse	Pintail mouse-genetic	Berry, 1960
	Mouse	Cmd aggrecan knockout	Watanabe et al., 1997; Watanabe and Yamada, 2002
	Mouse	Inherited kyphoscoliosis	Mason and Palfrey, 1984
	Mouse	Collagen II mutation	Sahlman et al., 2001
	Mouse	Collagen IX mutation	Kimura et al., 1996
	Mouse	Myostatin knockout	Hamrick et al., 2003
	Mouse	HLA-B27 transgenic spondylolisthesis	Weinreich et al., 1995
	Mouse	Defect at ank locus, ankylosing spondylitis	Sweet and Green, 1981
	Mouse	twy mouse—IVD calcification and ankylosis	Furuya et al., 2000
	Rat	HLA B27 transgenic, spondylolisthesis	Hammer et al., 1990; Taurog et al., 1999
	Sand rat	Accelerated ageing	Moskowitz et al., 1990
	Dog	Chondrodystrophy	Braund, 1974
	Baboon	Ageing	Lauerman et al., 1992
Structural (induced)			
Chemical			
	Rat		Norcross et al., 1991
	Rabbit	Chondroitinase ABC	Ando et al., 1995
	Dog		Yamada et al., 2001
	Rabbit	Fibronectin fragments	Anderson et al., 2003
	Dog	Chymopapain, krill proteases	Melrose et al. 1995; Melrose et al., 1996; Suguro et al., 1986
Antigen induced inflammation	Mouse (BALB/c)	Immunized with aggrecan and/or versican, develops spondylitis	Shi et al., 2003, Mikecz et al., 1987; Glant et al., 1987
Mechanical			
Disc compression	Rabbit	Static compression	Kroeber et al., 2002
	Pig	Compression injury, lumbar spine and caudal disc compression	Lundin et al., 1998; Lundin et al., 2000
Bipedal	Mouse, rat	Amputation of upper limbs and tail	Higuchi et al., 1983; Cassidy et al., 1988
EP damage	Pig	EP perforation	Holm et al., 2004
Hyperactivity (running)	Dog	Long distance running training	Puustjarvi et al., 1993; Puustjarvi et al., 1994; Saamanen et al., 1993
Fusion	Dog		Cole et al., 1985 a,b
	Rabbit	Lumbar arthrodesis	Phillips et al., 2002
	Sheep		Foster et al., 2002
Spinal distraction	Rabbit	Controlled dynamic distraction	Kroeber et al., 2005
Spinal instability	Mouse	Resection of spinous processes, Resection of facet joints	Ariga et al., 2001; Peng et al., 2001
	Rabbit		Stokes et al., 1989
	Pig		Kaigle et al., 1995
	Rabbit	Bilateral facet joint resection at L7S1 and rotational anipulation	Osterman and Osterman, 1996
	Rat	Facetectomy/capsulotomy torsional lumbar injury	Latorre et al., 1998
	Rabbit		Hadjipavlou et al., 1998b
	Rabbit	Distraction, rib resection and spinal rotation	Thometz et al., 2000

	Rabbit	Surgical narrowing of intervertebral neural foramen, vibrational stimulation of dorsal root ganglia	Pedrini-Mille et al., 1990
Disc lesions	Rabbit	Full depth anterior annular stab	Lipson and Muir, 1980; Lipson and Muir, 1981
	Rabbit	Multiple 5 mm stab incisions using 16, 18 or 21G needles	Kim et al., 2005 a,b, Masuda et al., 2005; Sobajima et al., 2005
	Rabbit	NP removal	Urayama, 1986
	Rabbit	Surgical resection of NP	Takaishi et al., 1997
	Sheep	3–5 mm outer anterolateral annular incision (rim-lesion)	Osti et al., 1990a; Melrose et al., 1992; Melrose et al., 1997 a,b,c; 1997; Melrose et al., 2002 a,b
	Sheep	Circumferential annular tear (delamellation)	Fazzalari et al., 2001; Thompson et al., 2004
	Pig	5 mm outer annular incision	Kaapa et al., 1994; Kaapa et al., 1995
	Dog	Full depth posterior annulotomy	Olsewski et al., 1996
Chronic AF, NP, facet joint lesion model	Pig	Combined lesions in AF, NP, facet joint and capsule	Kaigle et al., 1997
Pinealectomy models of scoliosis	Chicken	Pinealectomy	Cheung et al., 2003; Machida et al. 1993; Machida et al., 1995
	Rat	Pinealectomy + bipedal	Machida et al., 1999

o SHEEP MODEL IN SPINE RESEARCH

Sheep have been widely used as models in spinal research and several comparative studies have indicated the adequacy of this species as a model for IVD research questions due to specific biologic, anatomical and biomechanical characteristics similar to those present in human spine. (Wilke et al., 1997a; Wilke et al., 1997b, Kandziora et al., 2002; Reid et al., 2002; Smit, 2002; Hunter et al., 2004; O'Connell et al., 2007; Melrose et al., 2009; Schmidt et al., 2013).

Notochordal cells - In sheep as in humans, NCs predominate in the very young NP, their number decreases very rapidly after birth and no NCs are present by adulthood (Trout et al., 1982a; Trout et al., 1982b; Hunter et al., 2003). This is important because IVDs exhibiting NCs may respond differently to a degenerative stimulus than IVDs without NCs (Alini et al., 2008). As mentioned previously, NCs represent a completely different cell type in terms of morphology and function to the cells populating the adult NP (Hunter et al., 2004), and their disappearance seems to precede the onset of IVDD (Hunter et al., 2003).

Microscopic anatomy - Several microscopic IVD features have been described in sheep, demonstrating important analogous results to what has been reported in humans. Indeed, the water and collagen content of the IVD, as well as collagen fibre orientation angles, are similar in lumbar IVDs from sheep and humans (Reid et al., 2002).

A peculiar microscopic characteristic that has been identified both in sheep (Shea et al., 2001; Shea et al., 2002; Sinclair et al., 2013) and in humans (Boyce and Bloebaum, 1993; Bloebaum and Kopp, 2004) is represented by the presence of calcified fibrocartilage (CFC) in various anatomical sites. This tissue layer is also present on the vertebral EPs and shows lack of vascularization and of remodelling ability (Benjamin et al., 2000; Shea et al., 2002). Sheep can be therefore useful for translational research to observe how this CFC affects the supply of nutrients to the IVD space and how its presence may affect the outcome of spinal surgeries. Indeed, Sinclair et al. (2012) have observed that the incomplete removal of CFC during vertebral spinal fusion or total IVD replacement preparation inhibits skeletal attachment between the cortical EP and the intervertebral implant and obstruct successful fusion.

Anatomical characteristics - Anatomical variations between species are important to consider when selecting an appropriate animal model. In general, sheep spines consist of 7 cervical, 12-14 thoracic, and 6-7 lumbar vertebrae (Nickel et al., 1984); they are therefore different from human spines, which are consistently formed by 7 cervical, 12 thoracic and 5 lumbar vertebrae. Several differences and similarities in terms of shape, profile and relative sizes between sheep and human IVDs and vertebrae have been described. Sheep vertebrae are taller rather than wide, whereas human vertebrae are wider rather than tall; sheep vertebral bodies have a conic shape, whereas human vertebral bodies are cylindrical; sheep pedicles are ellipsoid, whereas human pedicle are nearly round; in the sheep spine, the cranial EP is convex and the caudal endplate concave, whereas both EPs are concave in the human spine (Wilke et al., 1997a; Kandziora et al., 2001). In humans, the antero-posterior diameter of the vertebral EPs

steadily increases from the cervical to the lumbar region, while in sheep this diameter almost stays the same over the whole spine (Wilke et al., 1997a). Therefore, compared to humans, this species has larger EP diameters in the cervical but smaller diameters in the lumbar spine. Despite the differences listed above, the trends of the two species in spinal canal width are nearly identical (Wilke et al., 1997a; Mageed et al., 2013) and similarities in the major dimensions have been reported to be strongest for the motion segment C5-C6 (Kandziora et al., 2001) and for the thoracic and lumbar regions (Wilke et al., 1997b). When comparing the macroscopic appearance of a sheep and a human motion segment, it is evident that their sizes greatly differ; in particular IVD height and endplate cross-section area of sheep IVDs are smaller than those of human (Schmidt and Reitmaier, 2013). This difference in sheep IVD size in comparison to human IVD may influence results interpretation (Elliott and Sarver, 2004); in fact size affects rates of biologic processes (West et al., 1997) and is influenced by competing biomechanical (Nakatsukasa and Hirose, 2003) and nutritional (Horner and Urban, 2001) demands. However, radiographic evaluation of IVD space height (IVD-SH) has shown an average of 6 mm in the sheep cervical spine, which is only approximately 1 mm (15%) higher than the IVD-SH in the human cervical spine (Kandziora et al., 26). In the lumbar spine, differences in intervertebral IVD-SH are higher (Wilke et al., 1997a; Green et al., 1993; Nachemson et al., 1979). Therefore, with regard to IVD-SH, the sheep cervical spine may represent a better model for human studies than sheep lumbar spine.

Biomechanical properties - Although the several variations of anatomical shapes and dimensions listed above influence the biomechanical behavior of the spinal segments, *in vivo* and *in vitro* studies have indicated that sheep may represent a valid model in spinal research. Sheep spinal range of motions (ROMs) present smaller absolute values in particular in flexion/extension of the lumbar spine, however the ROMs of sheep spines for different loads directions (flexion/extension, axial rotation right/left, lateral bending right/left) are qualitatively similar in their cranio-caudal trends to those of human

specimens reported in the literature (Ahlgren et al., 1994; Oxland et al., 1992; Panjabi, 1988; Panjabi et al., 1994; Wen et al., 1993; Wilke et al., 1995). Further similarities between sheep and humans are related to the relative DH loss and internal NP pressure after compression tests (Schmidt et al., 2013). It is nevertheless important to underline that differences in compressive forces are present between the two species; therefore, for example, pedicle screw systems and interspinous implants can be transferred from animal model to human but neither magnitude of the effect nor the statistical results can be compared.

Loading on the spine and IVDs - Another important aspect that needs to be considered is the fact that sheep are quadrupeds therefore, their spines supposedly are subjected to loads that differ considerably from those in humans (Bogdanffy et al., 1995; Frick et al., 1994; Goel and Gilbertson, 1997; Herkowitz, 1994; Robin and Stein, 1975; Yoganandan et al., 1996). In humans, the weight of the upper body acts on the lumbar spine, therefore the loading of the lumbar spine is often assumed to be larger than in quadrupeds. This, however, may not be correct since additional tensile forces from muscle contraction and tension of passive structures such as ligaments are necessary to control the posture of a quadruped spine as it cannot withstand substantial bending moments (Smit, 2002; Wilke et al., 2003). A finite element study has shown that the stress distributions in ovine and human motion segments under physiological loads are similar, thus strengthening the justification for their use as *in vivo* models for the study of the spine (Schmidt and Reitmaier, 2013). Furthermore, Smit (2002) demonstrated that quadrupeds' spine is mainly loaded by axial compression and that trabecular distribution in the vertebral bodies courses horizontally between their caudal and cranial EPs, implying that the main load within the vertebral body is indeed an axial compression force, as well as in human spine. An important point of difference, however, is that sheep are subjected to higher axial compression stress than humans (Smit, 2002), leading to a bone mineral density in the vertebrae up to fourfold higher than in humans (Wilke et al., 1996). Although

these differences should be considered on the transferability of the results of animal experiments, Kandziora et al. (2001) did not find significant differences between the bone mineral density value of human and sheep lower cervical spine, which therefore represents a suitable model for the testing of fixation devices such as plates, screws, and interbody fusion cages (Kandziora et al., 2001).

IVD changes with age and degeneration - The age of animals used for spine research must be closely monitored as naturally occurring changes, both histological and biochemical, occur with age. Several histologic, radiologic and biochemical changes, that are generally associated with pathology in human IVDs, have also been observed in sheep (Bayliss et al., 1988; Maeda et al., 2000). For example, common features of IVDD in both sheep and humans are represented by altered metabolism and PGs synthesis by the IVD fibrochondrocytes, decreased PGs aggregation levels with hyaluronan, increased PG hydrodynamic size and relative keratan sulphate content, increased serine proteinase activity and decreased serine proteinase inhibitory protein levels (Bayliss et al., 1988; Maeda and Kokubun, 2000). However, an important variation that should be considered is related to the fact that, in the aging sheep, the composition of IVD varies with the IVD location within the spine. In fact, lower PG levels are present in IVDs at the level of the thoracolumbar and lumbosacral junction (Melrose et al., 1994).

Disc calcification is a degenerative process, which has been described to occur in the IVDs of both humans and sheep (Melrose et al., 2009; Miller et al., 1988; Feinberg et al., 1990; Cheng et al., 1996; Chanchairujira et al., 2004). The aetiology remains unknown. It is characterized by hydroxyapatite (HA) crystals deposition and a decrease in IVD PGs content and size, suggesting that IVD calcification may be involved in the IVD degenerative process in ageing IVDs. The HA deposition seems to affect mainly the transitional zone between the AF and NP (Melrose et al., 2009).

Sheep provides a useful, naturally occurring model for investigation of the aetiology and pathogenesis of HA deposition, however direct comparison with human IVD

is inappropriate due to dissimilarities in IVD calcification between sheep and humans (Melrose et al., 2009). In sheep, HA deposition is restricted mainly to the lumbar region (L4-L5; L5-L6) whereas in humans the thoracic and upper lumbar regions are predominantly affected (Taylor et al., 1981). In sheep, IVD calcification seems to be secondary to a degenerative process whereas histological studies have indicated that metaplasia is the event, which leads to this form of calcification in humans (Depalma and Kruper, 1961; Uhthoff et al., 1976).

- ### *SURGICAL AND MRI ANATOMY OF THE OVINE LUMBAR SPINE*

A variation concerning the number of lumbar vertebrae is normal in the ovine species, as they can be either 6 or 7 (Lori et al., 2005). The curvature of sheep spine has a kyphotic shape (Barone, 2004). The vertebral body heights commonly exceed 40 mm (mean 42.49, SD 2.36) whilst DHs are usually only 4-5 mm (mean 4.48, SD 0.66) (Wilke et al., 1997). The IVDs and EPs appear as bulbous convex expansions in between concave elongated vertebral bodies. The tip of sheep transverse processes are large and easily palpable, and are visible in the flank region, serving as useful landmarks when performing surgery. Radicular veins and arteries run approximately 1 cm below the inferior endplates across the vertebral bodies and are variable in size and number. Muscular insertions into the lower lumbar vertebral bodies are usually thick and tendinous, whilst those higher in the lumbar spine are thin and easily divided. The spinal cord continues into the sacral region in the sheep (Baramki et al., 2000).

On MRI (1.5 Tesla) (Figure 13), the bone marrow has a characteristic distribution on sagittal T2w in all vertebrae with a zone of hyperintensity parallel to the endplate (Nisolle et al., 2013). This might be due to the characteristic presentation of secondary ossification centres that arise at the cranial and caudal aspects of the vertebral bodies, forming complete osseous plates above and below the physical plates (Alini et al., 2008). The facet joints appear as "J-shaped" lines, with the surfaces of the caudal and cranial articular processes being respectively concave and convex. The articular facet

cartilage, characterized in humans by a linear focus of high signal in T2w (synovial fluid), is not always visible in sheep due to the fact that are thin (Harnsberger et al., 2006). The ligaments appear hypointense in T2w, however only the supraspinous and interspinous ligaments can be well identified, whereas it is not always possible to differentiate the dorsal and ventral longitudinal ligaments from the low signal of the vertebral cortical bone or the AF (Harnsberger et al., 2006). This may be due to the fact that the ventral longitudinal ligament is very thin and narrow, while the dorsal ligament is thin but wider and spreading on the floor of the spinal canal (Nisolle et al., 2013). In the sheep, the ligamentum flavum is also difficult to identify by MR imaging due to the small space present between the capsule of the apophyseal joint and the junction of tha lamina with the spinous process, where the ligamentum generally extends (Nisolle et al., 2013). In high field MRI, in both T1w and T2w images, IVDs signal mirrors the water content that increases from outer to inner AF (74-82%), while the NP consists of 86% of water (Reid et al., 2002). Indeed, the moderately high signal for both NP and inner AF may be explained by these high percentages of water content. On transverse planes through the intervertebral foramen it is possible to identify the dorsal and ventral roots, the dorsal spinal ganglion and the ventral and dorsal branches of the spinal nerve. Due to the fact that in sheep the spinal cord ends at S1, a small subarachnoid space and conus medullaris are visible below the level of S1 vertebral body. Peripheral nerves can be identified in the centre of the neural foramen surrounded by hyperintense fat, with the same signal intensiy, in T1w and T2w images, of the spinal cord (Nisolle et al., 2013).
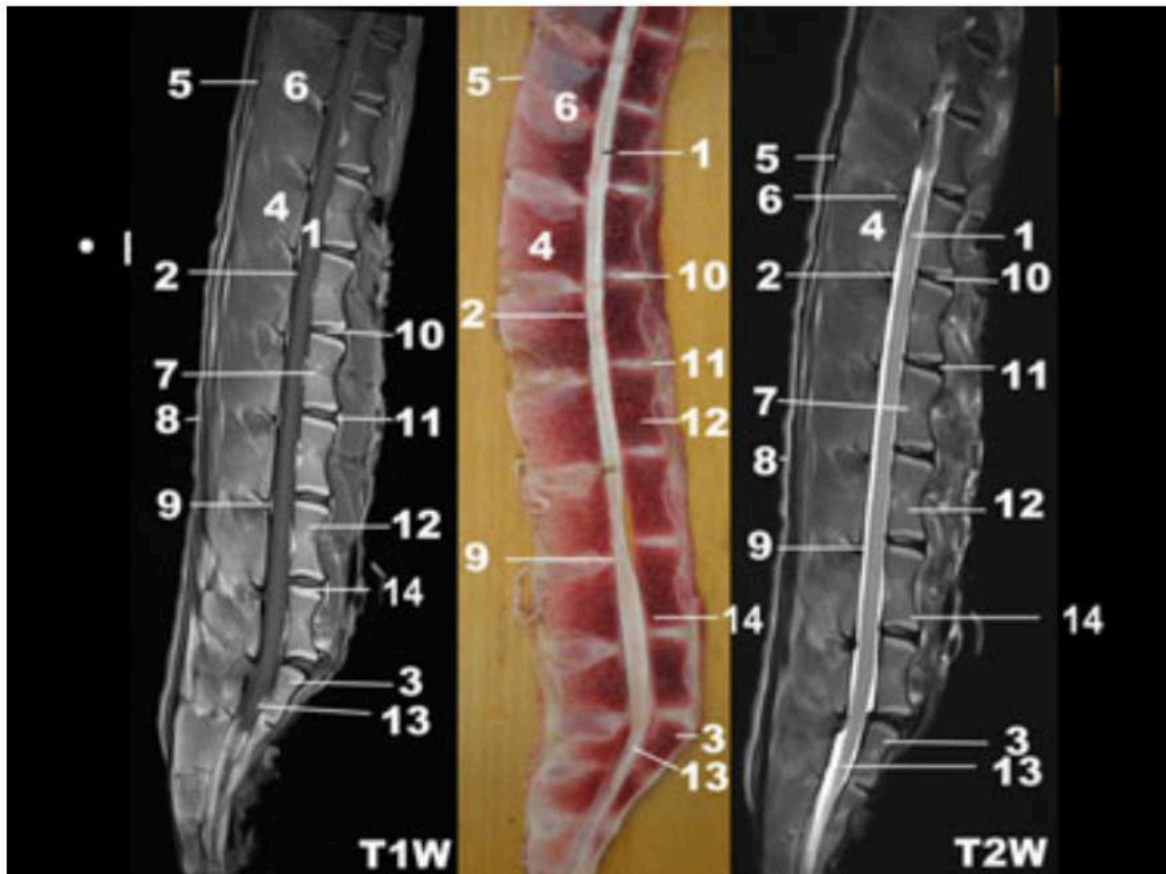
Figure 13. Sagittal view obtained at the median plane. 1. Spinal cord, 2. Cerebrospinal fluid, 3. First sacral vertebra, 4. Spinous process, 5. Supraspinous ligament, 6. Interspinous ligament, 7. Basivertebral veins, 8. Subcutaneous fat, 9. Epidural fat, 10. Nucleus pulposus and inner part of annulus fibrosus, 11. Outer part of annulus fibrosus, 12. Vertebral body, 13. End of spinal cord, 14. Vertebral plate. Note in T2w the nuclear cleft that appears as a hypointense spot in the centre of the nucleus pulposus (Nisolle et al., 2013).

o **THE TRANSPEDICULAR APPROACH**

As described above, IVD pathological changes affect all areas of the IVD. The NP is particularly affected in this degenerative process, therefore regenerative strategies are primarily focused on NP regeneration. The relatively homogeneous structure of NP tissue and its avascular compartmentalized microenvironment make easy to conceive molecular and engineering strategies toward tissue regeneration (Sowa et al., 2008). However, many issues still have to be overcome taking into account the biological, biophysical, and biomechanical environment.

Delivery of therapeutic growth factors, stem cells, and/or bioactive hydrogels for NP regeneration might be considered a straightforward task because of the easy accessibility of the NP through the AF. However, even a very modest AF injury may induce or enhance a degenerative cascade of the IVD (Elliott et al., 2008; Iatridis et al., 2009), affecting IVD biomechanics, cellularity, and biosynthesis (Korecki et al., 2008; Hsieh et al, 2009). A retrospective study, with ten years follow-up, showed how discography performed through small needle puncture resulted in accelerated IVDD, higher IVD herniation rate on the same side of the disc injection, and changes in the EP compared with matched control IVDs (Carragee et al., 2009). Furthermore, it has been recently shown on a rabbit IVDD model that the injection of MSCs into the NP through the AF route may lead to cell leakage and accelerated osteophyte formation (Vadalà et al,, 2012). Taking into account that the majority of regenerative strategies for IVD (molecular therapy, cell therapy, and biomaterial based tissue engineering) are traditionally delivered through the AF route, it should be considered that the resulting lesion might impair the expected outcomes leading to further degeneration, leakage of the biologically delivered material, and potential failure of the regenerative treatment. Therefore, alternative delivery methods and/or AF regeneration strategies have been considered.

The transpedicular approach has been recently described in a descriptive anatomical study on ovine and human cadaveric lumbar spinal segments, as an alternative route to deliver therapeutic agents to the IVD without disruption to the AF (Vadalà et al., 2013) (Figure 14).
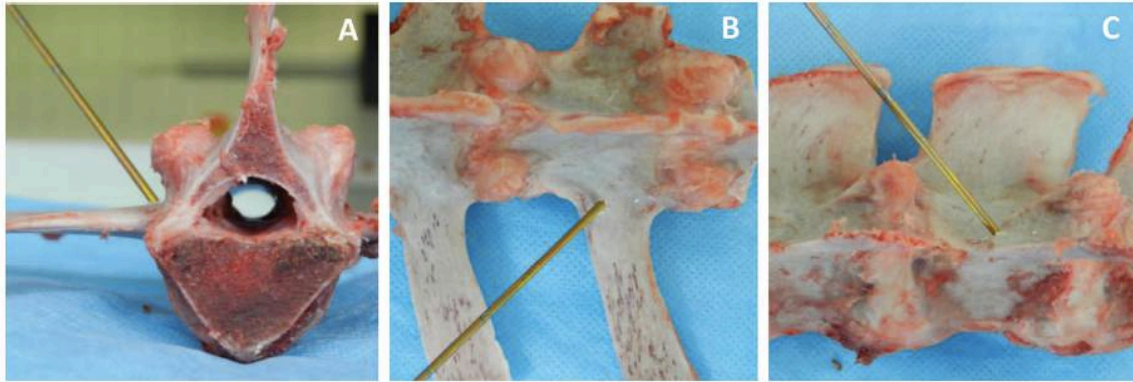
Figure 14. Representative images of the gross anatomy of the sheep spinal segments. The transpedicular technique approaches the disc through the EP, performing a tunnel through the pedicle with a specific angle. The K-wire angle to reach the center of the NP without affecting the AF is approximately 45° on coronal (A), frontal (B), and sagittal (C) planes (Vadalà et al., 2013).

The pedicle is a thin shell of cortical bone filled with cancellus bone that connects the vertebral body with the posterior arch. Despite its position close to vital neural structures, such as spinal cord and nerve roots, the pedicle can provide passage of biopsy instruments to the vertebral body, cannulae for cement injections in percutaneous vertebroplasty procedures, and screws for spinal fixation (Misenhimer at al., 1989). Furthermore, the pedicle morphology allows the insertion of instruments at various angles to assess any vertebral body lesion (Renfrew et al., 1991) or, orienting the instruments caudal to cranial, it is also possible to access the disc space (Vadalà et al., 2013). The transpedicular approach to the IVD is currently used as a way to perform biopsy and discectomy for the diagnosis and management of early discospondylitis (Figure 15), to facilitate the isolation of pathogens, natural healing, and immediate improvement of pain (Hajipavlou et al., 1998; Di Martino et al., 2012).
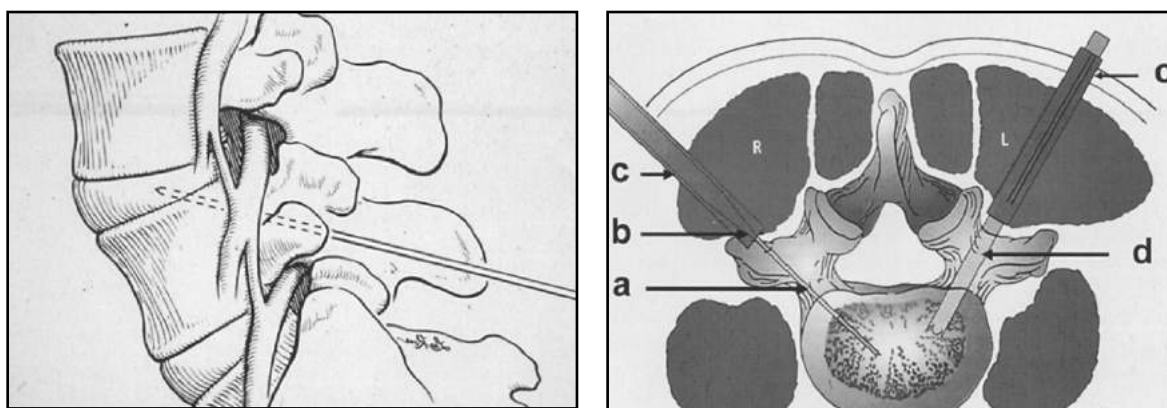
Figure 15. Lateral view of diagrammatic representation of transpedicular access at L4-L5 level that shows the guide pin introduced into the intervertebral disc space though the caudally located pedicle (A). Axial diagram illustrating the instrumentation for creating transpedicular channel for the insertion of discectomy instrumentation. A guide pin is first inserted percutaneously through the pedicle and subchondral bone into the disc space (a). Subsequently, a tissue dilator (b) is introduced over the guide pin, and over the tissue dilator, a sleeve (c) is placed to be used as a working channel. Then the dilator is removed and a toothed cutting bone tool (d) is inserted over the guide pin into the intended target (Hadjipavlou et al, 2004).

In a descriptive study (Vadalà et al., 2013) the transpedicular injection of a contrast agent demonstrated that drugs can diffuse into the whole NP tissue. Nucleotomy was obtained performing a very small diameter tunnel (2-mm) into the pedicle using an arthroscopic and/or endoscopic spine surgery device and the NP was replaced by an agarose gel. To avoid material leakage through the tunnel, biomechanical impairment, and diffusion of serum or blood cells into the disc space, a porous polyurethane biomaterial, with the ability to regenerate both bone tissue and cartilage tissue (Eglin et al., 2010), was used to seal the tunnel. Therefore, the small EP break generated by the 2-mm drill could be potentially closed/repaired by the biomaterial. The EP, which damage could trigger a degenerative cascade (Alini et al., 2008), is a paramount structure that supplies nutrients to the avascular IVD, therefore its impairment represents a potential limitation that needs to be carefully evaluated. Blood vessels in soft tissues provide the nutrients for the outer AF cells, while NP and inner AF cells rely on a capillary network in the subchondral EP through which nutrients diffuse. The reduction in nutritional supply is known to be one of the leading causes of IVDD (Urban et al., 2004). Holm et al. have described a technique to create IVDD in porcine lumbar spine by drilling a hole through

the central part of the EP into the NP. This model has been shown to trigger similar degenerative changes observed in degenerated human IVDs, such as alteration of water, PG, and cellular contents. However, this IVDD model is based on large damage to the EP (3.5 mm), which is quite extensive considering the relatively small geometry of the IVDs of the animal model used.

On the basis of different IVDD stages, the transpedicular approach could be used to deliver growth factors or drugs in early stages, or progenitor cells in moderate stages, of disc degeneration. Furthermore, it might also be used to introduce osteoinductive and/or osteoconductive agents to achieve interbody fusion in late stages of IVDD.

OBJECTIVES OF THE STUDY

The objectives of the study were divided into two main sections:

1. The first aim was to describe in detail and validate *in vivo* the transpedicular approach as an alternative route to the IVD, highlighting possible surgical-related difficulties and complications. The purpose of this novel approach was not only to provide a new model of IVDD without disruption of the AF, but also a new system for delivering therapeutic agents into the NP.

2. The second purpose was to collect qualitative and quantitative data from MRI, radiologic, macroscopic and histologic findings, with the aim of assessing the type and degree of IVDD changes obtained by performing four different surgical approaches to the IVD.

Section 1: in vivo characterization and validation of a new intervertebral disc degeneration model

MATERIALS AND METHODS

○ CASES SELECTION

Twelve skeletally mature (approximately three years of age), female Brogna breed sheep, weighing 34 to 42 kg, were included in the study. Ethical approval for the use of animals in this study was granted by the Italian Ministry of Health. All animal procedures and surgeries were performed at an accredited facility (Department of Animal Medicine, Productions and Health, Veterinary Teaching Hospital, University of Padua, Padua, Italy) where sheep were monitored at least once a day.

After arrival, a two-week period was provided to each animal to acclimate prior to any use for the experiments; this is important to reduce the stress associated with transportation and new environment which can have widespread effects on animals' physiological systems, including changes in cardiovascular, endocrine, immune, central nervous, and reproductive system. Blood analysis were performed as part of a general screening; subcutaneous injection with ivermectin (200 μg/kg) was administered to all animals, on arrival and 2 weeks later, to treat any possible infection and infestation due to gastrointestinal roundworms, lungworms, and larval stages of the nasal bot.

Sheep were followed serially before surgery (T0) and at 1 (T1), 3 (T2) and 6 (T3) months post surgical procedure.

○ IMAGING

X-RAY - Before the surgery and at each time point, conventional lateral plain radiographs of the lumbar spine were taken in each animal under sedation. The radiographs were analyzed qualitatively for evidence of changes in the vertebrae adjacent to the disc

spaces, looking for possible post-surgical alterations such as luxations, fractures, discospondylitis.

MRI - MR images of the lumbar spine were performed serially in 6 sheep, before surgery and at 1, 3, and 6 months post surgery. MR imaging scans were obtained using a 0,25 Tesla clinical magnet (Esaote Vet MR). Sheep were premedicated and anaesthetised and placed in lateral recumbency within the open magnet (Figure 16). A dorsal T1-weighted (T1w) localizer image (TR, 770 milliseconds; TE, 18 milliseconds) was obtained to establish the position of the lumbar discs from L1–L2 to L5–L6. A 4-mm thick midsagittal section was imaged, using a T2-weighted imaging sequence (TR, 2500 milliseconds; TE, 120 milliseconds) to highlight the signal from the NP. T1w (TR, 770 milliseconds; TE, 18 milliseconds) and 3D HYCE transverse images (TR, 10 milliseconds; TE, 5 milliseconds) were also obtained.

Figure 16. Sheep under anaesthesia placed in lateral recumbency within the open magnet

o **SURGICAL PROCEDURE**

Preparation - Sheep were fasted for 24 hours in order to prevent abdominal distension and aspiration of rumen fluids during surgery. Medetomidine hydrochloride (5-10 µg/kg IV)

was administrated to facilitate transport to the operating theatre, followed by intravenous injection of propofol (2-4 mg/kg IV) for anaesthetic induction. An endotracheal tube was inserted and anaesthesia maintained by isoflurane (2-3%) in oxygen and nitrous oxide. During surgery, replacement fluids (lactate Ringer's solution or 0.9% NaCl, 10mL/kg/h) and analgesia (alfentanil 60 µg/kg/h) were provided.

The lumbar region of each sheep was clipped from T10 to approximately the level of S3 vertebra. The sheep were placed on the operating table in sternal recumbency. The surgical site was aseptically prepared with chlorhexidine and alcoholic-iodide antiseptic wash followed by sterile draping. Local anaesthetic (lidocaine 0.5%) was subcutaneously injected around the incision site. Strict sterile precautions were maintained at all times.

Dorso-lateral approach to the lumbar IVD – Landmarks used for the incision were easily palpable; these were iliac crest, lumbar transverse processes and the costo-vertebral angle (Figure 17A); in addition a backhaus towel forcep was placed on one of the lumbar dorsal processes which was then identified on lateral X-Ray performed before starting surgery (Figure 17B).

A   **B**
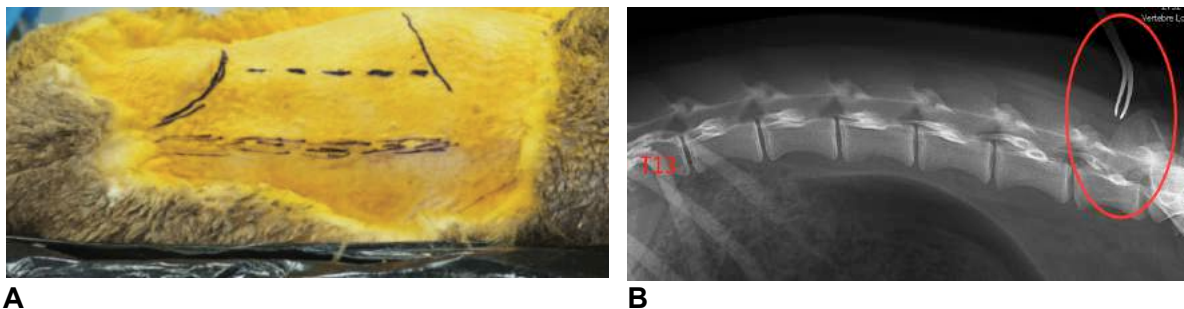
Figure 17. (A) Preoperative photo of sheep demonstrating lumbar spinous processes (lower dashed line), left lumbar transverse processes (upper dashed line), iliac crest (left) and costal margin (right) (Oeheme et al., 2012). (B) Radiographic landmark obtained by placing a backhause preoperatively (red circle); T13 can be easily identified due to the presence of the last pair of ribs.

A dorsal midline skin incision was extended from T12 to S1, using fluoroscopy to verify the correct localization in each animal. Following incision and retraction of the skin and superficial fascia, the deep fascia was incised unilaterally (left) around the tip of the spinous processes and retracted. Following left side dissection to the level of the synovial

joint of the articular processes, the incision was continued laterally and ventrally, by elevating the multifidus muscle attachments from the pedicles, allowing exposure of the articular and part of the transverse processes from L1 to L6. Electrocautery was used throughout the exposure to minimize bleeding. Once the procedure had been performed and haemostasis achieved, the wound was irrigated with Ringers' solution. Then, the transpedicular approach to the NP was performed by one surgeon. Five lumbar discs were assigned to different groups of treatment:

- L1-2: EP tunnel + nucleotomy;

- L2-3: EP tunnel;

- L3-4: EP tunnel + nucleotomy + EP repair with the polyurethane (PU) scaffold;

- L4-5: EP tunnel + EP repair with the PU scaffold;

- L5-6: intact control.

The different treatments are described below.

End-plate tunnel - Throughout a dorso-lateral surgical access to the lumbar spine, a 2-mm tunnel was drilled using a Kirschner wire (k-wire) into the pedicle of the vertebra to access the NP space of the cranial spinal segment under fluoroscopy guidance (Figure 18), checking the wire direction (mean angle degree ± standard deviation) in latero-lateral (Figure 18A) and dorso-ventral (Figure 18B) images, as already described (Vadalá et al., 2013). The k-wire was directed cranially and medially to reach the center of the NP, with an inclination of approximately 45°. A manual 2-mm drill was used to hole the EP and access the NP space.
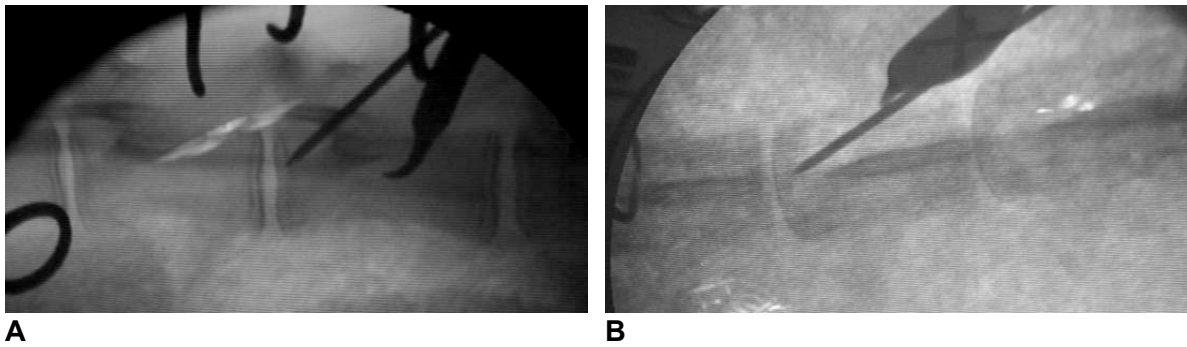
Figure 18. Representative intraoperative fluoroscopic images on the lateral (A) and dorsal (B) planes of the lumbar spine. It is possible to appreciate the k-wire reaching the center of the disc space through the transpedicular approach.

Nucleotomy - A 2-mm diameter shaver resector (Smith & Nephew Shaver Blades, 2.0 mm Full Radius, 7 cm length), powered by an arthroscopy shaver unit (Smith & Nephew, Dionics Inc. PS3500, Germany) and connected to a vacuum pump, was introduced through the 2-mm tunnel. NP tissue was removed maintaining the shaver blade in the IVD space oscillating at 4000 rpm for 5 minutes (Figure 19).
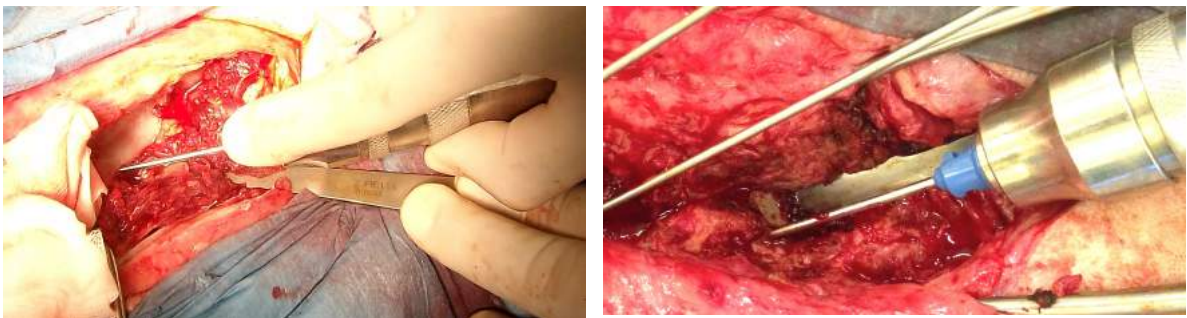
Figure 19. Surgical pictures showing placement of the 2-mm shaver dissector through the transpedicular approach in the disc space, used to perform nucleotomy under aspiration.

End-plate repair - The EP was repaired by sealing the edge of the tunnel using a press-fit porous polyurethane (PU) cylinder (2.2 mm diameter and 10 mm length) (Figure 20A) that was placed at the EP edge using a 14G cannula (Bonopty® Bone Biopsy System, AprioMed, Sweden) inserted through the tunnel (Figure 20B). The elastomeric PU cylinder was synthesized as previously described (Eglin et al., 2010; Laschke et al., 2010; Laschke et al., 2009). The scaffold was sterilized by cold ethylene oxide process and stored until the time of surgery.

At the end of the surgical procedure, the deep fascia, the subcutaneous layers and the skin were closed in a simple continuous pattern.
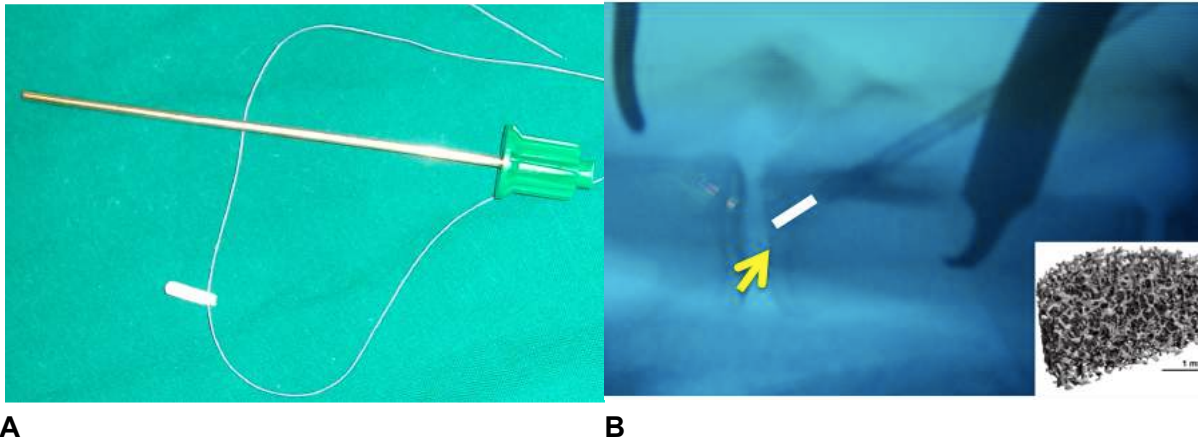
Figure 20. (A) A porous polyurethane (PU) cylinder was inserted using 14-G cannula (Bonopty - Bone Biopsy System, AprioMed, Sweden) at the edge of the tunnel performed through the vertebral body to repair the end-plate and seal the disc space. (B) Representative fluoroscopy image control showing the cannula placed into the transpedicular tunnel during the scaffold positioning (arrow).

o **PAIN MANAGEMENT AND POSTOPERATIVE CARE**

As soon as each sheep was breathing spontaneously, following cessation of isofluorane anaesthesia, it was extubated, transferred to a heated room and returned to the sheep housing, where it was given food when fully alert and standing. The sheep were observed for approximately one hour following surgery. All sheep received prophylactic antibiotics (Amoxicillin 15 mg/kg/q48 hours IM) perioperatively and postoperatively for 10 days. Tramadol (4 mg/kg/q12h) and Carprofen (4 mg/kg/q24h) were administered for postoperative analgesia at least for the first 5 days after surgery. Vital signs were monitored, neurological examination was performed postoperatively on a routine basis, and standard nursing care was provided. The sheep were monitored for normal feeding behaviour and cage activity twice daily to determine their general health. A wound inspection to check for possible infection or wound openings was performed on a daily basis until a complete healing.

o **EUTHANASIA**

At each time point (before and 1, 3, and 6 months post surgery), 3 sheep were anaesthetized with medetomidine (5-10 μg/kg IV) and propofol (2-4 mg/kg IV), and then euthanized with a solution of embutramide, mebenzonio ioduro and tetracaine chlorhydrate (0.3 ml/kg IV).

o **COMPLICATIONS**

Intra- and post-operative complications were recorded. Potential intraoperative complications included:

- Improper identification of the surgical site

- Inability to reach correctly the NP

- Excessive haemorrhage

- Incorrect k-wire inclination

- Iatrogenic damage to the spinal cord and nerve roots

Postoperative complications included:

- Persistent kyphosis

- Vertebral fracture and instability

- Pelvic limbs paresis/paralysis

- Seroma

- Wound infection

- Cutaneous fistula

- Discospondylitis

RESULTS

○ SURGICAL PROCEDURE

The transpedicular approach was feasible in all animals included in the study. In all the animals the K-wire was inserted correctly in the 4 discs treated (L1 to L5), allowing the correct placement of the shaver within the center of the NP.

The K-wire mean orientation angles (angle ± standard deviation) assessed on the latero-lateral and dorso-ventral fluoroscopy images were 50.6° ± 3.1 on the dorsal plane and 50.1° ± 6 on the sagittal plane. The average operation time was 92 minutes (range 74-110). The duration of the procedure to reach the NP, perform nucleotomy and place the PU scaffold became shorter over the course of the experimental period.

○ IMAGING

In animals that underwent MR imaging it was possible to detect the transpedicular tunnel throughout the vertebral body and pedicle of each treated disc, confirming the correct positioning of the k-wire (Figure 21).
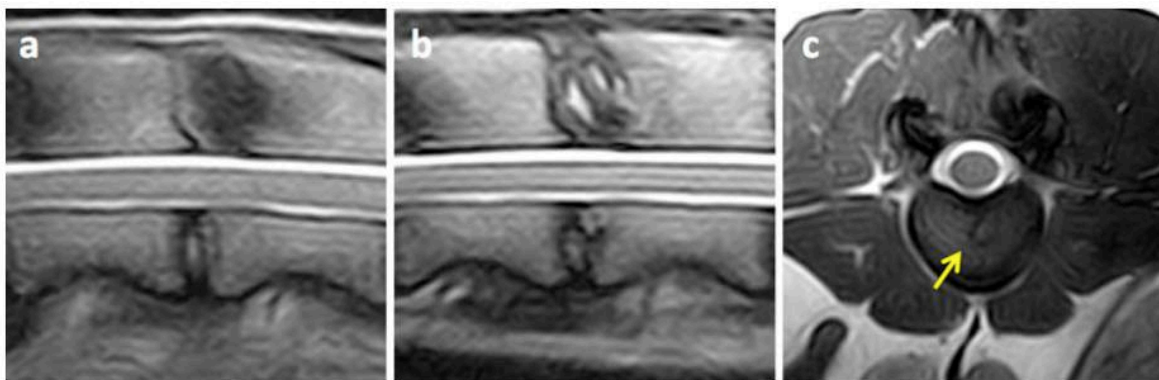
Figure 21. Representative middle-sagittal T2-weighted MR images showing the L3-L4 disc before the surgical approach (a) and after nucleotomy and scaffold placement at 3-month follow-up (b). The tunnel is visible on both sagittal (a) and transverse (c) images; furthermore the transverse MR image shows that the tunnel entry point on the end-plate is in its central area (c).

On parasagittal and transverse T2w images the tunnel appeared hypointense to the rest of the vertebral body (Figure 21b). Furthermore, loss of the NP signal intensity in the discs that underwent nucleotomy was visible in transverse images. The PU scaffold inserted in two of the treated discs in each sheep was not discernible from the surrounding bone.

○ **PERI- AND POST-OPERATIVE CARE AND COMPLICATIONS**

▪ *INTRAOPERATIVE DATA*

The only intraoperative complication was CSF leakage from the tunnel during the drilling process, that occurred in 2 of the 48 IVD spaces treated (complication rate 2.1%). Blood loss was minimal and no clinically apparent neural or great vessel injury was caused by any of the surgical procedures. There were no anaesthetic complications as confirmed by stable cardiovascular parameters.

▪ *POSTOPERATIVE DATA*

In the early post-operative period, no significant problems with mobility or pain have been encountered; all animals tolerated the procedure and within two hours from the end of the surgery were able to walk. After surgery all the sheep presented kyphosis, which had resolved after 3-5 days in 10/12 sheep. Post-operative complications verified in 3/12 sheep (25%). One sheep developed a sterile seroma, which reabsorbed completely after 7 days without causing any clinical problem. In none of the animal postoperative wound dehiscence did occur. A fracture to the cranial aspect of L4 vertebral body was detected radiologically in one sheep at 1-month follow-up (Figure 22a). The fracture evolved into L3-4 spondylarthritis after 3 months (Figure 22b). Apart from mild kyphosis the animal did not develop further clinical signs, such as discomfort and paresis, however was euthanized at 3-month follow-up. Through the analysis of the X-ray (Figure 22c) and MR images (Figure 22d) performed one month after surgery, discospondylitis at L1-2 (2.1% complication rate) was diagnosed in one sheep. The animal presented mild paraparesis,

ataxia and kyphosis and for ethical reasons was euthanized. Macroscopic changes attributed to discospondylitis were confirmed during autopsy.

Post-operative pain management was considered adecuate in all the sheep, with exception of the one that developed discospondylitis. Indeed, all the animals were walking, eating and drinking regularly and no evident reactions were elicited on spinal palpation. No weight loss was detected in any of the animal at their last time point; after the experimental period the animals weighed approximately 41 to 50 kg.
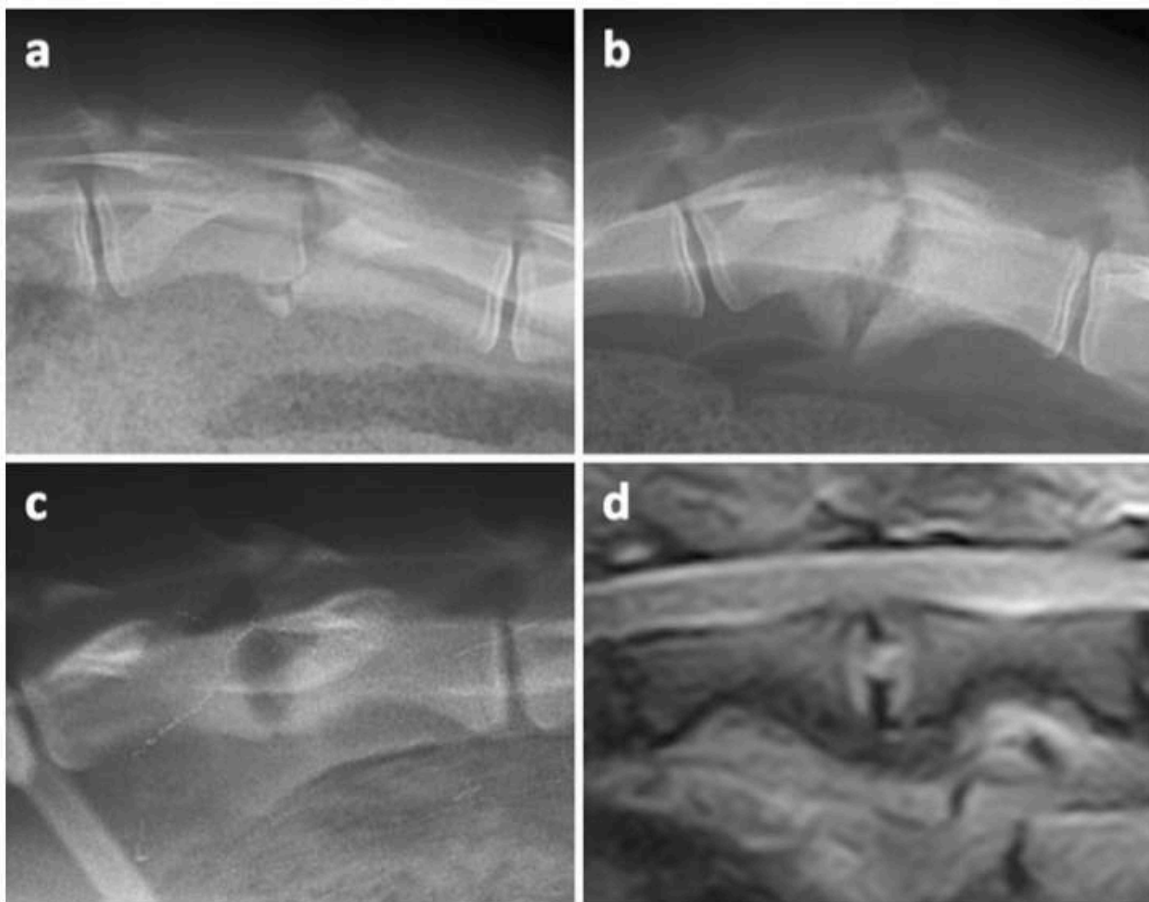
Figure 22. X-ray images showing a fracture of the cranial aspect of the vertebral body observed 1 month after the transpedicular approach (a) and that evolved into spondylarthritis after 3 months (b). Discospondylitis developed at L1-L2 as shown by the erosion of both end-plates and the consequent widening of disc space in letero-lateral X-ray image (c); T2-weighted MR image shows increase intensity of the disc and end-plates and apparent extension of the infection into the vertebral canal causing ventral compression of the spinal cord (d).

DISCUSSION

The recent consensus about the importance of maintaining the AF structural integrity (Elliott et al., 2008; Iatridis et al., 2009) has brought attention within the field of IVD regeneration on both novel AF repair strategies (Vadalá et al., 2012) and alternative ways to access the NP space. Indeed, taking into account that the majority of regenerative strategies for the IVD are traditionally delivered through the AF route, it should be considered that the resulting lesion might impair the expected outcomes leading to further degeneration, leakage of the biologically delivered material, and potential failure of the regenerative treatment (Vadalá et al., 2011).

The transpedicular approach has been described in a preliminary *ex vivo* study, which demonstrated that injections, nucleotomy and nucleoplasty were feasible by realizing a tunnel passing through the pedicle and the EP (Vadalá et al., 2013). The present study has proved that this alternative approach to the IVD is feasible *in vivo* with a relatively low morbidity rate. Indeed, both the transpedicular tunnel and nucleotomy were performed successfully in 48 and 24 IVD, respectively.

Technical surgical skills and a good knowledge of the regional anatomy are needed, however a remarkable progressive shortening of the surgical time was recorded, reflecting a quick rate of improvement of the learning curve.

The transpedicular approach provides good visualization and surgical access to the IVDs. The procedure can be performed from either the right or the left side of the lumbar spine. The only limitation is related to the realization of the technique caudally to L5, where the pelvis and the pelvic limbs can interfere with the acquisition of fluoroscopic lateral images.

Particular care must be taken to avoid any damage to the spinal cord. The inclination of the k-wire through the pedicle represents a key-point to perform this technique correctly and to reach the NP without causing any significant damage. On the

preliminary study (Vadalá et al., 2013) performed on lumbar ovine and human spinal segments, the k-wire angles which enabled to reach the centre of the NP were 47.5° ± 5.1° on the dorsal plane and 49.6° ± 6.2° on the sagittal plane. The angles recorded in the present study are very similar (50.6° ± 3.1° on the dorsal plane and 50.1° ± 6.0° on the sagittal plane), however it is possible that even a subtle difference in the inclination could explain the occurence of CSF leakage. Indeed, pedicles are paired, strong, tubular bony structures, made of hard cortical bone outside and cancellous bone inside and acting as thin lateral walls of the spinal canal. Due to the thin conformation of the pedicles and their proximity to the spinal cord even a small angle variation could cause severe consequences; it is therefore essential the careful evaluation of the anatomical landmarks and the k-wire inclination. Furthermore, when performing the transpedicular approach and before considering its application in human medicine, interspecies anatomical variations should be considered. In the light of this consideration and of the need of an experimental animal model able to reproduce the disc degenerative process, sheep spine was selected to minimize the differences with human spine. Sheep are readily available and show great homogeneity when selected for age, breed, and sex (Wilke, 1997a). Sheep have been widely used in spinal research and several comparative studies have pointed to similarities between the sheep and human IVD: (1) proportions are similare, though absolute size is smaller in sheep (Wilke et al., 1996), (2) the sheep spine is loaded along its long axis, like humans (Smit, 2002) and, (3) similar to adult human IVDs, no notochord cells are present in mature sheep discs (Trout et al., 1982 a,b). The skeletally mature sheep used in the present study showed uniform anatomical disc and vertebral patterns.

Several surgical approaches to the lumbar IVDs have been described in spinal research, however they can carry some limitation related to anatomical characteristics. For example, dorsal approaches to the lumbar spine, commonly used in human surgery, are difficult in sheep due to the risks related to the presence of the spinal cord within the lumbar spinal canal and due to the ossification of the dorsal longitudinal ligament (Oeheme et al., 2012). For this reason, the ovine lumbar IVD have traditionally been

accessed via a ventral or ventrolateral approach through the retroperitoneal or transperitoneal regions (Melrose et al., 2012; Baramki et al., 2000). These approaches carry significant risks, including bowel and great vessel injury, neural injury, and hernia formation. The procedure also requires a large abdominal incision with greater retraction of abdominal viscera, which can be harmful to the animal (Baramki et al., 2000). Recently, a minimally invasive retroperitoneal lateral approach has been described in an ovine model, allowing for a small focused incision and causing minimal morbidity (Oheme et al., 2012). Lateral approaches to the human lumbar spine, such as the extreme lateral interbody fusion procedure, have gained popularity as minimally invasive approaches to the lumbar IVDs. In the lateral body fusion procedure, a retroperitoneal transpsoas route is employed, requiring real-time neuromonitoring to ensure safe passage through the psoas without damaging the lumbar plexus (Youssef et al., 2010), which represents the main concern with this procedure. The transpedicular approach to the IVD is currently used, in humans, as a route to perform biopsy and discectomy for the diagnosis and management of early spondylodiscitis, to facilitate the isolation of pathogens, natural healing, and immediate improvement of pain (Hadjipavlou et al., 1998a; Di Martino et al., 2012). The technique is performed through a dorsal percutaneous approach; the advantage of this procedure is its minimal invasiveness that allows bacteriological and histological testing, drainage of infected material, as well as injection of therapies, permitting early patient mobilization (Arya et al., 1996; Hadjipavlou et al., 2004). The approach is simple, cost-effective and its diagnostic accuracy is comparable to that of open biopsy (Arya et al., 1996; Hadjipavlou et al., 2004). The transpedicular approach has been validated in spinal research both *ex vivo* by Vadalá et al. (2013) and *in vivo* with the present study, providing a model to perform biological and biomechanical studies of NP regenerative therapies (Vadalá et al., 2013). Further future perspectives are represented by the validation of CT/fluoroscopy guided minimally invasive approaches and by the clinical translation of new regenerative strategies for biological restoration of early and mild degenerative changes in IVD, which is crucial to improve present clinical treatments

and life quality of several patients.

Most of the structural injury IVDD models are based on a direct damage to the AF by performing different tear types (rim lesions, concentric and radiating annular tears) of different sizes, evaluating the evolution and progression of the biologic intradiscal alterations and demonstrating how these may affect the mechanics of the joint (Osti, 1990a; Melrose et al., 1992; Moore et al., 1992; Gunzburg et al., 1993; Ahlgren et al., 1994; Moore et al., 1996; Fazzalari et al., 2001; Melrose et al., 2002; Elliott et al., 2008). A porcine experimental model of IVDD, based on EP fractures or NP herniation through the EP, was described by Holm et al. (2004). Through a retroperitoneal approach, the cranial EP of the lumbar vertebra was perforated using a 3.5-mm drill bit inserted from the lateral cortex at mid-height, angulated at 45° so as to reach the central part of the EP. This model highlighted how the EP damage can trigger similar degenerative changes as those observed in degenerated human IVD, such as alteration of water, PG and cellular contents (Holm et al., 2004; Salo et al., 2008a,b). In contrast with this model, the transpedicular approach performed in the present study is based on a smaller EP damage (2-mm) and, in 2 of the 4 treated discs, the EP tunnel was sealed using conductive scaffolds with the aim of limiting the degradation cascade and preventing Schmorl's nodes formation or material leakage. The histological evaluation of the degeneration obtained in the IVDs treated and of the changes related to the use of the scaffold will be discussed in the second part.

A moderately low rate of intraoperative (2.1%) and postoperative complications (25%) occurred in the present study. The CSF leakage reported in two sheep is likely to be secondary to dural tear provoked by the incorrect k-wire positioning during the realization of the transpedicular tunnel. To our knowledge, neural complications related to the perforation of the dura have not occurred as the animals recovered uneventfully. Vertebral subluxation and discospondylitis, localized at L3-4 and L1-2 IVDs respectively, were observed during the postoperative period in two different sheep; the two lesions were likely to be iatrogenic. The fact that both the affected discs were nucleotomized may

imply that nucleotomy could contribute to increasing the risk of potential complications. Experimentally, it is generally agreed that the structural damage due to *in vitro* nucleotomy significantly destabilizes the motion segment (Zollner et al., 2000). However, *in vivo* biomechanical tests suggested that post-operative instability might not be exclusively a consequence of the trauma to the IVD, but that dorsal passive-spine supportive structures integrity (articular facets, spinous processes) play a crucial role in maintaining motion segments stability (Reitmaier et al., 2014). In the current study, dorsal vertebral structures remained intact, however we cannot rule out that the retraction of the lumbar epaxial muscles may have contributed to reducing the strength of the motion segments involved.

Iatrogenic IVD space infection represents one of the possible complications occurring after spinal surgery. In humans, discospondylitis represents a common complication following microsurgical discectomy, percutaneous laser disc decompression (Farrar et al., 1998), automated percutaneous lumbar nucleotomy operations (Dullerud et al., 1997), and discography (Guyer et al., 1997; Osti et al., 1990b). In the present case, the occurence of discospondylitis could represent a consequence of either iatrogenic bacterial inoculation into the NP or hematogenous spread. Further laboratory and histologic analysis were not performed to confirm the diagnosis and identify a pathogen, however the characteristic radiologic and post-mortem macroscopic changes are highly supportive of IVD infection. MRI analysis has high sensitivity and specificity for the evaluation of pyogenic discospondylitis (Lucio et al., 2000). Characteristic MRI findings of discospondylitis include decreased signal from the disc and adjacent portion of vertebral bodies on T1w sequences and an increased signal from these structures on T2w sequences; contrast uptake can be detected in the adjacent vertebral bone marrow, in the disc space and in the dorsal AF (Lucio et al., 2000). In the present study post contrast images were not available, however T1w and T2w images showed alterations similar to those described. The peculiar radiographic changes, characterized by erosion of the EPs and widening of the IVD space, and the macroscopic bone remodeling observed on the ventral aspect of L1-2 vertebral bodies during necroscopy, supported the diagnosis of disc

infection.

Summarizing, the transpedicular approach represents an alternative route to the traditional ventral and ventrolateral approaches through the AF. This new pathway to the IVD provides a new model to study biologic and biomechanical alterations in relation to both IVD degenerative processes and potential NP regenerative therapies.

<u>Section 2</u>: evaluation of quantitative and qualitative data of the intervertebral disc degeneration model

MATERIALS AND METHODS

o QUALITATIVE ANALYSIS

MR images, macroscopic and histologic samples of the intact and injured discs were analysed qualitatively for evidence of degenerative changes.

▪ *MAGNETIC RESONANCE IMAGES ANALYSIS*

MRI images, acquired as described in the first part of the study, were analysed qualitatively. Disc morphologic changes, as seen on sagittal T2w images, were recorded and divided into 5 categories according to the Pfirrmann grading scale (Pfirrmann et al., 2001). Variations of signal intensity, IVD structure, distinction between NP and AF, and IVD height were evaluated for each treated and control disc at each time point.

▪ *GROSS ANATOMY AND HISTOLOGICAL EVALUATION*

At sacrifice, the lumbar spines were removed from the sheep (Figure 23a), and the discs (L1 to L6) together with intact adjacent vertebral body bone (Figure 23b) were fixed in 10% neutral buffered formalin for at least 1 week, decalcified in ethylenediaminetetraacetic acid, and processed for paraffin sectioning. Blocks of tissue (5 mm in thickness) were embedded in paraffin. The blocks of tissue were then cut into sections of 5 µm in thickness using a microtome and stained with Safranin O/Fast Green and hematoxylin and eosin (H&E).
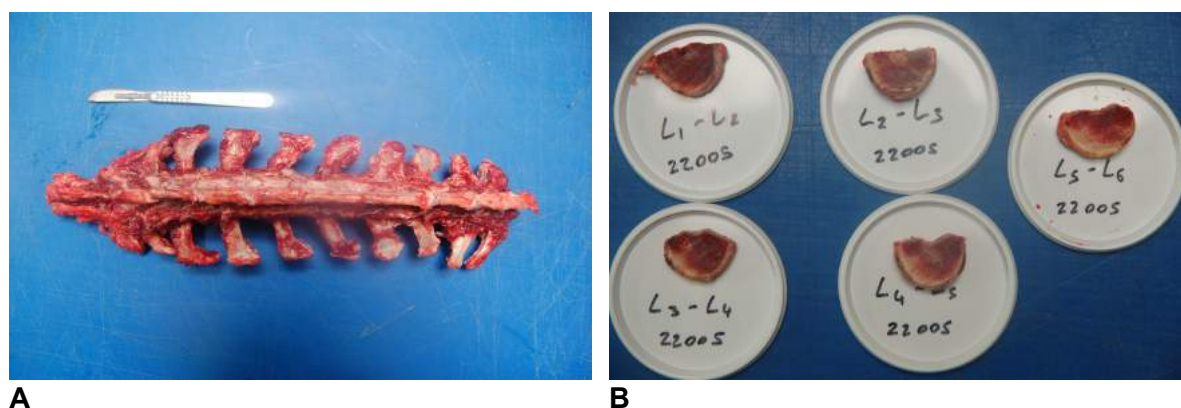
Figure 23. (A) Post-operative photo of one of the sheep spine (L1-S3) harvested after euthanasia; perispinal muscles have been resected. (B) Representative picture of treated (L1-L5) and control (L5-L6) removed from the spine.

Based on the previously described grading scale (Thompson et al., 1990), all midsagittal sections of the harvested discs within each single sheep were compared to each others, to discs of all other sheep and to the control discs. Anatomical characteristics and degenerative changes were evaluated for the NP, AF, EPs and vertebral bodies of each disc. More in detail, in the NP the progressive replacement of the bulging gel with fibrous tissue and the presence of clefts formation were evaluated; in the AF and EP, changes in the organization of the lamellae in the composition and structure of the hyaline cartilage were observed; finally, margins shape and osteophytes formation were recorded for the vertebral bodies.

Qualitative histological analysis was performed under a light microscope (Nikon Eclipse E800, Nikon, Melville, NY), at magnifications ranging from 10 to 200X. In particular, evidence of changes in NP cells composition and the presence of possible cells leaking from the tunnels were recorded.

o **QUANTITATIVE ANALYSIS**

The effect of the different degeneration modalities performed on each disc was evaluated quantitatively through the analysis of X-ray and MR images performed at each time point. Quantitative analysis of the images was performed by transferring the images to a

commercially available image processing software (OsiriX Imaging Software, www.osirix-viewer.com) as follows.

- ### *DISC HEIGHT INDEX (DHi)*

Under lateral view, vertebral body and DHs were measured in each segment from L1 to L6. Disc and vertebral body heights were derived by averaging the distance between EPs at 3 places obtained from the dorsal, middle, and ventral portions of the disc normalized to the average length of 2 adjacent vertebral bodies in each section (Figure 24). The preoperative radiograph was used as a baseline measurement. The data were then transferred to the Excel sofware program (Microsoft Excel, 2010) and the DHi was calculated using the method described by Masuda et al. (2004) (Figure 24).

$$DHi = 2 \times (D+E+F) / (A+B+C+G+H+I)$$
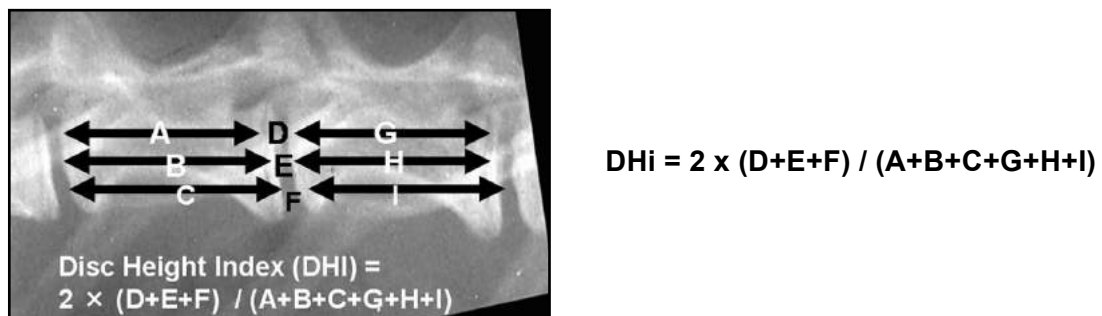
Figure 24. Using digitized radiographs, measurements including the vertebral body heights and DH were analyzed by Osirix software. IVD height was calculated by averaging the measurements obtained from the dorsal, middle, and ventral portions of the IVD and dividing that by the average of adjacent vertebral body heights (Masuda et al., 2004).

- ### *MRI INDEX (MRi)*

The T2w midsagittal images of the intact and treated discs were analyzed quantitavely calculating the MRi (Sobajiama et al., 2004). The NP of each disc was outlined manually to define the region of interest (ROI), as shown in Figure 25. The area and average signal intensity (gray scale value) of this ROI were then computed automatically using the Osirix

software, and their product resulted in an MRi for each IVD (Figure 25). Considering that MRI images of a NP of a degenerating disc potentially could exhibit changes in area, signal intensity, or both, the MRi was computed to serve as a more comprehensive measure of NP degenerative changes.
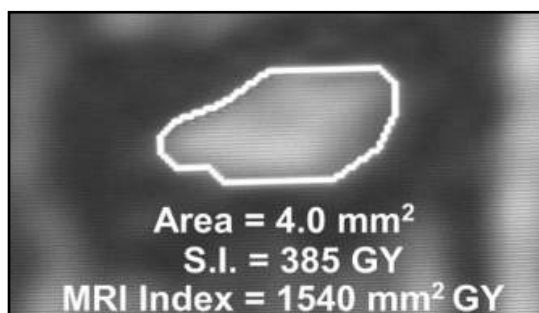
$$\text{MRi} = \text{Area (mm}^2) \times \text{Signal Intensity (GY)}$$

Figure 25. T2-weighted MRI image of a representative rabbit lumbar disc with NP outlined to define ROI. The measured NP area, signal intensity, and MRi (product of area and signal intensity) are shown (Sobajima et al., 2004).

o **STATISTICAL ANALYSIS**

Data regarding DHI and MRi were collected in a spreadsheet (Microsoft Excel 2016, Microsoft Corporation, Redmond, WA, USA) and analyzed using commercially available software (JMP Pro 11, SAS Institute, Cary, NC, USA). Normal distribution of the residuals, symmetrical distribution of differences, and homoscedasticity of data were visually assessed. When necessary, a Shapiro-Wilk test and a Levene test were used to confirm or reject the aforementioned assumptions.

Two different sets of analyses were performed both on MRi and on DHI data in order to identify differences between treatments (discs) and differences between time-points.

Difference between techniques – Each individual DHI and MRi score at T1, T2, and T3 were subtracted from the corresponding T0 value from the same individual, in order to obtain a score independent from individual variations in magnitude of DHI and MRi

possibly present at T0. The different treatments (discs) were therefore compared to the control group using a Dunn's test.

Difference between time-points – For each treatment group (discs) a Wilcoxon Signed Rank was used to identify differences in DHI and MRi scores of the same disc at different time-points (T1 vs. T0, T2 vs. T0, T3 vs. T0, T2 vs. T1, T3 vs. T1, T3 vs. T2).

P-values were Bonferroni adjusted when necessary and a $p < 0.05$ was considered significant for all the tests performed.

RESULTS

○ QUALITATIVE ANALYSIS

▪ *MRI ANALYSIS*

Representative serial MRI scans of the lumbar spine of one sheep are shown in figure 26, consisting of T2w, midsagittal images obtained before and 1, 3 and 6 months after surgery. Progressive decrease in NP area and signal intensity was evident for each of the 4 treated discs (L1-2, L2-3, L3-4, L4-5) over the 6-month period. Furthermore, different degrees (Pfirrmann scale) of disc degeneration could be assigned to each disc at time point 3 (6 months), depending on the surgical technique used. As shown in figure 26, lower degrees of IVDD (Grade II and III) were achieved by performing only the tunnel through the vertebral body, while higher degrees of degeneration were obtained by performing nucleotomy. The sealing of the tunnel with the PU scaffold seemed to lead to a lesser degree of disc degeneration at L3-4 and L4-5, if compared to L2-3 and L1-2 respectively (Figure 26). MRI appearance of the NP of the intact control disc (L5-6) remained relatively constant over the same period. Qualitative MRI observations are provided in Table 4.

▪ *GROSS ANATOMY AND HISTOLOGY*

On gross inspection of the lumbar spines removed at sacrifice variable degenerative changes, depending on the surgical technique, were seen. In figure 27 are shown representative lumbar IVD specimens of three sheep collected at time point 3. Five categories (Thompson grading scale) of IVDD were observed for each IVD considered. In the two nucleotomized IVDs (L1-2, L3-4) macroscopic signs of degeneration, such as defects in EP cartilage, fibrous appearance of the NP, focal disruption of the AF and pointed vertebral bodies margins were observed. L2-3 and

L4-5 IVDs were degenerated as well, although to a lesser degree (Table 5). In figure 27 it is possible to observe how control IVDs were showing the characteristic bulging gel NP, with uniform hyaline EPs in the three sheep represented. These macroscopic findings seemed to overlap with the MRI changes and the five grades of degeneration attributed to each treated IVD (Figure 30).

The Safranin O/Fast Green (figure 28) and H&E histologic sections revealed a range of morphologies from normal to severely degenerated which were consistent in relation to the IVD observed, therefore to the surgical technique used. Normal-looking IVDs matched with the control group and displayed an intact AF with a normal pattern of well-organized fibrocartilage lamellar sheets and a well-defined border between the AF and the NP. The NP was rounded, bloated-looking and consisted of numerous chondrocyte-like cells. With progression of the degree of IVDD, the AF aquired a wavy appearance due to its disorganization and infolding and gradual loss of NP cells was observed. Cracks and fissures were progressively more evident in the AF, and a general loss of definition between the AF and NP was noticed. The NP was gradually occupied by disorganized, hypocellular fibrocartilagineous tissue. The qualitative histologic findings are summarized in Table 5. Further observations were made about possible differences between the discs where the tunnel was sealed with the PU scaffold (L3-4, L4-5) and those where the cylinder was not inserted (L1-2, L2-3). An important aspect observed was the presence of leakage of NP cells through the tunnel in non-sealed discs (Figure 29); moreover remodeling of the scaffold was noted.
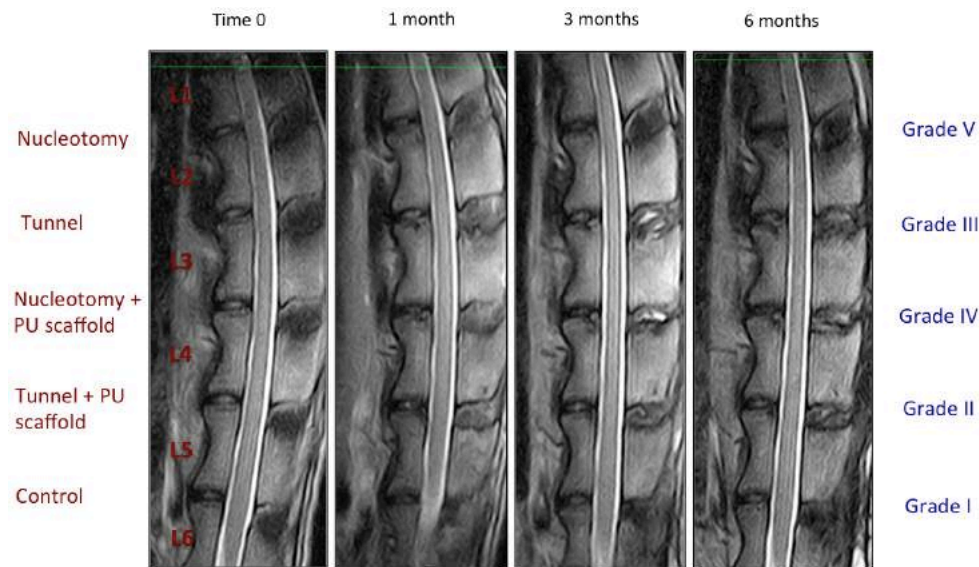
Figure 26. Representative serial MRI scans of lumbar spine of one sheep, showing Tw, midsagittal plane images obtained before and 1, 3 and 6 months after surgery. On L1-2, L2-3, L3-4 and L4-5 IVDs four different surgical techniques were performed; L5-6 was considered as control disc. Progressive decrease in NP area and signal intensity for each of the four treated discs over the 6-month period is present. In contrast, area and signal intensity of the NP of the intact control disc (L5-6) seem to remain relatively constant over the same period.
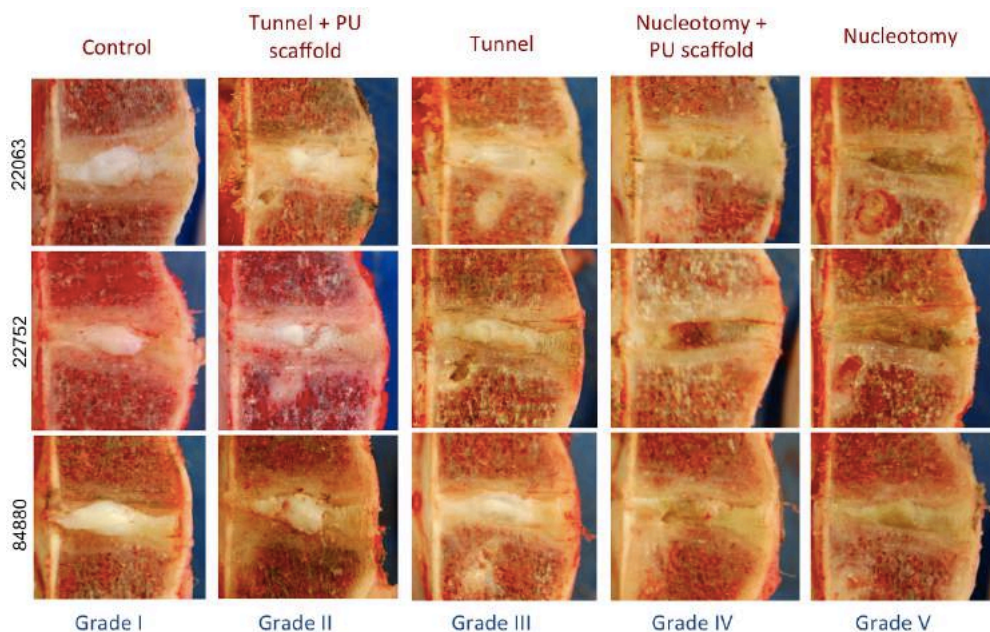
Figure 27. Midsagittal plane IVD samples of three sheep are represented. The specimen were collected at 6-month follow-up.

Figure 28. Representative histologic sections (Safranin O/Fast Green staining) of L1 to L6 IVDs, 6 months after surgery. A progressive narrowing of the EPs can be observed; disorganization and fragmentation of the AF and NP matrix appear gradually increased depending on the surgical technique performed.
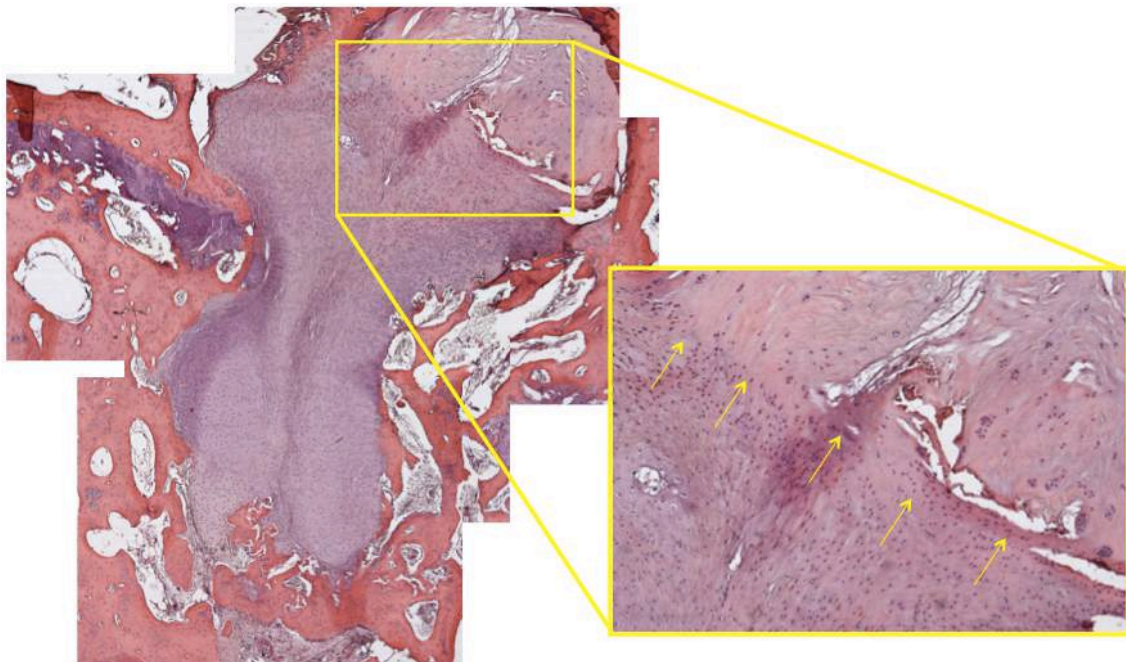
Figure 29. NP tissue leakage within the tunnel without PU scaffold (H&E) (yellow arrows).

Summarizing, the qualitative MRI, macroscopic and histologic findings, similar and consistent results were observed for each disc evaluated (Figure 30). With the model of IVDD described in this study, four progressive degree of IVDD were obtained by performing either a transpedicular tunnel or nucleotomy technique, with or without the use of a PU scaffold.
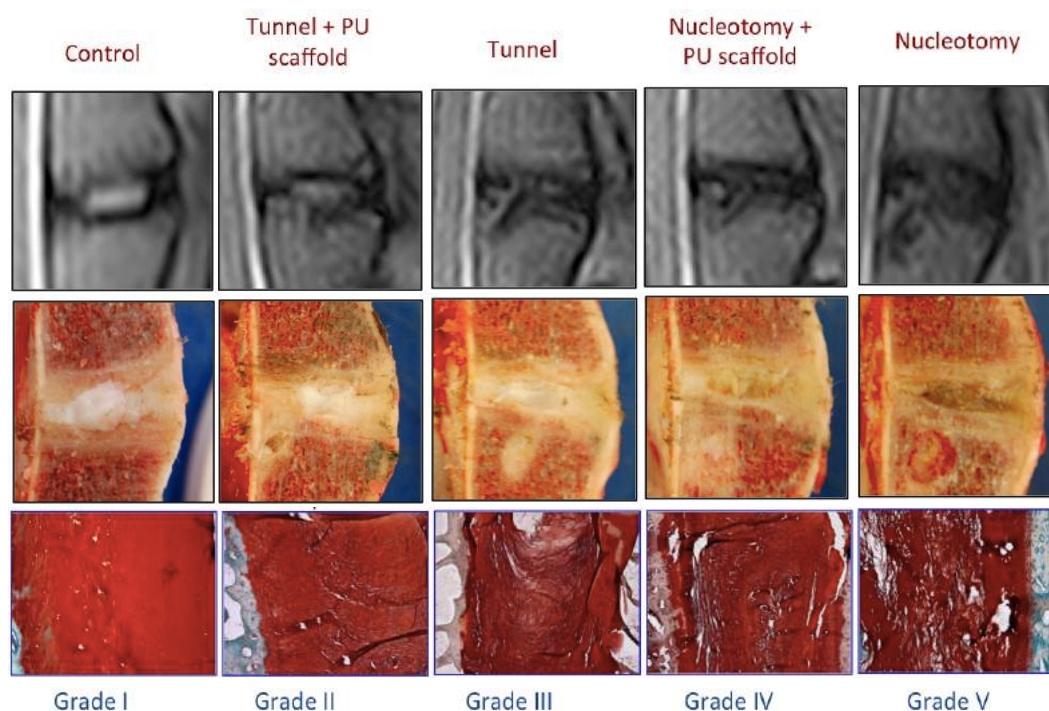
Figure 30. Representative MRI, macroscopic and histologic images of L1 to L6 IVDs at time point 3. Correspondence between the findings is observed and each grade of degeneration reflects a differet surgical technique, demonstrating progressive and reproducible changes similar to changes seen in human IDD.

Table 5. Summary of MRI, macroscopic and histologic observations of the treated and control discs at 6-month follow-up

IVD	Surgical technique	MRI	Gross anatomy	Histology
L1-2	Nucleotomy	Extensive decrease in NP area and signal intensity and increasing dark signal of the NP; loss of distinction between AF and NP	Fibrotic appearance of both NP and AF, diffuse EP sclerosis and pointed vertbral body's margins	Loss of definition between NP and AF; cracks and fissures in AF; NP tissue leakage within the tunnel
L2-3	Tunnel	Irregular NP and reduced area and signal intensity; decreased distinction between AF and NP	Reduction in anular-nuclear demarcation; defects in EP cartilage	Apparent decrease in number off chondrocyte-like cells; infolding of inner AF
L3-4	Nucleotomy+PU scaffold	Dark/grey signal of NP and reduction of its area; low definition between AF and NP	Progressive fibrous appearance of the NP; irregularity and sclerosis in subchondral bone; smoothed vertebral body's margins	Hypocellular fibrocartilage evident in NP; loss of definition between AF and NP
L4-5	Tunnel + PU scaffold	Mild decrease in NP signal intensity	Altered NP structure, irregular EP thickness	Reduced number of chondrocyte-like cells in NP
L5-6	Control	Homogeneous, bright NP; clear distinction between NP and AF	Bulging gel NP with fibrous lammellar AF and uniform hyaline EPs	Homogeneous population of chondrocyte-like cells in NP

o   QUANTITATIVE ANALYSIS

DHi and MRi were calculated at each time point (T0 to T3) in 6 and 5 cases, respectively.

In 4 sheep X-Ray were available until T1 or T2. The two animals that developed

discospondylitis and vertebral fracture were omitted from the study (Table 6).

Table 6. Survival time and diagnostic test performed

Case N.	Survival time (months)	Diagnostic test
22063	6	Rx+MRI
84480	6	Rx+MRI
22752	6	Rx+MRI
85936	6	Rx+MRI
83734	6	Rx+MRI
84320	6	Rx
85184	3	Rx
85233	3	Rx
22002	1	Rx
22005	1	Rx
23389*	3	Rx
22542*	1	Rx+MRI

* Cases eliminated from the study

In table 6 are represented the differences, expressed in percentage, of DHi and MRi of

each time point (T1, T2, T3) in comparison to the baseline (T0). Each IVD showed an

overall reduction of both indices over the 6 months, apart from L4-5 IVD, which presented

an increased DHi when T3 was compared to T0 (Table 7).

	T0 to T1	T0 to T2	T0 to T3
L1-L2	-30%	-14%	-28%
L2-L3	-12%	-31%	-27%
L3-L4	-29%	-45%	-57%
L4-L5	-16%	-28%	-30%
L5-L6	-4%	-11%	-15%

MRi

	T0 to T1	T0 to T2	T0 to T3
L1-L2	2%	-5%	-3%
L2-L3	6%	-4%	-2%
L3-L4	-7%	-10%	-2%
L4-L5	0%	-6%	5%
L5-L6	-2%	-6%	-9%

DHi

Table 7. Percentage of variation of MRi and DHi comparing each time point to the baseline (T0)

In figure 31 it is represented the trend of the two indices evaluated over the 6-month experimental period. Each index is inversely proportional to the degree of degeneration obtained, therefore the overall negative trend shown in both DHi and MRi curves indicates a progressive increasing in IVDD over time (Figure 31). In the control IVDs was observed a gradual and progressive decrease in DHi and MRi among time points; this regular trend was not seen in the treated discs, which exhibited fluctuations over the time points. In the treated discs, major disc space narrowing was observed 3 months after surgery (time point 2), followed by an apparent widening of the disc heights at 6 months. MRi scores exhibited similar results in term of progressive reduction of the values noted at T3 if compared to T0.

Figure 31. Graphic representation of the trend of DHi and MRi averages for each disc over 6 months
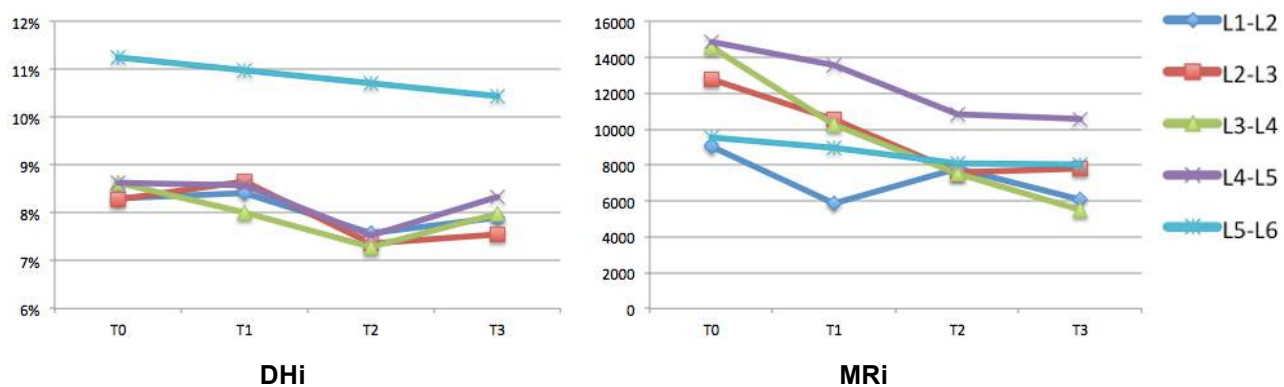
Differences between techniques - Figure 32 shows the mean DHi and MRi of the pooled data of the treated discs (L1 to L5) and the intact control discs (L5–L6), plotted against time. Each IVD treated was then compared to the control disc (L5-6). No statistically significant differences were detected in these data for DHi (P > 0.05).

However, when the treated discs data where compared to the control disc, significantly higher higher values were observed for L4-5 at T3.

 On MRi analysis was observed that the nuclotomy+scaffold technique significantly affected some results throughout the experimental period. The MRi was significantly lower at L3-4 than control group at T2 and T3. Further differences among the remaining discs were not detected.

Differences between time points – DHi and MRi were evaluated for each disc by comparing the results obtained in two different time points (T0 to T1, T0 to T2, T0 to T3, T1 to T2, T1 to T3, T2 to T3) to judge which of each entitity had the lowest amount (increased degeneration) of the quantitative data (Figure 33). Disc height (Figure 33a) exhibited a significant narrowing at L2-3 IVD space between T0 and T2 and T1 and T2. The disc height of the control disc was significantly reduced when T3 was compared to T0. Statistically significant results were observed in the degree of degeneration obtained by calculating MRi (Figure 34b) for L1-2 ($p< 0.03$: T1-T0), L2-3 ($p< 0.03$: T2-T0), L3-4 ($p< 0.03$: T1-T0; T2-T0; T2-T1; T3-T0; T3-T1) and L4-5 ($p< 0.03$: T2-T0; T3-T0) (Figure 33b). The degree of IVDD significantly increased throughout the experimental period in the four treated disc levels. Not all the time points where involved in the changes and in none of the discs significant degeneration was observed between T2 and T3.

Figure 32. Difference between techniques (Dunn's test)
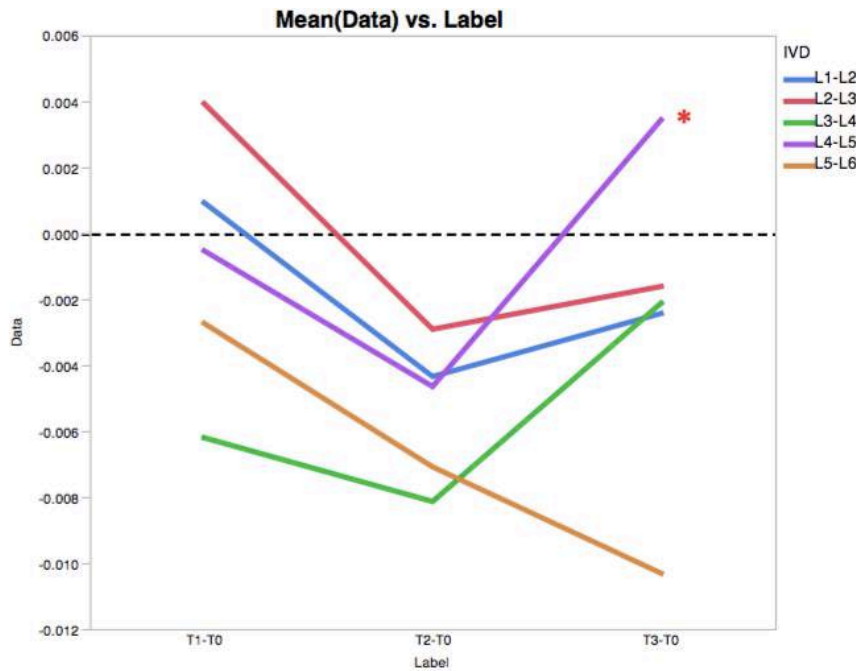
(a) DHi. Changes in the IVD height were assessed quantitaviley and postsurgical results (T1, T2, T3) were normalized to the baseline (T0). When the effect of each technique was analyzed (L1-2: nucleotomy; L2-3: tunnel; L3-4: nucleotomy+scaffold; L4-5: tunnel +scaffold) a narrowing of the disc space was observed at T2 when compared to control; however this was not significant. At T3 the curve shows increasing results, with a significant difference between L4-5 and the control disc.
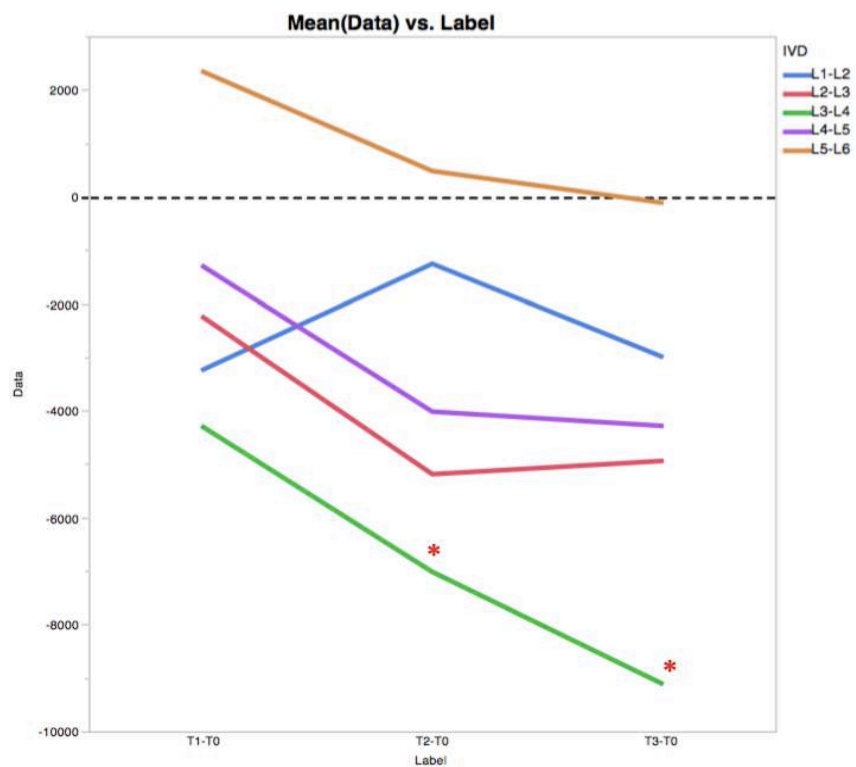
(b) MRi. Statistically significant differences were detected in disc L3-4 (nucleotomy+scaffold) when compared to the control disc. The disc was significantly and progressively more degenerated at time point 2 and 3.

Figure 33. Difference between time points (Wilcoxon test)

Matched Pairs IVD=L1-L2

Wilcoxon Signed Rank

	T1-T0	T2-T0	T2-T1	T3-T0	T3-T1	T3-T2
Test Statistic S	-4.500	-4.500	-3.500	-0.500	-2.500	3.500
Prob>|S|	0.4375	0.4375	0.5625	1.0000	0.6875	0.5625
Prob>S	0.7813	0.7813	0.7188	0.5000	0.6563	0.2813
Prob<S	0.2188	0.2188	0.2813	0.5000	0.3438	0.7188

Matched Pairs IVD=L2-L3

Wilcoxon Signed Rank

	T1-T0	T2-T0	T2-T1	T3-T0	T3-T1	T3-T2
Test Statistic S	5.500	-9.500	-9.500	-1.500	-4.500	6.500
Prob>|S|	0.3125	0.0625	0.0625	0.8438	0.4375	0.2188
Prob>S	0.1563	0.9688	0.9688	0.5781	0.7813	0.1094
* Prob<S	0.8438	0.0313*	0.0313*	0.4219	0.2188	0.8906

Matched Pairs IVD=L3-L4

Wilcoxon Signed Rank

	T1-T0	T2-T0	T2-T1	T3-T0	T3-T1	T3-T2
Test Statistic S	-7.500	-6.500	-3.500	-4.500	3.500	4.500
Prob>|S|	0.1563	0.2188	0.5625	0.4375	0.5625	0.4375
Prob>S	0.9219	0.8906	0.7188	0.7813	0.2813	0.2188
Prob<S	0.0781	0.1094	0.2813	0.2188	0.7188	0.7813

Matched Pairs IVD=L4-L5

Wilcoxon Signed Rank

	T1-T0	T2-T0	T2-T1	T3-T0	T3-T1	T3-T2
Test Statistic S	-0.500	-3.500	-3.500	2.500	5.500	4.500
Prob>|S|	1.0000	0.5625	0.5625	0.6875	0.3125	0.4375
Prob>S	0.5000	0.7188	0.7188	0.3438	0.1563	0.2188
Prob<S	0.5000	0.2813	0.2813	0.6563	0.8438	0.7813

Matched Pairs IVD=L5-L6

Wilcoxon Signed Rank

	T1-T0	T2-T0	T2-T1	T3-T0	T3-T1	T3-T2
Test Statistic S	-7.500	-4.500	-1.500	-7.500	-6.500	-5.500
Prob>|S|	0.1563	0.4375	0.8438	0.0625	0.2188	0.3125
Prob>S	0.9219	0.7813	0.5781	0.9688	0.8906	0.8438
* Prob<S	0.0781	0.2188	0.4219	0.0313*	0.1094	0.1563

Matched Pairs IVD=L1-L2

Wilcoxon Signed Rank

	T1-T0	T2-T0	T2-T1	T3-T0	T3-T1	T3-T2
Test Statistic S	-7.500	-3.500	3.500	-4.500	1.500	-4.500
Prob>|S|	0.0625	0.4375	0.4375	0.3125	0.8125	0.3125
Prob>S	0.9688	0.7813	0.2188	0.8438	0.4063	0.8438
* Prob<S	0.0313*	0.2188	0.7813	0.1563	0.5938	0.1563

Matched Pairs IVD=L2-L3

Wilcoxon Signed Rank

	T1-T0	T2-T0	T2-T1	T3-T0	T3-T1	T3-T2
Test Statistic S	-4.500	-7.500	-4.500	-6.500	-4.500	0.500
Prob>|S|	0.3125	0.0625	0.3125	0.1250	0.3125	1.0000
Prob>S	0.8438	0.9688	0.8438	0.9375	0.8438	0.5000
Prob<S	0.1563	0.0313*	0.1563	0.0625	0.1563	0.5000

Matched Pairs IVD=L3-L4

Wilcoxon Signed Rank

	T1-T0	T2-T0	T2-T1	T3-T0	T3-T1	T3-T2
Test Statistic S	-7.500	-7.500	-7.500	-7.500	-7.500	-5.500
Prob>|S|	0.0625	0.0625	0.0625	0.0625	0.0625	0.0938
Prob>S	0.9688	0.9688	0.9688	0.9688	0.9688	0.9063
* Prob<S	0.0313*	0.0313*	0.0313*	0.0313*	0.0313*	0.0938

Matched Pairs IVD=L4-L5

Wilcoxon Signed Rank

	T1-T0	T2-T0	T2-T1	T3-T0	T3-T1	T3-T2
Test Statistic S	-2.500	-7.500	-1.500	-7.500	-6.500	-1.500
Prob>|S|	0.6250	0.0625	0.8125	0.0625	0.1250	0.8125
Prob>S	0.6875	0.9688	0.5938	0.9688	0.9375	0.5938
* Prob<S	0.3125	0.0313*	0.4063	0.0313*	0.0625	0.4063

Matched Pairs IVD=L5-L6

Wilcoxon Signed Rank

	T1-T0	T2-T0	T2-T1	T3-T0	T3-T1	T3-T2
Test Statistic S	-0.500	-2.500	-4.500	-2.500	-6.500	-3.500
Prob>|S|	1.0000	0.6250	0.6250	0.6250	0.1250	0.4375
Prob>S	0.5000	0.6875	0.8438	0.6875	0.9375	0.7813
Prob<S	0.5000	0.3125	0.1563	0.3125	0.0625	0.2188

(a) DHi. Statistically significant results (P < 0.05) were detected for L3-4 and L5-6 (red asterisk)

(b) MRi. Statistically significan results where detected for the four disc levels where surgery was performed.

DISCUSSION

○ QUALITATIVE ANALYSIS

In the present study, four different IVDD techniques were performed through the transpedicular route in lumbar IVDs of skeletally mature sheep. Different degrees of degeneration were obtained by performing distinct types of surgical approaches to four lumbar IVDs. Through the transpedicular route, the IVDs from L1 to L5 were addressed by performing (1) nucleotomy, (2) tunnel, (3) nucleotomy + PU scaffold and (4) tunnel + PU scaffold, respectively. Variations in IVD degenerative changes were detected by quantitative MRI, macroscopic and histologic evaluations, in order to follow the IVDD process secondary to EP and NP injury.

The 4 transpedicular IVDD models led to slowly progressive MRI changes, similar to those observed in human IVDD. Through the analysis of MRI images, quantitative alterations in IVD hydration or composition can be detected non-invasively with a sufficient degree of accuracy (Boos et al., 1995). Indeed, the signal loss of IVDs on T2w images correlates with progressive degenerative changes of IVDs (Modic et al., 1988), reflecting true biochemical IVDD (Tertti et al., 1991). Furthermore, the brightness of the NP has been demonstrated to correlate directly with PG concentration (Pearce et al., 1991). Over the 6-month experimental period, the NP of all the treated IVDs displayed a progressive decrease of MRI signal intensity in T2w mid-sagittal image, exhibiting different degrees of degeneration in line with the type of treatment performed. According to Pfirrmann grading scale, the control group (L5-6) maintained a grade I of degeneration at all time points; at T3, group L1-2 appeared as grade V, group L2-3 looked as grade III and group L3-4 and L4-5 appeared as grade IV and II, respectively.

These observations were further supported by macroscopic and histologic analysis. Morphologically, progressive increasing in IVD narrowing, fragmentation of the

NP matrix and loss of definition between NP and AF were observed at T3 in correlation to each technique performed. All stages of the degenerative process, from Thompson grade I to grade V, were observed with the same association of the Pfirrmann degenerative grade. The Thompson score reviews different aspects of the IVD (NP, EP and vertebral body) and subsequently a grade is assigned, ranging between I (normal disc) and V (severe degeneration) (Thompson et al., 1990). This scale has been widely accepted as a tool to measure IVDD (Battie and Videman, 2006; Bogduk, 1995), therefore represents a reliable parameter to evaluate IVD changes.

The histologic evaluation to assess IVDD showed a consistency to MRI and macroscopic findings at T3. The correlation between histologic and MRI findings supported the concept that the MRI findings correlate with changes, such as cellularity, and matrix of the NP, and border changes of the NP and AF. Although the MRI machine available for this research had a small magnet, the data obtained suggested that *in vivo* MRI might hold promise for assessing the NP integrity.

The histologic evaluation provided interesting considerations regarding the efficacy of the PU scaffold. Unlike the spinal segments where the tunnel was sealed with the scaffold (L3-4, L4-5), in those segments where the device was not introduced at the EP edge (L1-2 and L2-3), NP tissue was observed within the tunnel with infiltration of inflammatory cells. This observation indicates that the PU scaffold prevents the NP from leaking within the tunnel. This is important for several reasons. The EP damage, caused by the 2-mm tunnel, represents a potential limitation of this technique. Indeed, the importance of the EP for IVD nutrition is well known and a lesion created by the proposed approach might induce Schmorl's nodes, alter the nutrition supply to the centre of the IVD and cause further degeneration (Holm et al., 2004; Urban et al., 2004; Papalia et al., 2015). These changes could be prevented or at least reduced by the use of the scaffold. Furthermore, when drugs, growth factors, stem cells, and viscoelastic biomaterials are delivered into the NP, the sealing of the tunnel would prevent the material from leaking

and might promote the restoration of intradiscal pressure, allowing the realization of biomechanical studies. Scaffolds should provide a three-dimensional matrix for the cells to attach, proliferate and finally form a functional tissue construct. They should exhibit a porous structure with interconnecting pores to allow a rapid and sufficient vascularization (Lashke, 2000). In particular, PU is regarded as a kind of bone repair material for its mechanical property and its special shape memory function. PUs have controlled degradation rate and the degradation time can take few months, which is compatible with the growth rate of osteoblasts (Guelcher et al., 2005; Guelcher et al., 2008). In the present study, evident signs of bone formation, in relation to the presence of the PU scaffold, were not observed; this could be related either to inadequate time for the surrounding cells to proliferate or to inadequate scaffold characteristics. Indeed, the biological quality of the scaffold determines to a great extent the regenerative potential of a tissue. *In vitro*, among the factors determining the cell-scaffold interactions are the biocompatibility of the scaffold's material and its degradation products, the physicochemical characteristics of the scaffold's surface, and the morphology, density, and size of pores in the scaffold (Gugala and Gogolewski, 2005).

The data collected from the qualitative findings suggest that the injury induced in this study is a reliable method for initiating a progressive form of IVDD in the adult sheep, obtaining different grades of IVDD depending on the type of lesion performed. The EP damage itself, caused by the realization of the transpedicular tunnel, led to IVD degenerative changes, although less severe than those caused by performing nucleotomy, which represents a more invasive and aggressive approach to the IVD.

This stepwise model could be suitable for studying pathogenesis and pathophysiology of IDD evaluated at the different stages of degeneration. Moreover, the model could be used to test safety and efficacy of novel treatments for IDD. Since has been proved that the sealing of the tunnel prevents the NP leakage into the cavity, growth factors and drugs could be tested in grade II model (tunnel + PU scaffold), while

biomaterials and cells as well as tissue engineering constructs might be tested in grade IV model (nucleotomy + PU scaffold) (Zhang et al., 2011). Moreover the intact AF would prevent leakage trough the AF allowing also reliable biomechanical tests (Vadalá et al., 2013).

The above mentioned parameters, excluding the histology measures, represent indirect measurements of degeneration; therefore, despite the good correlation disclosed between the different scales, further quantitative analysis were performed to better determine the degenerative changes obtained.

o **QUANTITATIVE ANALYSIS**

The parameters analyzed in the present experiment are commonly used to study IVDD (Krijnen et al., 2006; Loeser, 2002; Masuda et al., 2005; Sobajiama et al., 2005; Sakai et al., 2006). Both the DHi and the MRi are useful tools to quantify the results based on imaging techniques. Over the 6-month duration of the present study, the IVDs exhibited a progressive reduction in both indices if compared to the preoperative values.

MRI currently is the gold standard to evaluate IVDD in the (pre)clinical setting (Vaga et al., 2008). The MRI score and the MRi have been reported to correlate well with IVDD and are used to analyze the MRI images (Lu et al., 2008; Fan et al., 2012). The MRi assesses both the area and the signal intensity of the NP, which are both affected by IVDD (Fan et al., 2012). Three of the treated IVDs (L1-2, L2-3, L4-5) presented a similar reduction in mean MRi at T3 (approximately 30%), whereas the "nucleotomy + PU scaffold" group showed a mean decrease of 57%, which was significantly higher than the control group at T2 and T3, when compared to the baseline. These results may indicate that the degree of degeneration induced was major and more consistent at L3-4, however no significant differences were found when treated discs were compared to each other. The intact control discs (L5-6) of the present model underwent some mild degenerative changes (15%) as well, possibly due to their proximity to and

interaction with the degenerated IVDs (Philips et al., 2002). When the variations of the MRi were evaluated for each treated IVD between the different time points, significant degree of degeneration were detected in all of them, demonstrating the potential effectiveness of each corresponding IVDD model. Interestingly, none of the IVDs presented significant indices variations between T2 and T3, which might indicate that most of the changes occurred during the first months of the study or may be related to the onset of reversal changes or spontaneous recovery between T2 and T3. When interpreting MRi results it is important to consider that several variables may influence the NP average signal intensity and its area. High signal intensity in the NP can be determined not only by the water content, but also by localized fluid collection in a fissure or the vacuum phenomenon (Schweitzer et al., 1998), that could represent rare but potential pitfalls for the assessment of the IVD. Increased NP signal intensity, secondary to the potential inflammatory process triggered by the nucleotomy, may also represent a limit for results interpretation. Limits linked to the outlined NP area could be related to the low field MRI machine and to the fact that the line was drawn manually, leading to reduced images detail and precision, respectively. In addition, the application of a phantom-based method (Luoma et al., 1997) to normalize the signal intensity at the different time points would have increased the accuracy of the MRI measurements.

Controversial results were observed for the DHi. At T3, the DH lost was only between 2 and 9% in 3 of the treated IVDs, whereas L4-5 presented a greater DH. Loss of DH is widely accepted as a measure of IVDD and the DHi enables the quantification of this phenomenon (Miyakoshi et al., 2000; Sasaki et al., 2001; Shao et al., 2002; Masuda et al., 2005). The DHi neutralizes the effects of the sheep size and the magnification of the X-ray, allowing an inter-animal control of these values (Miyakoshi et al., 2000; Sasaki et al., 2001; Shao et al., 2002; Masuda et al., 2004). The curves in Figure 33a are represented by "v-shape" lines, indicating an increased DHi when T3 was compared to T0. This result may imply the presence of spontaneous recovery or reversal

changes with consequent widening of the space. However, this variation must be evaluated cautiously; indeed, for practical reasons a consistent level of anaesthesia was not maintained during radiography of each animal and at each time point, leading to different degrees of muscle relaxation, which may have affected the DHi by causing a false increasing in the DH.

Animal models play a central role in current regenerative or reparative disc response studies (Alini et al., 2008). Different animal species, anatomical sites (spine or tale), and methods to induce IVDD are currently considered adequate to represent human IVD degenerative changes. In the present study, a variable degree of IVDD was induced by performing distinct type of injury, providing different models suitable to study different stages of IVDD in human. The nucleotomy produced a direct and fast damage to the NP, whereas the realization of the transpedicular tunnel through the EP induced a less severe and slower IVD damage. The time course of the modeled IVDD is relevant from several perspectives. The classic stab model developed by Lipson and Muir (1981) results in fast degeneration by immediate herniation of the NP and therefore might not mimic the process of human IVDD. Further, the rapid development of severe degenerative changes in this model does not allow the study of the mild changes occurring in early phase IVDD. Recently, new models have been developed to induce mild and slowly progressive degeneration by a needle puncture (Masuda et al., 2005; Sobajiama et al., 2005). These models provide an excellent and cost-effective method to study new regenerative therapies. However, the rabbit, used in these models, has some shortcomings in its comparability to humans, as it is much smaller and also retains the notochordal cells in the NP in maturity (Hunter et al., 2004). Therefore, a large animal model is needed to study the feasibility of newly developed therapies before moving towards clinical application. The present transpedicular sheep model is suitable for this purpose as it lacks notochordal cells at the skeletally mature age (Hunter et al., 2004) and its IVD has comparable proportions as humans (Reid et al., 2002); furthermore, it provides different

progressive stages of IVDD. To determine whether the induced degeneration is truly mimicking human IVDD, biochemical and biological parameters need to be evaluated.

The present study has a number of limitations that have been partially discussed throughout the text (e.g. EP damage, use of low field MRI, possible imprecisions related to quantitative measures). Further limitations of this model are represented by the fact that, being an injury model, may not truly represent human IVDD, by the measurable costs and by time to generate a consistent IVD injury. In order to study a sufficient number of animals to test a new intervention procedure or a drug, this model is a reasonable testing model, although the results obtained should be confirmed in a larger number of animals.

CONCLUSIONS

The present study has demonstrated the feasibility of the transpedicular approach *in vivo* and its potential for studying IVDD physiopathology and for future clinical applications for delivering drugs, growth factors, stem cells, and viscoelastic biomaterials directly into the NP without affecting the AF. By sealing the transpedicular tunnel with a PU scaffold, will be also possible to perform additional biomechanical studies of the new NP regenerative therapies. Mechanical EP injury and nucleotomy of skeletally mature sheep lumbar IVDs has been performed via the EP route through the transpedicular approach, resulting in different degrees of MRI, radiographic, macroscopic and histologic IVDD changes. The IVDD seemed to occur with specific degrees of degeneration according to the group of surgical treatment at 6-month follow-up. The present IVDD model will be a significant contribution towards the translation to the therapeutic arsenal of new regenerative strategies for biological restoration of degenerative changes in the IVD, which is crucial to improve present clinical treatments and life quality of several patients.

BIBLIOGRAPHY

1. Adams MA, Roughley PJ. What is intervertebral disc degeneration, and what causes it ?. *Spine (Phila Pa 1976)* 2006; 31, 2151- 2161

2. Adler JH, Schoenbaum M, Silberberg R. Early onset of disk degeneration and spondylosis in sand rats (*Psammomys obesus*). *Vet Pathol* 1983; 20, 13–22

3. Ahlgren BD, Vasava MS, Brower RS, Lydon C, Herkowitz MD, Panjabi MM. Anular incision technique on the strength and multidirectional flexibility of the healing intervertebral disc. *Spine* 1994; 19: 948-54

4. Alini M, Eisenstein SM, Ito K, Little C, Kettler AA, Masuda K, Melrose J, Ralphs J, Stokes I, Wilke HJ. Are animal models useful for studying human disc disorders/degeneration?. *Eur Spine J* 2008; 17: 2–19

5. Anderson DG, Izzo MW, Hall DJ, Vaccaro AR, Hilibrand A, Arnold W, Tuan RS, Albert TJ. Comparative gene expression profiling of normal and degenerative discs: analysis of a rabbit annular laceration model. *Spine* 2002; 27, 1291–1296

6. Anderson GD, Li X, Tannoury T, Beck G, Balian G. A fibronectin fragment stimulates intervertebral disc degeneration in vivo. *Spine* 2003; 28: 2338–2345

7. Ando T, Kato F, Mimatsu K, Iwata H. Effects of chon- droitinase ABC on degenerative intervertebral discs. *Clin Orthop Relat Res* 1995; 318: 214–221

8. Antoniou J, Steffen T, Nelson F, Winterbottom N, Hollander AP, Poole RA, Aebi M, Alini M. The human lumbar intervertebral disc: evidence for changes in the biosynthesis and denaturation of the extracellular matrix with growth, maturation, ageing, and degeneration. *J Clin Invest* 1996; 98: 996-1003

9. Ariga K, Miyamoto S, Nakase T, Okuda S, Meng W, Yonenobu K, Yoshikawa H. The relationship between apoptosis of endplate chondrocytes and aging and degeneration of the intervertebral disc. *Spine*, 2001; 26: 2414 –20

10. Arya S, Crow WN, Hadjipavlou AG, Nauta HJW, Borowski AM, Vierra LA, Walser E. Percutaneous transpedicular management of discitis. *J Vasc Interv Radiol* 1996; 7: 921-927

11. Aszodi A, Chan D, Hunziker E, Bateman JF, Fassler R. Collagen II is essential for the removal of the notochord and the formation of intervertebral discs. *J Cell Biol* 1998; 143, 1399-1412

12. Baramki HG, Papin P, Steffen T. A surgical approach to the ventral aspect of the lumbar vertebrae in the sheep model. *Surg Radiol Anat* 2000; 22: 25-27

13. Barone R (2004). *Anatomie comparée des mammiféres domestiques*. Paris, Vigot

14. Battié MC, Videman T, Gibbons LE, Manninen H, Gill K, Pope M, Kaprio J. Occupational driving and lumbar disc degeneration: a case-control study. *Lancet* 2002; 360: 1369-74

15. Bayliss MT, Johnstone B, O'Brien JP. 1988 Volvo award in basic science. Proteoglycan synthesis in the human intervertebral disc. Variation with age, region and pathology. *Spine* 1988; 13: 972-81.

16. Benjamin M, Rufal A, Ralphs JR. The mechanism of formation of bony spurs (enthesophytes) in the Achilles tendon. *Arthritis Rheum* 2000; 43: 576-583

17. Berry RJ. Genetical studies on the skeleton of the mouse 26. Pintail. *Genet Res* 1960; 1:439–451

18. Bloebaum RD, Kopp DV. Remodeling capacity of calcified fibrocartilage of the hip. *Anat Rec* 2004; 279: 736-739

19. Blummenkrantz G, Lindsey CT, Dunn TC, Jin H, Ries MD, Link TM, Steinbach LS, Majumdar S. A pilot, two-year longitudinal study of the interrelationship between trabecular bone and articular cartilage in the osteoarthritic knee. *Osteoarthritis Cartilage* 2004; 12, 977-1005

20. Boden SD, Davis DO, Dina TS, Patronas NJ, Wiesel SW. Abnormal magnetic-resonance scans of the lumbar spine in asymptomatic subjects. A prospective investigation. *J Bone Joint Surg Am* 1990; 72: 403–408

21. Bogdanffy GM, Ohnmeiss DD, Guyer RD. Early changes in bone mineral density above a combined antero-posterior L4-S1 lumbar spinal fusion: a clinical investigation. *Spine* 1995; 20:1674-8

22. Bogduk N. The anatomical basis for spinal pain syndromes. *J.Manipulative Physiol Ther* 1995; 18: 603-5

23. Boos N, Rieder R, Schade V, Spratt KF, Semmer N, Aebi M. Volvo Award in clinical sciences. The diagnostic accuracy of magnetic resonance imaging, work perception, and psychosocial factors in identifying symptomatic disc herniations. *Spine* 1995; 20: 2613-2625

24. Boos N, Weissbach S, Rohrbach H, Weiler C , Spratt KF, Nerlich AG. Classification of age-related changes in lumbar intervertebral discs: 2002 Volvo Award in basic science. *Spine* 2002; 27:2631-2644

25. Boos N, Weissbach S, Rohrbach H, Weiler C, Spratt KF, Nerlich AG. Classification of age-related changes in lumbar intervertebral discs: 2002 Volvo Award in basic science. *Spine* 2002; 27: 2631–44

26. Bowles, R. D., Williams, R. M., Zipfel, W. R. and Bonassar, L. J. (2010). Self-assembly of aligned tissue-engineered annulus fibrosus and intervertebral disc composite via collagen gel contraction. *Tissue Eng. Part A*. 16, 1339-1348

27. Boyce TM, Bloebaum RD. Cortical aging differences and fracture implications for the human femoral neck. *Bone* 1993; 14: 769-778

28. Braund KG (1974). *Some aspects of structure and function of the canine intervertebral disc.* Ph.D. thesis, University of Sydney

29. Brittberg M, Lindahl A, Nilsson A, Ohlsson C, Isaksson O, Peterson L. Treatment of deep cartilage defects in the knee with autologous chondrocyte transplantation. *N Engl J Med* 1994; 331: 889-895

30. Bruehlmann SB, Rattner JB, Matyas JR, Duncan NA. Regional variations in the cellular matrix of the annulus fibrosus of the intervertebral disc. *J Anat* 2002; 201: 159-171

31. Buckwalter JA. Aging and degeneration of the human intervertebral disc. *Spine* 1995; 20: 1307–14

32. Burkus JK, Zdeblick TA (2004). *Lumbar disc disease*. Frymoyer JW, Wiesel SW, editors. The adult & pediatric spine. 844-899. Philadelphia, Lippincott, Williams & Wilkins

33. Butler WF (1989) .*Comparative anatomy and development of the mammalian disc.* In *The Biology of the Intervertebral Disc* (ed. Gosh P), pp. 84–108. Boca Raton: CRC Press

34. Cappello R, Bird JL, Pfeiffer D, Bayliss MT, Dudhia J. Notochordal cell produce and assemble extracellular matrix in a distinct manner, which may be responsible for the maintenance of healthy nucleus pulposus. *Spine* 2006; 31, 873-882

35. Carragee EJ, Don AS, Hurwitz EL, Cuellar JM, Carrino JA, Herzog R. 2009 ISSLS prize winner: does discography cause accelerated progression of degeneration changes in the lumbar disc: a ten-year matched cohort study. *Spine (Phila Pa 1976)* 2009; 34: 2338 – 45

36. Cassidy JD, Yong-Hing K, Kirkaldy-Willis WH, Wilkinson AA. A study of the effects of bipedism and upright posture on the lumbosacral spine and paravertebral muscles of the Wistar rat. *Spine* 1988; 13: 301–308

37. Cavanaugh JM. Neural mechanisms of lumbar pain. *Spine* 1995; 20: 1804-1809

38. Chanchairujira K, Chung CB, Kim JY, Papakonstantinou O, Lee MH, Clopton P, Resnick D. Intervertebral disk calcification of the spine in an elderly population: radiographic prevalence, location, and distribution and correlation with spinal degeneration. *Radiology* 2004; 230: 499-503

39. Cheng XG, Brys P, Nijs J, Nicholson P, Jiang Y, Baert AL, Dequeker J. Radiological prevalence of lumbar   intervertebral disc calcification in the elderly: an autopsy study. *Skeletal Radiol* 1996; 25: 231-5

40. Cheung KM, Lu DS, Poon AM, Wang T, Luk KD, Leong JC. Effect of melatonin suppression on scoliosis develop ment in chickens by either constant light or surgical pinealectomy. *Spine* 2003; 28: 1941–1944

41. Choi KS, Cohn MJ, Harfe BD. Identification of nucleus pulposus precursor cells and notochordal remnants in the mouse: implications for disk degeneration and chordoma formation. *Dev Dyn* 2008; 237, 3953-3958

42. Cole TC, Burkhardt D, Frost L, Ghosh P. The proteo- glycans of the canine intervertebral disc. *Biochim Biophys Acta* 1985 (a); 839: 127–138

43. Cole TC, Burkhardt D, Ghosh P, Ryan M, Taylor T. Effects of spinal fusion on the proteoglycans of the canine intervertebral disc. *J Orthop Res* 1985 (b); 3: 277–291

44. Coppes MH, Marani E, Thomeer RT, Groen GJ. Innervation of "painful" lumbar discs. *Spine*, 1997; 22: 2342– 2349.

45. Crock HV, Goldwasser M, Yoshizawa H (1991). Vascular anatomy related to the intervertebral disc. In: Biology of the Intervertebral Disc. Edited by Ghosh P. Boca Raton: CRC Press

46. Depalma AF, Kruper JS. Long-term study of shoulder joints afflicted with and treated for calcific tendinitis. *Clin Orthop Relat Res* 1961; 20:61-72

47. Di Martino A, Papapietro N, Lanotte A, Russo F, Vadalá G, Denaro V. Spondylodiscitis standards of current treatment. *Curr Med Res Opin* 2012; 2: 689–99

48. Diamant B, Karlsson, Nachemson A. Correlation between lactate levels and pH in discs of patients with lumbar rhizopathies. *Experientia* 1986; 24, 1159-1196

49. Drissi H, Zuscik M, Rosier R, O'Keefe R. Transcriptional regulation of chondrocyte maturation: potential involvement of transcription factors in OA pathogenesis. *Mol Aspects Med* 2005; 26, 169-179

50. Duance VC, Crean JK, Sims TJ, Avery N, Smith S, Menage J, Eisenstein SM, Roberts S. Changes in collagen cross-linking in degenerative disc disease and scoliosis. *Spine* 1998; 23: 2545-2551

51. Dullerud R, Nakstad PH. Side effects and complications of automated percutaneous lumbar nucleotomy. *Neuroradiology* 1997; 39: 282-285

52. Eck JC, Humphreys SC, Hodges SD. Adjacent-segment degeneration after lumbar fusion: a review of clinical, biomechanical, and radiologic studies. *Am J Orthop*, 1999, 28: 336-340

53. Eglin D, Griffon S, Alini M. Thiol-containing degradable poly(thiourethane-urethane)s for tissue engineering . *J Biomater Sci Polym Ed*, 2010; 21: 477 – 91

54. Eijkelkamp MF, et al. (2002) *On the development of an artificial intervertebral disc.* Faculty of Medical Sciences, Thesis. Groningen, The Netherlands: University of Groningen; 2002: 106

55. Elliott DM, Sarver JJ. Young investigator award winner: validation of the mouse and rat disc as mechanical models of the human lumbar disc. *Spine* 2004; 29: 713-22

56. Elliott DM, Yerramalli CS, Beckstein JC, Boxberger JI, Johannessen W, Vresilovic EJ. The effect of relative needle diameter in puncture and sham injection animal models of degeneration. *Spine (Phila Pa 1976)* 2008; 33: 588–96

57. Errington RJ, Puustjarvi K, White IR, Roberts S, Urban JP. Characterisation of cytoplasm-filled processes in cells of the intervertebral disc. *J Anat* 1998; 192: 369-378

58. Eyre DR, Muir H. Quantitative analysis of types I and II collagens in human intervertebral discs at various ages. Biochimi Biophys Acta 1977; 27: 29-42

59. Eyre DR, Wu JJ, Fernandes RJ, Pietka TA, Weis MA. Recent developments in cartilage research: matrix biology of the collagen II/IX/XI heterofibril network. *Biochem Soc Trans* 2001; 30: 93-899

60. Eyre DR, Wu JJ, Fernandes RJ, Pietka TA, Weis MA. Recent developments in cartilage research: matrix biology of the collagen II/IX/XI heterofibril network. *Biochem Soc Trans* 2001; 30: 893-899

61. Fan SW, Zhou ZJ, Hu ZJ, Fang XQ, Zhao FD, Zhang J. Quantitative MRI analysis of the surface area, signal intensity and MRI index of the central bright area for the evaluation of early adjacent disc degeneration after lumbar fusion. *Eur Spine J* 2012; 21: 1709-1715

62. Farrar MJ, Walker A, Cowling P. Possible salmonella osteomyelitis of spine following laser disc decompression. *Eur Spine J* 1998; 7: 509-511

63. Fazzalari NL, Costi JJ, Hearn TC, Fraser RD, Vernon-Roberts B, Hutchinson J, Manthey BA, Parkinson IH, Sinclair C. Mechanical and pathologic consequences of induced concentric anular tears in an ovine model. *Spine* 2001; 26: 2575– 81

64. Feinberg J, Boachie-Adjei O, Bullough PG, Boskey AL. The distribution of calcific deposits in intervertebral discs of the lumbosacral spine. *Clin Orthop Relat Res* 1990; 254, 303-310

65. Feinberg J, Boachie-Adjei O, Bullough PG, Boskey AL. The distribution of calcific deposits in intervertebral discs of the lumbosacral spine. *Clin Orthop Relat Res* 1990; 254: 303-10.

66. Ferguson SJ, Steffen T. Biomechanics of the aging spine. *Eur Spine J* 2003; 12 (suppl 2): S97–103

67. Fleming A, Keynes RJ, Tannahill D. The role of the notochord in vertebral column formation. *Anat* 2001; 199, 177-180

68. Foster MR, Allen MJ, Schoonmaker JE, Yuan HA, Kanazawa A, Park SA, Liu B. Characterization of a developing lumbar arthrodesis in a sheep model with quantitative instability. *Spine J* 2002; 2: 244-50

69. Freemont AJ, Peacock TE, Goupille P, Hoyland JA, O'Brien J, Jayson MI. Nerve ingrowth into diseased intervertebral disc in chronic back pain. *Lancet*, 1997; 350: 178–181

70. Freemont AJ, Watkins A, Le Maitre C, Baird P, Jeziorska M, Knight MT, Ross ER, O'Brian JP, Hoyland JA. Nerve growth factor expression and innervation of the painful intervertebral disc. *J Pathol* 2002; 197: 286–292

71. Freemont AJ. The cellular pathobiology of the degenerate intervertebral disc and discogenic back pain. *Rheumatology (Oxford)*, 2009; 48: 5–10

72. Frick SL, Hanley EN Jr, Meyer RA Jr, Ramp WK, Chapman TM. Lumbar intervertebral disc transfer. A canine study. *Spine* 1994; 19: 1826-34.

73. Frick SL, Hanley EN, Meyer RA, Ramp WK Jr, Chapman TM Jr. Lumbar intervertebral disc transfer. A canine study. *Spine* 1994; 19, 1826–1834

74. Furuya S, Ohtsuki T, Yabe Y, Hosoda Y. Ultrastructural study on calcification of cartilage: comparing ICR and twy mice. *J Bone Miner Metab* 2000; 18:140–147

75. Ganey T, Libera J, Moos V, Alasevic O, Fritsch KG, Meisel HJ, Hutton WC. Disc chondrocyte transplantation in a canine model: a treatment for degenerated or damaged intervertebral disc. *Spine* 2003; 28, 2609–2620

76. Ghosh P, Taylor TK, Braund KG, Larsen LH. The collagenous and non-collagenous protein of the canine intervertebral disc and their variation with age, spinal level and breed. *Gerontology* 1976; 22: 124–34

77. Glant TT, Mikecz K, Arzoumanian A, Poole AR. Proteoglycan-induced arthritis in BALB/c mice. Clinical features and histopathology. *Arthritis Rheum* 1987; 30: 201–212

78. Goel VK, Gilbertson LG. Basic science of spinal instrumentation. *Clin Orthop* 1997; 335: 10-31

79. Green TP, Adams MA, Dolan P. Tensile properties of the anulus fibrosus: Ultimate tensile strength and fatigue life. *Eur Spine J* 1993; 2: 209 -14

80. Groen GJ, Baljet B, Drukker J. Nerves and nerve plexuses of the human vertebral column. *Am J Anat* 1990; 188: 282 – 296

81. Gruber HE, Hanley EN Jr. Ultrastructure of the human intervertebral disc during aging and degeneration: comparison of surgical and control specimens. *Spine* 2002; 27: 798–805

82. Gruber HE, Hanley EN. Analysis of aging and degeneration of the human intervertebral disc - Comparison of surgical specimens with normal controls. *Spine* 1998; 23:751-757

83. Guehring T, Nerlich A, Kroeber M, Richter W, Omlor GW. Sensitivity of notochordal disc cells to mechanical loading: an experimental animal study. *Eur Spine J* 2010; 19, 113-121

84. Guelcher SA, Gallagher K. Synthesis of biocompatible segmented polyurethanes from aliphatic diisocyanates and diureadiol chain extenders. *Acta Biomaterialia* 2005; 1, 471−484

85. Guelcher SA. Synthesis, mechanical properties, bio- compatibility, and biodegradation of polyurethane networks from lysine polyisocyanates. *Biomaterials* 2008; 29, 1762−1775

86. Gugala Z, Gogolewski S. The in vitro growth and activity of sheep osteoblasts on three-dimensional scaffolds from poly(L/DL-lactide) 80/20%. *J Biomed Mater Res A* 2005; 75: 702-9

87. Guyer RD, Ohnmeiss DD, Mason SL, Shelokov QP. Complications of cervical discography: findings in a large series. *J Spinal Disord* 1997; 10: 95-101

88. Hadjipavlou AG, Crow WN, Borowski A, Mader JT, Adesokan A, Jensen RE. Percutaneous transpedicular discectomy and drainage in pyogenic spondylodiscitis. *Am J Orthop (Belle Mead NJ)* 1998 (a); 27: 188–97

89. Hadjipavlou AG, Simmons JW, Yang JP, Bi LX, Ansari GA, Kaphalia BS, Simmons DJ, Nicodemus CL, Necessary JT, Lane R, Esch O. Torsional injury resulting in disc degeneration: I. An in vivo rabbit model. *J Spinal Disord* 1998 (b); 11: 312–317

90. Haefeli M, Kalberer F, Saefesser D, Nerlich AG, Boos N, Paesolf G. The course of macroscopic degeneration in the human lumbar intervertebral disc. *Spine* 2006; 31, 1522-1531

91. Hammer RE, Maika SD, Richardson JA, Tang JP, Taurog JD. Spontaneous inflammatory disease in transgenic rats expressing HLA-B27 and human beta 2m: an animal model of HLA-B27-associated human disorders. *Cell* 1990; 63: 1099–1112

92. Hamrick MW, Pennington C, Byron CD. Bone architecture and disc degeneration in the lumbar spine of mice lacking GDF-8 (myostatin). *J Orthop Res* 2003; 21: 1025–1032

93. Hansen HJ. A pathologic-anatomical interpretation of disc degeneration in dogs. *Acta Orthop Scand* 1952; 20, 280-293

94. Hansen HJ. A pathologic-anatomical interpretation of disc degeneration in dogs. *Acta Orthop Scand* 1951; 20: 280 – 93

95. Hansen HJ. Comparative views on the pathology of disk degeneration in animals. *Lab Invest* 1959; 8, 1242–1265

96. Harnsberger HR, Osborn AG, Macdonald AJ, Ross JS (2006). Diagnostic and surgical Imaging anatomy. Salt Lake City Utah: Amirsys

97. Hastreiter D, Ozuna RM, Spector M. Regional variations in certain cellular characteristics in human lumbar intervertebral discs, including the presence of alpha-smooth muscle actin. *J Orthop Res* 2001; 19:597-604

98. Heggeness MH, Doherty BJ. Discography causes end plate deflection. *Spine* 1993; 18: 1050–1053

99. Heikkila JK, Koskenvuo M, Heliovaara M, Kurppa K, Riihimaki H, Heikkila K, Rita H, Videman T. Genetic and environmental factors in sciatica. Evidence from a nationwide panel of 9365 adult twin pairs. *Ann Med* 1989; 21: 393-398

100. Herkowitz HN. Point of view. *Spine* 1994; 19: 1444

101. Higuchi M, Abe K, Kaneda K. Changes in the nucleus pulposus of the intervertebral disc in bipedal mice. A light and electron microscopic study. *Clin Orthop Relat Res* 1983; 175:251–257

102. Hollander AP, Heathfield TF, Liu JJ, Pidoux I, Roughley PJ, Mort JS, Poole AR. Enhanced denaturation of the alpha (II) chains of type-II collagen in normal adult human intervertebral discs compared with femoral articular cartilage. *J Orthop Res* 1996, 14:61-66

103. Holm S, Holm AK, Ekstro̊m L, Karladani A, Hansson T. Experimental disc degeneration due to endplate injury. *J Spinal Disord Tech* 2004; 17:64–71

104. Holm S, Nachemson A. Nutrition of the intervertebral disc: acute effects of cigarette smoking. An experimental animal study. *Ups J Med Sci* 1988; 93: 91-99

105. Holm S, Nachemson A. Nutritional changes in the canine intervertebral disc after spinal fusion. *Clin Orthop* 1982; 169: 243-258

106. Holm S, Nachemson A. Variation in the nutrition of the canine intervertebral disc induced by motion. *Spine* 1983; 8: 866-874

107. Horner HA, Urban JP. 2001 Volvo Award Winner in Basic Science Studies: effect of nutrient supply on the viability of cells from the nucleus pulposus of the intervertebral disc. *Spine* 2001; 26: 2543-9

108. Horner HA, Urban JP. 2001 Volvo Award Winner in Basic Science Studies: effect of nutrient supply on the viability of cells from the nucleus pulposus of the intervertebral disc. *Spine* 2001; 26: 2543-9

109. Horwitz T (1977) The Human Notochord: a Study of its Development and Regression, Variations, and Pathologic Derivative, Chordoma. Indianapolis: Horwitz

110.	Hsieh AH, D Hwang, DA Ryan, AK Freeman, H Kim. Degenerative anular changes induced by puncture are associated with insufficiency of disc biomechanical function. *Spine (Phila Pa 1976)* 2009; 34: 998 – 1005

111.	Huang CY, Gu WY. Effects of mechanical compression on metabolism and distribution of oxygen and lactate in intervertebral disc. *J Biomech* 2008; 41, 1184-1196

112.	Hughes SPF, Freemont AJ, DWL Hukins, McGregor AH, Roberts S. The pathogenesis of degeneration of the intervertebral disc and emerging therapies in the management of back pain. *J Bone Joint Surg Br* 2012; 94-b, 1298-1304

113.	Hunter CJ, Matyas JR, Duncan NA. Cytomorphology of notochordal and chondrocytic cells from the nucleus pulposus: a species comparison. *J Anat* 2004; 205, 357-362

114.	Hunter CJ, Matyas JR, Duncan NA. Cytomorphology of notochordal and chondrocytic cells from the nucleus pulposus: a species comparison. *J Anat* 2004; 205: 357-62

115.	Hunter CJ, Matyas JR, Duncan NA. The notochordal cell in the nucleus pulposus: a review in the context of tissue engineering. *Tissue Eng* 2003 (a); 9, 667- 677

116.	Hunter CJ, Matyas JR, Duncan NA. The three-dimensional architecture of the notochordal nucleus pulposus: novel observations on cell structures in the canine intervertebral disc. *J Anat* 2003b; 202, 279-291

117.	Hurri H, Karppinen J. Discogenic pain. *Pain* 2004; 112: 225–228

118.	Hutton WC, Ganey TM, Elmer WA, Kozlowska E, Ugbo JL, Doh ES, Whitesides TE Jr. Does long-term compressive loading on the intervertebral disc cause degeneration? *Spine* 2000; 25, 2993–3004

119.	Iatridis JC, Mente PL, Stokes IA, Aronsson DD, Alini M. Compression-induced changes in intervertebral disc proper- ties in a rat tail model. *Spine* 1999; 24, 996–1002

120.	Iatridis JC, Mente PL, Stokes IA, Aronsson DD, Alini M. Compression-induced changes in intervertebral disc properties in a rat tail model. *Spine* 1999; 24: 996-1002.

121.	Iatridis JC, Michalek AJ, Purmessur D, Korecki CL. Localized intervertebral disc injury leads to organ level changes in structure, cellularity, and biosynthesis. *Cell Mol Bioeng* 2009; 2: 437 – 47

122.	Inoue H. Three-dimensional architecture of lumbar intervertebral discs. *Spine* 1981; 6:139-146

123.	Ishihara H, Urban JP. Effects of low oxygen concentrations and metabolic inhibitors on proteoglycan and protein synthesis rates in the intervertebral disc. *J Orthop Res* 1999; 17:829-835

124.	Johnson WE, Evans H, Menage J, Eisenstein SM, El Haj A, Roberts S. Immunohistochemical detection of Schwann cells in innervated and vascularized human intervertebral discs. *Spine*, 2001; 26: 2550-2557

125. Johnstone B, Bayliss MT. The large proteoglycans of the human intervertebral disc. Changes in their biosynthesis and structure with age, topography, and pathology. *Spine* 1995; 20: 674-684.

126. Kaapa E, Han X, Holm S, Peltonen J, Takala T, Vanharanta . Collagen synthesis and types I, III, IV, and VI collagens in an animal model of disc degeneration. *Spine* 1995; 20: 59–66

127. Kaapa E, Holm S, Han X, Takala T, Kovanen V, Vanharanta H. Collagens in the injured porcine intervertebral disc. *J Orthop Res* 1994; 12: 93–102

128. Kadoya K, Kotani Y, Abumi K, Takada T, Shimamoto N, Shikinami Y, Kadosawa T, Kaneda K. Biomechanical and morphologic evaluation of a three-dimensional fabric sheep artificial intervertebral disc: in vitro and in vivo analysis. *Spine* 2001; 26, 1562–1569

129. Kaigle AM, Holm SH, Hansson TH. 1997 Volvo Award winner in biomechanical studies. Kinematic behavior of the porcine lumbar spine: a chronic lesion model. *Spine* 1997; 22: 2796– 2806

130. Kaigle AM, Holm SH, Hansson TH. Experimental instability in the lumbar spine. *Spine* 1995; 20: 421–430

131. Kalson NS, Richardson S, Hoyland JA. Strategies for regeneration of the intervertebral disc. *Regen Med* 2008; 3: 717-29

132. Kandziora F, Pflugmacher R, Scholz M, Schnake K, Lucke M, Schröder R, Mittlmeier T. Comparison between sheep and human cervical spines. *Spine* 2001; 26: 1028-37

133. Kang JD, Georgescu HI, McIntyre-Larkin L, Stefanovic-Racic M, Donaldson WF, Evans CH. Herniated lumbar intervertebral discs spontaneously produced matrix metalloproteinases, nitric oxide, interleukin-6, and prostag- landin E2. *Spine* 1996; 21: 271-277

134. Kathmann I, Cizinauskas S, Rytz U, Lang J, Jaggy A. Spontaneous lumbar intervertebral disc protrusion in cats: literature review and case presentations. *J Feline Med Surg* 2000; 2, 207–212

135. Katsuura A, Hukuda S. Experimental study of intervertebral disc allografting in the dog. *Spine* 1994; 19, 2426–2432

136. Kauppila LI, McAlindon T, Evans S, Wilson PW, Kiel D, Felson DT. Disc degeneration/back pain and calcification of the abdominal aorta. A 25-year follow-up study in Framingham. *Spine*, 1997 (a); 22 1642-1647

137. Kauppila LI. Prevalence of stenotic changes in arteries supplying the lumbar spine. A postmortem angiographic study on 140 subjects. *Ann Rheum Dis*, 1997 (b); 56: 591-595

138. Kawakami M, Tamaki T, Weinstein JN, Hashizume H, Nishi H, Meller ST. Pathomechanism of pain-related behavior r produced by allografts of intervertebral disc in the rat. *Spine* 1996; 21: 2101-2107

139. Kawchuk GN, Kaigle AM, Holm SH, Rod FO, Ekstrom L, Hansson T. The diagnostic performance of vertebral displacement measurements derived from ultrasonic indentation in an in vivo model of degenerative disc dis- ease. *Spine* 2001; 26, 1348–1355

140.   Kim KS, Yoon ST, Li J, Park JS, Hutton WC. Disc degeneration in the rabbit: a biochemical and radiological comparison between four disc injury models. Spine 2005 (a) 30: 33–37

141.   Kim KW, Ha KY, Park JB, Woo YK, Chung HN, An HS. Expressions of membrane-type I matrix metalloproteinase, Ki- 67 protein, and type II collagen by chondrocytes migrating from cartilage endplate into nucleus pulposus in rat intervertebral discs: a cartilage endplate-fracture model using an intervertebral disc organ culture. *Spine* 2005 (b); 30: 1373–1378

142.   Kim KW, Lim TH, Kim JG, Jeong ST, Masuda K, An HS. The origin of chondrocytes in the nucleus pulposus and histologic findings associated with the transition of a notochordal nucleus pulposus to a fibrocartilaginous nucleus pulposus in intact rabbit intervertebral discs. *Spine 2003;* 28, 982-990

143.   Kimura T, Nakata K, Tsumaki N, Miyamoto S, Matsui Y, Ebara S, Ochi T. Progressive degeneration of articular cartilage and intervertebral discs. An experimental study in transgenic mice bearing a type IX collagen mutation. *Int Orthop* 1996; 20: 177– 181

144.   Korecki CL, Costi JJ, Iatridis JC. Needle puncture injury affects intervertebral disc mechanics and biology in an organ culture model. *Spine (Phila Pa 1976)* 2008; 33: 235 – 41

145.   Krijnen MR, Valstar ER, Smit TH, Wuisman OI. Does bioresorbable cage material influence segment stability in spinal interbody fusion?. *Clin Orthop Relat Res* 2006; 448: 33-8

146.   Kroeber M, Unglaub F, Guehring T, Nerlich A, Hadi T, Lotz J, Carstens C. Effects of controlled dynamic disc distraction on degenerated intervertebral discs: an in vivo study on the rabbit lumbar spine model. *Spine* 2005; 30: 181–187

147.   Kroeber MW, Unglaub F, Wang HL, Schmid C, Thomsen M, Nerlich A, Richter W. New in vivo animal model to create intervertebral disc degeneration and to investigate the effects of therapeutic strategies to stimulate disc regeneration. *Spine* 2002; 27: 2684–2690

148.   Laschke MW, Strohe A, Scheuer C, Eglin D, Verrier S, Alini M, Pohlemann T, Menger MD. In vivo biocompatibility and vascularization of biodegradable porous polyurethane scaffolds for tissue engineering. *Acta Biomater* 2009; 5: 1991-2001

149.   Latorre A, Albareda J, Castiella T, Lasierra JM, Seral F. Experimental model of multidirectional disc hernia in rats. *Int Orthop* 1998; 22: 44–48

150.   Lauerman WC, Platenberg RC, Cain JE, Deeney VF. Age-related disk degeneration: preliminary report of a naturally occurring baboon model. *J Spinal Disord* 1992; 5: 170–174

151.   Leung VY, Chan D, Cheung KMC. Regeneration of intervertebral disc by mesenchymal stem cells: potentials, limitations, and future direction. Eur Spine J 2006; 15: S406-413

152.   Lipson SJ, Muir H. 1980 Volvo award in basic science. Proteoglycans in experimental intervertebral disc degeneration. *Spine* 1981; 6: 194–210

153.   Lipson SJ, Muir H. Vertebral osteophyte formation in experimental disc degeneration. Morphologic and proteoglycan changes over time. *Arthritis Rheum* 1980; 23: 319–324

154.   Loeser RF. Integrins and cell signaling in chondrocytes. *Biorheology* 2002; 39:119-24

155.   Lori DN, MacLeay JM, Turner AS. Variation in the lumbar spine of the mature ewe: a descriptive study. *Vet Radiol Ultrasound* 2005; 46: 105–107

156.   Lotz J, Colliou O, Chin J, Duncan NA, Liebenberg E. Compression-induced degeneration of the intervertebral disc: an in vivo mouse model and finite-element study. *Spine* 1998; 23: 2493–506

157.   Lotz JC, Chin JR. Intervertebral disc cell death is dependent on the magnitude and duration of spinal loading. *Spine* 2000; 25, 1477–1483

158.   Lotz JC, Hsieh AH, Walsh AL, Palmer EI, Chin JR. Mechanobiology of the intervertebral disc. *Biochem Soc Trans* 2002; 30: 853–8

159.   Lotz JC. Animal models of intervertebral disc degeneration: lessons learned. *Spine*, 2004; 29: 2742 – 50

160.   Lu ZF, Zandieh DB, Wuisman PI, Bank RA, Helder MN. Influence of collagen type II and nucleus pulposus cells on aggregation and differentiation of adipose tissue-derived stem cells. *J Cell Mol Med* 2008; 12: 2812-22

161.   Lucio E, Adesokan A, Hadjipavlou AG, Crow WN, Adegboyega PA. Pyogenic spondylodiskitis: A radiologic/pathologic and culture correlation studies. *Arch Pathol Lab Med* 2000; 124: 712-716

162.   Ludwinski FE, Gnanalingham K, Richardson SM, Hoyland JA. Understanding the native nucleus pulposus cell phenotype has important implications for intervertebral disc regeneration strategies. *Regen Med* 2013; 8: 75-87. 2013

163.   Lundin O, Ekstrom L, Hellstrom M, Holm S, Sward L. Exposure of the porcine spine to mechanical compression: differences in injury pattern between adolescents and adults. *Eur Spine J* 2000; 9: 466–471

164.   Lundin O, Ekstrom L, Hellstrom M, Holm S, Sward L. Injuries in the adolescent porcine spine exposed to mechanical compression. *Spine* 1998; 23: 2574–2579

165.   Luo X, Pietrobon R, Sun SX, Liu GG, Hey L. Estimates and patterns of direct health care expenditures among individuals with back pan in the United States. *Spine*, 2004; 29: 79-86

166.   Luoma EK, Raininko R, Nummi PJ, Luukkonen R, Manninen HI, Riihimaki. Suitability of cerebrospinal fluid as a signal-intensity reference on MRI: evaluation of signal-intensity variations in the lumbosacral dural sac. *Neuroradiology* 1997; 39: 728-732

167.   Lyons G, Eisenstein SM, Sweet MB. Biochemical changes in intervertebral disc degeneration. *Biochim Biophys Acta* 1981; 673:443-453

168.   Machida M, Dubousset J, Imamura Y, Iwaya T, Yamada T, Kimura. Role of melatonin deficiency in the develop- ment of scoliosis in pinealectomised chickens. *J Bone Joint Surg Br* 1995; 77:v134–138

169.   Machida M, Dubousset J, Imamura Y, Iwaya T, Yamada T, Kimura J. An experimental study in chickens for the pathogenesis of idiopathic scoliosis. *Spine* 1993; 18: 1609–1615

170.   Machida M, Murai I, Miyashita Y, Dubousset J, Yamada T, Kimura J. Pathogenesis of idiopathic scoliosis. Experimental study in rats. *Spine* 1999; 24: v1985–1989

171.   MacLean JJ, Lee CR, Grad S, Ito K, Alini M, Iatridis JC. Effects of immobilization and dynamic compression on intervertebral disc cell gene expression in vivo. *Spine* 2003; 28, 973–981

172.   Maeda S, Kokubun S. Changes with age in proteoglycan synthesis in cells cultured in vitro from the inner and outer rabbit annulus fibrosus. Responses to interleukin-1 and interleukin-1 receptor antagonist protein. *Spine* 2000; 25: 166-9.

173.   Mageed M, Berner D, Jülke H, Hohaus C, Brehm W, Gerlach K. Is sheep lumbar spine a suitablet alternative model for human spinal research? Morphometrical comparison study. *Lab Anim Res* 2013; 29: 183-189

174.   Maldonado BA, Oegema TRJ. Initial characterization of the metabolism of intervertebral disc cells encapsulated in microspheres. *J Orthop Res* 1992; 10, 677–690

175.   Marchand F, Ahmed AM. Investigation of the laminate structure of lumbar disc anulus fibrosus. *Spine* 1990, 15: 402-410

176.   Maroudas A, Nachemson A, Stockwell R, Urban J. Some factors involved in the nutrition of the intervertebral disc. *J Anat* 1975; 120: 113-130

177.   Mason RM, Palfrey AJ. Intervertebral disc degeneration in adult mice with hereditary kyphoscoliosis. *J Orthop Res* 1984; 2: 333–338

178.   Masuda K, Aota Y, Muehleman C, Imai Y, Okuma M, Thonar EJ, Andersson GB, An HS. A novel rabbit model of mild, reproducible disc degeneration by an anulus needle puncture: correlation between the degree of disc injury and radiological and histological appearances of disc degeneration. *Spine (Phila Pa 1976)* 2005; 30: 5 – 14

179.   Matsui H, Kanamori M, Ishihara H, Yudoh K, Naruse Y, Tsuji H. Familial predisposition for lumbar degenerative disc disease. A case-control study. *Spine* 1998; 23: 1029-1034

180.   Matsuzaki H, Wakabayashi K, Ishihara K, Ishikawa H, Ohkawa A. Allografting intervertebral discs in dogs: a possible clinical application. *Spine* 1996; 21, 178–183

181.   Meisel HJ, Ganey T, Hutton WC, Libera J, Minkus Y, Alasevic O. Clinical experience in cell-based therapeutics: Intervention and outcome. *Eur Spine J* 2006; 15: S397-S405

182.   Meisel HJ, Siodla V, Ganey T, Minkus Y, Hutton WC, Alasevic OJ. Clinical experience in cell-based therapeutics: Disc chondrocyte transplantation: A

treatment for degenerated or damaged intervertebral disc. *Biomol Eng* 2007; 24: 5-21

183.   Melrose C, Shu C, Young AA, Smith SS, Gooden B, Dart A, Podadera J, Appleyard RC, Little CB. Mechanical destabilization induced by controlled annular incision of the intervertebral disc dysregulates metalloproteinase expression and induces disc degeneration. *Spine (Phila Pa 1976)* 2012; 37: 18–25

184.   Melrose J, Burkhardt D, Taylor TKF, Dillon CT, Read R, Cake M, Little CB. Calcification in the ovine intervertebral disc: a model of hydroxyapatite deposition disease. *Eur Spine J* 2009; 18: 479-89

185.   Melrose J, Ghosh P, Taylor TK, Hall A, Osti OL, Vernon- Roberts B, Fraser RD. A longitudinal study of the matrix changes induced in the intervertebral disc by surgical damage to the annulus fibrosus. *J Orthop Res* 1992; 10: 665–676

186.   Melrose J, Ghosh P, Taylor TK, Latham J, Moore R. Topographical variation in the catabolism of aggrecan in an ovine annular lesion model of experimental disc degeneration. *J Spinal Disord* 1997 (a); 10: 55–67

187.   Melrose J, Ghosh P, Taylor TK, McAuley L. Variation in the composition of the ovine intervertebral disc with spinal level and in its constituent proteoglycans. *Vet Comp Orthop Traumatol* 1994; 7: 70-6

188.   Melrose J, Ghosh P, Taylor TK, Vernon-Roberts B, Latham J, Moore R. Elevated synthesis of biglycan and decorin in an ovine annular lesion model of experimental disc degeneration. *Eur Spine J* 1997 (b); 6:376–384

189.   Melrose J, Ghosh P, Taylor TK. A comparative analysis of the differential spatial and temporal distributions of the large (aggrecan, versican) and small (decorin, biglycan, fibromodulin) proteoglycans of the intervertebral disc. *J Anat* 2001; 198: 3-15

190.   Melrose J, Hall A, Macpherson C, Bellenger CR, Ghosh P. Evaluation of digestive proteinases from the Antarctic krill Eu-280 phasia superba as potential chemonucleolytic agents. In vitro and in vivo studies. *Arch Orthop Trauma Surg* 1995; 114: 145–152

191.   Melrose J, Roberts S, Smith S, Menage J, Ghosh P. Increased nerve and blood vessel ingrowth associated with proteoglycan depletion in an ovine anular lesion model of experimental disc degeneration. *Spine* 2002; 27:1278–1285

192.   Melrose J, Smith S, Little CB, Kitson J, Hwa SY, Ghosh P. Spatial and temporal localization of transforming growth factor-beta, fibroblast growth factor-2, and osteonectin, and identification of cells expressing alpha-smooth muscle actin in the injured anulus fibrosus: implications for extracellular matrix repair. *Spine* 2002; 27: 1756–1764

193.   Melrose J, Taylor TK, Ghosh P, Holbert C, Macpherson C, Bellenger CR. Intervertebral disc reconstitution after chemonucleolysis with chymopapain is dependent on dosage. *Spine* 1996; 21: 9–17

194.   Melrose J, Taylor TK, Ghosh P. The serine proteinase inhibitory proteins of the chondrodystrophoid (beagle) and non- chondrodystrophoid (greyhound) canine intervertebral disc. *Electrophoresis* 1997 (c); 18: 1059–1063

195.   Mente PL, Aronsson DD, Stokes IA, Iatridis JC. Mechanical modulation of growth for the correction of vertebral wedge deformities. *J Orthop Res* 1999; 17, 518–524

196.   Mikecz K, Glant TT, Poole AR. Immunity to cartilage proteoglycans in BALB/c mice with progressive polyarthritis and ankylosing spondylitis induced by injection of human cartilage proteoglycan. *Arthritis Rheum* 1987; 30: 306–318

197.   Miller JA, Schmatz C, Schultz AB. Lumbar disc degeneration: correlation with age, sex, and spine level in 600 autopsy specimens. *Spine* 1988; 13: 173-8

198.   Mirza SK, Deyo RA. Systematic review of randomized trials comparing lumbar fusion surgery to nonoperative care for treatment of chronic back pain. *Spine* 2007; 32, 816-823

199.   Misenhimer GR, Peek RD, Wiltse LL, Rothman SL, Widell EH Jr. Anatomic analysis pedicle cortical and cancellous diameter as related to screw size. *Spine (Phila Pa 1976)* 1989; 14: 367–72

200.   Miyakoshi N, Abe E, Shimada Y, Okuyama K, Suzuki T, Sato K. Outcome of one-level posterior lumbar interbody fusion for spondylolisthesis and postoperative intervertebral disc degeneration adjacent to the fusion. *Spine* 2000; 25: 1837-1842

201.   Mizuno H, Roy AK, Zaporojan V, Vacanti CA, Ueda M, Bonassar LJ. Biomechanical and biochemical characterization of composite tissue-engineered intervertebral discs. *Biomaterials* 2006; 27, 362-370

202.   Modic MT, Masaryk TJ, Ross JS, Carter JR. Imaging of degenerative disk disease. *Radiology* 1988; 168: 177– 86

203.   Morinaga T, Takahashi K, Yamagata M, Chiba T, Tanaka K, Takahashi Y, NakamuraS, Suseki K, Moriya H. Sensory innervation to the anterior portion of lumbar intervertebral disc. *Spine* 1996; 21: 1848–1851

204.   Moskowitz RW, Ziv I, Denko CW, Boja B, Jones PK, Adler JH. Spondylosis in sand rats: a model of intervertebral disc degeneration and hyperostosis. *J Orthop Res* 1990; 8: 401–411

205.   Nachemson A, Lewin T, Maroudas A, Freeman MAF. In vitro diffusion of dye through the end-plates and annulus fibrosus of human lumbar intervertebral discs. *Acta Orthop Scand* 1970; 41: 589-607

206.   Nachemson A, Schiltz AB, Berkson MH. Mechanical properties of human lumbar spine motion segments: Influence of age, sex, disc level, and degeneration. *Spine* 1979; 4: 1-8

207.   Nakatsukasa M, Hirose Y. Scaling of lumbar vertebrae in anthropoids and implications for evolution of the hominoid axial skeleton. *Primates* 2003; 44:127-35

208.   Nerlich AG, Schaaf R, Walchli B, Boos N. Temporo-spatial distribution of blood vessels in human lumbar intervertebral discs. *Eur Spine J* 2007; 16, 547-555

209.   Nerurkar NL, Elliott DM, Mauck RL. Mechanical design criteria for intervertebral disc tissue engineering. *J. Biomech* 2010*; 43, 1017-1030

210.   Nesti LJ, Li WJ, Shanti RM, Jiang YJ, Jackson W, Freedman BA, Kuklo TR, Giuliani JR, Tuan RS. Intervertebral disc tissue engineering using a novel hyaluronic acid-nanofibrous scaffold (HANFS) amalgam. *Tissue Eng. Part A* 2008; 14, 1527-1537

211.   Neufeld JH, Machado T, Margolin L. Variables affecting disc size in the lumbar spine of rabbits: anesthesia, paralysis, and disc injury. *J Orthop Res* 1991; 9:104–112

212.   Nguyen-minh C, Haughton VM, Papke RA, An H, Censky CS. Measuring diffusion of solutes into intervertebral disks with MR imaging and paramagnetic contrast medium. *Am J Neuroradiol* 1998; 19, 1781-1784

213.   Nickel R, Schummer A, Seiferle E. *Lehrbuch der Anatomie der Haustiere.* Vol 1. Berlin und Hamburg: Verlag Paul Parey, 1984

214.   Nishimura K, Mochida J. Percutaneous reinsertion of the nucleus pulposus. An experimental study. *Spine* 1998; 23, 1531–1538

215.   Nisolle JF, Wang XQ, Squélart M, Hontoir F, Kirschvink N, Clegg P, Vandeweerd JM. Magnetic resonance imaging (MRI) anatomy of the ovine lumbar spine. *Anat Histol Embryol* 2013; 43: 203-209

216.   Nomura T, Mochida J, Okuma M, Nishimura K, Sakabe K. Nucleus pulposus allograft retards intervertebral disc degeneration. *Clin Orthop* 2001; 1, 94–101

217.   O'Connell GD, Vresilovic EJ, Elliott DM. Comparison of animals used in disc research to human lumbar disc geometry. *Spine* (Phila Pa 1976) 2007; 32: 328-33

218.   O'Halloran DM, Pandit AS. Tissue-engineering approach to regenerating the intervertebral disc. *Tissue Eng* 2007; 13: 1927-54

219.   Oeheme D, Goldschlager T, Rosenfeld J, Danks A, Ghosh P, Gibbon A, Jenkin G. Lateral surgical approach to lumbar intervertebral disc in an ovine model. Sci World J 2012; 2012: 873726

220.   Oh WS, Shim JC. A randomized controlled trial of radiofrequency denervation of the ramus communicans nerve for chronic discogenic low back pain. *Clin J Pain* 2004; 20: 55–60

221.   Ohshima H, Urban JPG. Effect of lactate concentrations and pH on matrix synthesis rates in the intervertebral disc. *Spine* 1992; 17 1079-1082

222.   Ohtori S, Takahashi K, Chiba T, Yamagata M, Sameda H, Moriya H. Sensory innervation of the dorsal portion of the lumbar intervertebral disc in rats. *Spine* 1999; 24: 2295–2299

223.   Olmarker K, Rydevik B (2002). Disc Herniation and sciatica; the basic science platform. In: Gunzburg R, Szpalski M, eds. *Lumbar Disc Herniation.* Philadelphia: Lippincott. Williams & Wilkins

224.   Olsewski JM, Schendel MJ, Wallace LJ, Ogilvie JW, Gundry CR. Magnetic resonance imaging and biological changes in injured intervertebral discs under normal and increased mechanical demands. *Spine* 1996; 21: 1945–1951

225.   Osterman K, Osterman H. Experimental lumbar spondylolisthesis in growing rabbits. *Clin Orthop Relat Res* 1996; 332: 274–280

226.   Osti O, Vernon-Roberts B, Fraser R. Annulus tears and intervertebral disc degeneration. *Spine* 1990 (a); 15: 762–7

227.   Osti OL, Fraser RD, Vernon-Roberts B. Discitis after discography. The role of prophylactic antibiotics. *J Bone Joint Surg Br* 1990 (b); 72: 271-274

228.   Oxland TR, Lin R-M, Panjabi MM. Three dimensional mechanical properties of the thoracolumbar junction. *J Orthop Res* 1992; 10: 573-80

229.   Panjabi MM, Oda T, Crisco JJ, Dvorak J, Grob D. Posture affects motion coupling patterns of the upper cervical spine. *Spine* 1993; 11: 525-36

230.   Panjabi MM, Oxland TR, Yamamoto I, Crisco JJ. Mechanical behavior of the human lumbar and lumbosacral spine as shown by three-dimensional load-displacement curves. *J Bone Joint Surg [Am]* 1994; 76: 413-24

231.   Panjabi MM. Biomechanical evaluation of spinal fication devices: I. A conceptual framework. *Spine* 1988: 13: 1129-34

232.   Papalia R, Albo E, Vadalá G, D'Adamio S, Lanotte A, Di Martino A, Denaro V. Is there a role for endothelial dysfunction in the pathogenesis of lumbar disc degeneration? A hypothesis that needs to be tested. *Med Hypotheses* 84: 249-51

233.   Pazzaglia UE, Salisbury JR, Byers PD. Development and involution of the notochord in the human spine. *J R Soc Med* 1989; 82, 413-415

234.   Peacock A. Observations on the postnatal development of the intervertebral disc in man. *J Anat* 1952; 86, 162-179

235.   Peacock A. Observations on the prenatal development of the intervertebral disc in man. *J Anat* 1951; 85, 260-274

236.   Pearce RH, Thompson JP, Bebault GM, Flak B. Magnetic resonance imaging reflects the chemical changes of aging degeneration in the human intervertebral disk. *J Rheumatol Suppl* 1991; 27: 42–3

237.   Pedrini-Mille A, Weinstein JN, Found EM, Chung CB, Goel VK. Stimulation of dorsal root ganglia and degradation of rabbit annulus fibrosus. *Spine* 1990; 15: 1252–1256

238.   Peng B, Chen J, Kuang Z, Li D, Pang X, Zhang X. Expression and role of connective tissue growth factor in painful disc fibrosis and degeneration. *Spine (Phila Pa 1976)*, 2009; 34: E178–E182

239.   Peng B, Hao J, Hou S, Wu W, Jiang D, Fu X, Yang Y. Possible pathogenesis of painful intervertebral disc degeneration. *Spine (Phila Pa 1976)* 2006; 31: 560–566

240.   Peng B, Wu W, Hou S, Li P, Zhang C, Yang Y. The pathogenesis of discogenic low back pain. *J Bone Joint Surg Br* 2005; 87: 62–67

241.   Peng BG, Hou SX, Shi Q, Jia LS. The relationship be- tween cartilage end-plate calcification and disc degeneration: an experimental study. *Chin Med J* 2001; 114:308–312

242.   Pfirrmann CW, Metzdorf A, Zanetti M, Hodler J, Boos N. Magnetic resonance classification of lumbar intervertebral disc degeneration. *Spine* 2001; 1873-1878

243.   Phillips FM, Reuben J, Wetzel FT. Intervertebral disc degeneration adjacent to a lumbar fusion. An experimental rabbit model. *J Bone Joint Surg Br* 2002; 84: 289-94

244.   Prescher A. Anatomy and pathology of the aging spine. *Eur J Radiol* 1998; 27, 181-195

245.   Puustjarvi K, Lammi M, Helminen H, Inkinen R, Tammi M. Proteoglycans in the intervertebral disc of young dogs following strenuous running exercise. *Connect Tissue Res* 1994; 30: 225–240

246.   Puustjarvi K, Lammi M, Kiviranta I, Helminen HJ, Tammi M. Proteoglycan synthesis in canine intervertebral discs after long-distance running training. *J Orthop Res* 1993; 11: 738–746

247.   Puustjarvi K, Takala T, Wang W, Tammi M, Helminen H, Inkinen R. Proteoglycans in the interverterbal disc of young dogs following strenuous running exercise. *Conn Tiss Res* 1993; 30: 1-16

248.   Radin EL, Rose RM. Role of subchondral bone in the initiation and progression of cartilage damage. *Clin Orthop Relat Res* 1986; 231, 34-40

249.   Raj PP. Intervertebral disc: anatomy-physiology-pathophysiology-treatment. *Pain Pract* 2008; 8: 18-44

250.   Rastogi A, Thakore P, Leung A, Benavides M, Machado M, Morschauser MA, Hsieh AH. Environmental regulation of notochordal gene expression in nucleus pulposus cells. *J. Cell Physiol* 2009; 220, 698-705

251.   Rea W, Kapur S, Mutagi H. Intervertebral disc as a source of pain. *Contin Educ Anaesth Crit Care Pain* 2012; 12: 279-282

252.   Reid JE, Meakin JR Robins, SP, Skakle JM, Hukins DW. Sheep lumbar intervertebral discs as models for human discs. *Clin Biomech* (Bristol, Avon) 2002; 17: 312–14

253.   Renfrew DL, Whitten CG, Wiese JA, el-Khoury GY, Harris KG. CT-guided percutaneous transpedicular biopsy of the spine. *Radiology* 1991; 180: 574 – 6

254.   Retimaier S, Volkheimer D, Berger-Roscher N, Wilke HJ, Ignatius A. Increase or decrease in stability after nucleotomy? Conflicting in vitro and in vivo results in the sheep model. *J R Soc Interface* 2014; 11: 20140650

255.   Risbud MV, Schaer TP, Shapiro IM. Toward an understanding of the role of notochordal cells in the adult intervertebral disc: from discord to accord. *Dev. Dyn* 2010; 239, 2141-2148.

256.   Roberts S, Caterson B, Menage J, Evans EH, Jaffray DC, Eisenstein SM. Matrix metalloproteinases and aggrecanase: their role in disorders of the human intervertebral disc. *Spine* 2000; 25: 3005-3013

257.   Roberts S, Eisenstein SM, Menage J, Evans EH, Ashton IK. Mechanoreceptors in intervertebral discs. Morphology, distribution, and neuropeptides. *Spine* 1995; 20: 2645-2651

258.   Roberts S, Evans H, Trivedi J, Menage J. Histology and pathology of the human intervertebral disc. *J Bone Joint Surg Am* 2006; 88: 10-4

259.   Roberts S, Menage J, Duance V, Wotton S, Ayad S. 1991 Volvo award in basic sciences: Collagen types around the cells of the intervertebral disc and cartilage end plate: An immunolocalization study. *Spine* 1991; 16: 1030-1038

260.   Roberts S, Menage J, Eisenstein SM. The cartilage end-plate and intervertebral disc in scoliosis: calcification and other sequelae. *J Orthop Res* 1993; 11: 747-757

261.   Roberts S, Menage J, Urban JP. Biomechanical and structural properties of the cartilage end-plate and its relation to the intervertebral disc. *Spine (Phila Pa 1976)* 1989; 14: 166-74

262.   Roberts S, Menage J, Urban JPG. Biochemical and structural properties of the cartilage end-plate and its relation to the intervertebral disc. *Spine* 1989; 14: 166-174

263.   Roberts S, Urban JPG, Evans H, Eisenstein SM. Transport properties of the human cartilage endplate in relation to its composition and calcification. *Spine* 1996; 21: 415-420

264.   Robin GC, Stein H. Experimental scoliosis in primates. Failure of a technique. *J Bone Joint Surg* 1975; 57-A: 142-5

265.   Roughley PJ, Alini M, Antoniou J. The role of proteoglycans in aging, degeneration and repair of the intervertebral disc. *Biochem Soc Trans* 2002; 30: 869–74

266.   Rufai A, Benjamin M, Ralphs JR. The development of fibrocartilage in the rat intervertebral disc. *Anat Embryol (Berl)* 1995; 192, 53-62

267.   Rutges JP, Duit RA, Kummer JA, Oner FC, van Rijen MH, Verbout AJ, Castelein RM, Dhert WJA, Creemers LB. Hypertrophic differentiation and calcification during intervertebral disc degeneration. *Osteoarthritis Cartilage* 2010; 18, 1487-1495

268.   Saamanen AM, Puustjarvi K, Ilves K, Lammi M, Kiviranta I, Jurvelin J, Helminen HJ, Tammi M. Effect of running exercise on proteoglycans and collagen content in the interver- tebral disc of young dogs. *Int J Sports Med* 1993; 14:48–51

269.   Sahlman J, Inkinen R, Hirvonen T, Lammi MJ, Lammi PE, Nieminen J, Lapvetelainen T, Prockop DJ, Arita M, Li SW, Hyttinen MM, Helminen HJ, Puustjarvi K. Premature vertebral endplate ossification and mild disc degeneration in mice after inactivation of one allele belonging to the Col2a1 gene for Type II collagen. *Spine* 2001; 26: 2558–2565

270.   Sakai D, Mochida J, Iwashina T et al. Differentiation of mesenchymal stem cells transplanted to a rabbit degenerative disc model: potential and limitations for stem cell therapy in disc regeneration. *Spine* 2005; 30:2379-87

271.   Sakai D, Mochida J, Iwashina T, Hiyama A, Omi H, Imai M, Najai T, Ando K, Hotta T. Regenerative effects of transplanting mesenchymal stem cells embedded in atelocollagen to the degenerated intervertebral disc. *Biomaterials* 2006; 27:335-345

272.   Salo J, Kaigle Holm A, Indahl A, Mackiewicz Z, Sukura A, Holm S, Jämsen E, Konttinen YT. Expression of vascular endothelial growth factor receptors coincide with blood vessel in-growth and reactive bone remodelling in experimental intervertebral disc degeneration. *Clin Exp Rheumatol* 2008 (a); 26: 1018–26

273.   Salo J, Mackiewicz Z, Indahl A, et al. Plasmin-matrix metallopro- teinase cascades in spinal response to an experimental disc lesion in pig. *Spine (Phila Pa 1976)* 2008 (b); 33: 839–44

274.   Sandstrom C. Calcifications of the intervertebral discs and the relationship between various types of calcifications in the soft tissues of the body. *Acta radiol* 1951; 36, 217-233

275.   Sasaki M, Takahashi T, Miyahara K, Hirose T. Effects of chondroitinase ABC on intradiscal pressure in sheep. An *in vivo* study. *Spine* 2001; 26: 463-468

276.   Schmidt H, Reitmaier S. Is the ovine intervertebral disc a small human one? A finite element model study. *J Mech Behav Biomed Mater* 2013; 17: 229-41

277.   Schweitzer ME, el-Noueam KI. Vacuum disc: frequency of high signal intensity on T2-weighted MR images. *Skeletal Radiol* 1998; 27: 83-6

278.   Scott NA, Harris PF, Bagnall KM. A morphological and histological study of the postnatal development of intervertebral discs in the lumbar spine of the rabbit. *J Anat* 1980; 130, 75–81

279.   Shao Z, Rompe G, Schiltenwolf M. Radiographic changes in the lumbar intervertebral discs and lumbar vertebrae with age. *Spine* 2002; 27: 263-268

280.   Shea JE, Hallows RK, Bloebaum RD. Experimental confirmation of the sheep model for studying the role of calcified fibro-cartilage in hip fractures and tendon attachments. *Anat Rec* 2002 (a); 266:177-183.

281.   Shea JE, Hallows RK, Ricks S, Bloebaum RD. Microvascularization of the hypermineralized calcified fibrocartilage and cortical bone in the sheep proximal femur. *Anat Rec* 2002 (b); 268: 365-370

282.   Shea JE, Vajda EG, Bloebaum RD. Evidence of a hypermineralized calcified fibrocartilage on the human femoral neck and lesser trochanter. *J Anat* 2001; 198: 153-162.

283.   Shi S, Ciurli C, Cartman A, Pidoux I, Poole AR, Zhang Y. Experimental immunity to the G1 domain of the proteoglycan versican induces spondylitis and sacroilitis, of a kind seen in human spondylarthropathies. *Arthritis Rheum* 2003; 48: 2903–2915

284.   Silberberg R. Histologic and morphometric observations on vertebral bone of aging sand rats. *Spine* 1988; 13: 202-8

285.   Sinclair SK, Bell S, Epperson RT, Bloebaum RD. The significance of calcified fibrocartilage on the cortical endplate of the translational sheep spine model. *Anat Rec* 2013; 296: 736-44

286.   Sinclair SK, Konz GJ, Dawson JM, Epperson RT, Bloebaum RD. Host bone response to polyetheretherketone versus porous tantalum implants for cervical spinal fusion in a goat model. *Spine* (Phila Pa 1976) 2012; 37-E: 571-80

287.   Singh K, Masuda K, An HS. Animal models for human disc degeneration. *Spine J* 2005; 5: 267S-279S

288.   Smit TH. The use of a quadruped as an in vivo model for the study of the spine - biomechanical considerations. *Eur Spine J* 2002; 11: 137-44

289.   Smith JW, Serafini-Fracassini A. The distribution of the protein-polysaccharide complex in the nucleus pulposus matrix in young rabbits. *J Cell Sci* 1968; 3, 33–40

290.   Smith LJ, Nerurjar NL, Choi KS, Harfe BD, Elliott DM. Degeneration and regeneration of the intervertebral disc: lessons from development. *Dis Model Mech* 2011; 4, 31-41

291.   Sobajima S, Kim JS, Gilbertson LG, Kang JD. Gene therapy for degenerative disc disease. *Gene Ther* 2004; 11: 390-401

292.   Sobajima S, Kompel JF, Kim JS et al. A slowly progressive and reproducible animal model of intervertebral disc degeneration characterized by MRI, X-ray, and histology. *Spine* 2005; 30: 15-24

293.   Sowa G, Vadalà G, Studer R, Kompel J, Iucu C, Georgescu H, Gilbertson L, Kang J. Characterization of intervertebral disc aging: longitudinal analysis of a rabbit model by magnetic resonance imaging, histology, and gene expression. *Spine (Phila Pa 1976)*, 2008; 33 : 1821 – 8

294.   Stemple DL Structure and function of the notochord: an essential organ for chordate development. *Development* 2005; 132, 2503-2512

295.   Stokes IA, Counts DF, Frymoyer JW. Experimental instability in the rabbit lumbar spine. *Spine* 1989; 14: 68–72

296.   Suguro T, Oegema TR Jr, Bradford DS. Ultrastructural study of the short-term effects of chymopapain on the inter- vertebral disc. *J Orthop Res* 1986; 4: 281–287

297.   Suseki K, Takahashi Y, Takahashi K, Chiba T, Yamagata M, Moriya H. Sensory nerve fibres from lumbar intervertebral discs pass through rami communicantes. A possible pathway for discogenic low back pain. *J Bone Joint Surg Br* 1998; 80: 737–742

298.   Sweet HO, Green MC. Progressive ankylosis, a new skeletal mutation in the mouse. *J Hered* 1981; 72: 87–93

299.   Sztrolovics R, Alini M, Roughley PJ, Mort JS. Aggrecan degradation in human intervertebral disc and articular cartilage. *Biochem J* 1997; 326: 235-241

300.   Taher F, Essig D, Lebl DR, Hughes AP, Sama AA, Cammisa FP, Girardi FP. Lumbar degenerative disc disease: current and future concepts of diagnosis and management. *Adv Orthop* 2012; 970752

301.   Takaishi H, Nemoto O, Shiota M, Kikuchi T, Yamada H, Yamagishi M, Yabe Y. Type-II collagen gene expression is transiently upregulated in experimentally induced degeneration of rabbit intervertebral disc. *J Orthop Res* 1997; 15:528–538

302.   Taurog JD, Maika SD, Satumtira N, Dorris ML, McLean IL, Yanagisawa H, Sayad A, Stagg AJ, Fox GM, Le O'Brien A, Rehman M, Zhou M, Weiner AL,

Splawski JB, Richardson JA, Hammer RE. Inflammatory disease in HLA-B27 trans- genic rats. *Immunol Rev* 1999; 169: 209–223

303.   Taylor TKF, Ghosh P, Bushell GR, Stephens RW. *Scientific basis of the treatment of intervertebral disc disorders*. London: Heinemann Medical Books, 1981

304.   Tertti M, Paajanen H, Laato M, Aho H, Komu M, Kormano M. Disc degeneration in magnetic resonance imaging: a comparative biochemical, histologic, and radiologic study in cadaver spines. *Spine* 1991; 16: 629 –34

305.   Thometz JG, Liu XC, Lyon R. Three-dimensional rota- tions of the thoracic spine after distraction with and without rib resection: a kinematic evaluation of the apical vertebra in rabbits with induced scoliosis. *J Spinal Disord* 2000; 13: 108–112

306.   Thompson JP, Pearce RH, Schechter MT, Adams ME, Tsang IKY, Bishop PB. Preliminary evaluation of a scheme for grading the gross morphology of the human intervertebral disc. *Spine* 1990; 15, 411-415

307.   Thompson RE, Pearcy MJ, Barker TM. The mechanical effects of intervertebral disc lesions. *Clin Biomech* 2004; 19:v448–455

308.   Trout JJ, Buckwalter JA, Moore KC, Landas S K. (1982a). Ultrastructure of the human intervertebral disc. I. Changes in notochordal cells with age. *Tissue Cell* 1982 (a); 14, 359-369

309.   Trout JJ, Buckwalter JA, Moore KC. Ultrastructure of the human intervertebral disc. II. Cells of the nucleus pulposus. *Anat Rec* 1982 (b); 207, 307-314

310.   Twomey LT, Taylor JR. Age changes in lumbar vertebrae and intervertebral discs. *Clin Orthop* 1987; 224: 97-104.

311.   Uhthoff HK, Sarkar K, Maynard JA. Calcifying tendinitis: a new concept of its pathogenesis. *Clin Orthop Relat Res* 1976; 118:164-8

312.   Urayama. Histological and ultrastructural study of degeneration of the lumbar intervertebral disc in the rabbit following nucleotomy, with special reference to the topographical distribution pattern of the degeneration. *Nippon Seikeigeka Gakkai Zasshi* 1986; 60: 649–662

313.   Urban J (1996). *Disc biochemistry in relation to function*. In *The Lumbar Spine* (ed. S. W. Wiesel, J. N. Weinstein, H. N. Herkowitz, J. Dvorak and G. Bell), pp. 271-280. Philadelphia: Saunders

314.   Urban JP, Holm S, Maroudas A. Diffusion of small solutes into the intervertebral disc: as in vivo study. *Biorheology* 1978; 15: 203-221

315.   Urban JP, Maroudas A, Bayliss MT, Dillon J. Swelling pressures of proteoglycans at the concentrations found in cartilaginous tissues. *Biorheology* 1979; 16: 447-464

316.   Urban JP, Roberts S. Development and degeneration of the intervertebral discs. *Mol Med Today* 1995; 1, 329-335

317.   Urban JP, Smith S, Fairbank JC. Nutrition of the intervertebral disc. *Spine (Phila Pa 1976)* 2004; 29: 2700-9

318.   Urban MR, Fairbank JC, Etherington PJ, Loh FL, Winlove CP, Urban JP. Electrochemical measurement of transport into scoliotic intervertebral discs in vivo using nitrous oxide as a tracer. *Spine* 2001; 26: 984-990

319.   Vadalá G, Mozetic P, Rainer A, Centola M, Loppini M, Trombetta M, Denaro V. Bioactive electrospun scaffold for annulus fibrosus repair and regeneration. *Eur Spine J* 2012; 21: S20-6

320.   Vadalà G, Russo F, Pattappa G, Peroglio M, Stadelmann VA, Roughley P, Grad S, Alini M, Denaro V. A nucleotomy model with intact annulus fibrosus to test intervertebral disc regeneration strategies. *Tissue Eng Part C Methods* 2015; 21: 1117-24

321.   Vadalà G, Russo F, Pattappa G, Schiuma D, Peroglio M, Benneker L, Grad S, Alini M, Denaro V. The transpedicular approach as an alternative route for intervertebral disc regeneration. *Spine* 2013; 38-E: 319-24

322.   Vadalà G, Sowa G, Hubert M, Gilbertson LG, Denaro V, Kang JD. Mesenchymal stem cells injection in degenerated intervertebral disc: cell leakage may induce osteophyte formation. *J Tissue Eng Regen Med* 2011; 6: 348 – 55

323.   Vaga S, Raimondi MT, Caiani EG, Costa F, Giordano C, Perona F, Zerbi A, Fornari M. Quantitative assessment of intervertebral disc glrycosaminoglycan distribution by gadolinium-enhanced MRI in orthopedic patients. *Magn Reson Med* 2008; 59: 85-95

324.   Varlotta GP, Brown MD, Kelsey JL, Golden AL. Familial predisposition for herniation of a lumbar disc in patients who are less than twenty-one years old. *J Bone Joint Surg Am* 1991; 73:124-128

325.   Wallach CJ, Kim JS, Sobajima S, Wallach CJ, James W, Larson III JW, MD, Robbins PD, Xiao X, Juan L, Vadalá G, Gilbertson LG, Kang JD. Safety assessment of intradiscal gene transfer: a pilot study. *Spine J* 2006*; 6, 107–112

326.   Walmsley R. The development and growth of the intervertebral disc. *Edinb Med J* 1953; 60, 341-364

327.   Walsh AJ, Lotz JC. Biological response of the intervertebral disc to dynamic loading. *J Biomech* 2004; 37, 329–337

328.   Wang H, Zhang J, Sub Q, Yang X. Altered gene expression in articular chondrocytes of Smad3ex8/ex8 mice, revealed by gene profiling using microarrays. *J Genet Genomics* 2007; 34, 698-708

329.   Watanabe H, Nakata K, Kimata K, Nakanishi I, Yamada Y. Dwarfism and age-associated spinal degeneration of heterozygote cmd mice defective in aggrecan. *Proc Natl Acad Sci USA* 1997; 94: 6943–6947

330.   Watanabe H, Yamada Y. Chondrodysplasia of gene knockout mice for aggrecan and link protein. *Glycoconj J* 2002; 19: 269–273

331.   Weiler C, Nerlich AG, Zipperer J, Bachmeier BE, Boos N. 2002 SSE Award Competition in Basic Science: expression of major matrix metalloproteinases is associated with intervertebral disc degradation and resorption. *Eur Spine J* 2002; 11: 308-320

332.	Weinreich S, Hoebe B, Ivanyi P. Maternal age influences risk for HLA-B27 associated ankylosing enthesopathy in trans- genic mice. *Ann Rheum Dis* 1995; 54:754–756

333.	Wells DJ. Gene therapy progress and prospects: electroporation and other physical methods. *Gene Ther 2004;* 11, 1363–1369

334.	Wen N, Lavaste F, Santin JJ, Lassau JP. Three-dimensional biomechanical properties of the human cervical spine in vitro. *Eur Spine J* 1993; 2: 2-47

335.	West GB, Brown JH, Enquist BJ. A general model for the origin of allometric scaling laws in biology. *Science* 1997; 276: 122-6

336.	Wiley JJ, Macnab I, Wortzman G. Lumbar discography and its clinical applications. *Can J Surg* 1986; 11: 280– 289

337.	Wilke H-J, Wolf S, Claes LE, Arand M, Wiesend A. Stability increase of the lumbar spine with different muscle groups. *Spine* 1995: 20 192-8

338.	Wilke HJ, Kettler A, Gosh P, Claes LE. Are sheep spines a valid biomechanical model for human spines? *Spine* 1997 (b); 22: 2365-74

339.	Wilke HJ, Kettler A, Wenger KH, Claes LE. Anatomy of the sheep spine and its comparison to the human spine. *Anat Rec* 1997 (a); 247: 542-55

340.	Wilke HJ, Krischak S, Claes L. Biomechanical comparison of calf and human spines. *J Orthop Res* 1996; 14: 500-3

341.	Wilke HJ, RohlmannA, Neller S, Graichen F, Claes L, Bergmann G. ISSLS prize winner: a nove approach to determine trunk muscle forces during flexion and extension: a comparison of data from an in vitro experiment and in vivo measurements. *Spine* 2003; 28: 2585-93

342.	Wilste LL, Newman PH, Macnab I. Classification of spondylolisis and spondylolisthesis. *Clin Orthop Relat Res* 1976; 117: 23-29

343.	Wolfe HJ, Pustchar WGJ, Vickery AL. Role of the notochord in human intervertebral disk. I. Human and infant. *Clin Orthop Relat Res* 1965; 39, 205-212

344.	Yamada K, Tanabe S, Eueno H, Oinuma A, Ytakahashi T, Mityauchi S, Shigeno S, Hirose T, Miyahara K, Sato M. Investigation of the short term effect of chemonucleolysis with chondroitinase ABC. *J Vet Med* Sci 2001; 63: 521–525

345.	Yoganandan N, Kumaresan S, Voo L, Pintar FA. Finite element applications in human cervical spine modeling. *Spine* 1996; 21:1824-34

346.	Youssef JA, McAfee PC, Patty CA, Raley E, DeBauche S, Shucosky E, Chotikul L. Minimally invasive surgery: lateral approach interbody fusion: results and review. *Spine* 2010; 35: S302–S311

347.	Yu J, Winlove CP, Roberts S, Urban JP. Elastic fibre organization in the intervertebral discs of the bovine tail. *J Anat* 2002; 201: 465-475

348.	Zhang Y, Chee A, Thonar E, An HS. Intervertebral disk repair by protein, gene, or cell injection: a framework for rehabilitation-focused biologics in the spine. *PM R* 2011; 3: S88-S95

349.   Zollner J, Heine J, Eysel P. Effect of enucleation on the biomechanical behavior of the lumbar motion segment. *Zentralbl Neurochir* 2000; 61, 138–42